Thomas Holler

Mikrobiologische Studien zur anaeroben Oxidation von Methan (AOM)

Mikrobiologische Studien zur anaeroben Oxidation von Methan (AOM)

Dissertation
zur
Erlangung des Grades eines
Doktors der Naturwissenschaften
– Dr. rer. nat. –

Dem Fachbereich Biologie/Chemie der
Universität Bremen vorgelegt von

Thomas Holler
aus Halle an der Saale

Bremen 2010

Die vorliegende Arbeit wurde im Rahmen des Programms „The International Max Planck Research School of Marine Microbiology“ in der Abteilung Mikrobiologie am Max-Planck-Institut für marine Mikrobiologie in Bremen angefertigt.

1. Gutachter: Prof. Dr. Antje Boetius

2. Gutachter: PD Dr. Jens Harder

Tag des Promotionskolloquiums: 20. Dezember 2010

Inhaltsverzeichnis

Zusammenfassung

In marinen Sedimenten wird mehr als 90% des gebildeten Methans durch die anaerobe Oxidation von Methan mit Sulfat als Elektronenakzeptor (AOM) abgebaut. Dadurch gelangt nur wenig Methan, ein relevantes Treibhausgas, aus dem Meer in die Atmosphäre. Die AOM wird von Konsortien anaerober methanotropher Archaeen (ANME) und Sulfat-reduzierender Bakterien (SRB) katalysiert. Die Interaktion der beteiligten Mikroorganismen ist noch nicht vollständig verstanden. Phylogenetisch sind ANME mit methanogenen Archaeen verwandt. Daher wird vermutet, dass die Aktivierung des Methans eine Umkehrreaktion der Methanogenese ist. Der bakterielle Partner ist ebenfalls phylogenetisch charakterisiert, konnte jedoch noch nicht isoliert werden. Ziel der Dissertation war es, die an der AOM beteiligten Organismen zu kultivieren und anzureichern. Zu Beginn dieser Arbeit gab es nur eine sedimentfreie AOM-Anreicherungskultur. Daher wurden verschieden AOM-aktive marine Sedimente anaerob inkubiert und auf die Umsetzung von Methan untersucht. Unter optimierten Anreicherungsmethoden wurden weitere sedimentfreie, hoch aktive AOM-Kulturen gewonnen. Das Aktivitätsoptimum einiger dieser Kulturen liegt bei maximal 20 °C. Ein weiteres Ziel der Arbeit war die Anreicherung methanotropher Konsortien bei höheren Temperaturen. Aus marinen hydrothermalen Sedimenten wurden ANME angereichert, die ein Aktivitäts- und Wachstumsoptimum bis zu 60 °C aufweisen. Dabei handelt es sich um die erste wachsende Anreicherung von Methanotrophen des ANME-1 Clusters. Weiterhin wurde mittels Inkubation und radioisotopischen Methoden AOM für ein nicht marines Habitat nachgewiesen. Sedimente eines Schlammvulkans in den Karpaten, Rumänien, zeigten erstmals *in vitro* AOM-Aktivität für ein terrestrisches Habitat.

Mit den gewonnenen AOM-Anreicherungen aus marinen Sedimenten wurde die Isotopenfraktionierung von Methan während der AOM untersucht. In Inkubations-experimenten wurden Fraktionierungsfaktoren für Kohlenstoff und Wasserstoff des Methans ermittelt, welche signifikant größer waren als die aus Untersuchungen von marinen Porenwasserprofilen.

Untersuchungen zur Umkehrreaktion der AOM in den Anreicherungskulturen zeigten deutliche Austauschreaktionen zwischen den Produkt- und Substrat-Pools, womit das erste Mal die Reversibilität für einen vollständigen katabolen Prozess gezeigt wurde. Die Umkehrung der AOM entsprach bis zu 13% der Nettorate. Eine Umkehrung im Sinne einer vollständigen Methanogenese konnte nicht gezeigt werden. Dies lässt vermuten, dass ANME-Archaeen obligate methanotrophe Organismen sind.

Abstract

In marine sediments more than 90% of the produced methane is consumed by the anaerobic oxidation of methane with sulfate as terminal electron acceptor (AOM). Due to this, the contribution of the oceans as source of climate-relevant methane is rather low. AOM is catalyzed by consortia of methanotrophic archaea (ANME) and sulfate-reducing bacteria (SRB). The interaction of these two organisms is so far poorly understood. ANME are phylogenetically closely related to methanogenic archaea. Hence, it is thought that the activation of methane acts in a reverse reaction of methanogenesis. The bacterial partner of ANME is also phylogenetically characterized. However both organisms are not isolated yet.

Hence, the first aim of this thesis was to achieve (sediment-free) enrichment cultures and the further characterization of the organisms. Therefore AOM-active sediments from different habitats were incubated with methane and sulfate as sole substrates, tested for their growth optima and repeatedly diluted, which yielded finally sediment-free AOM-enrichments. The growth optima of cultures from marine cold seeps were between 4 and 20 °C. Incubations from hydrothermally influenced sediment succeeded the first thermophilic enrichments of AOM with a growth optimum between 50 and 60 °C. These are the first successfully growing enrichments of the ANME-1 cluster. Furthermore presence of AOM was also shown for a terrestrial mud volcano, one of the first described non-marine AOM-habitats.

The obtained enrichment cultures from marine cold seeps were used to determine the isotope fraction factors of methane during its anaerobic oxidation. We defined the first experimentally derived carbon and hydrogen isotope fractionation factors for AOM. Those are significantly higher than fractionation factors calculated from isotope profiles of sedimentary marine pore waters.

Furthermore, the enrichments were used to test it for the enzymatic back-reaction during AOM, which can be described as exchange reactions between product and substrate pools. The reversibility of AOM was about 13% of the net-metabolic rate. Back reaction, defined as a complete reversal of AOM (“true” methanogenesis) was excluded.

I. Einleitung

Methan (CH_4, MW = 16,04) ist ein farb- und geruchloses Gas (Schmelzpunkt, –183 °C; Siedepunkt, –164 °C) und kann abiotischen oder biotischen Ursprungs sein. Der Großteil des auf der Erde vorkommenden Methans (ca. 69%) entsteht durch mikrobielle Reduktion von Kohlenstoffverbindungen (biotisch/biogenen Ursprungs, Conrad, 2009). Methanogenese findet überall dort statt, wo Sauerstoff und andere potenzielle Elektronenakzeptoren (biologische Oxidationsmittel) wie Nitrat/Nitrit, Mangan(IV), Eisen(III) und Sulfat veratmet oder assimiliert sind. Typische Habitate der biogenen Methanproduktion sind Reisfelder, der Darmtrakt von Wiederkäuern und Termiten, Feuchtbiotope, Mülldeponien, Stauwasserböden sowie limnische und marine Sedimente. Nach Schätzungen werden 10–20% des in Böden und Sedimente eingetragenen organischen Materials zu Methan reduziert. In marinen anoxischen (sauerstofffreien) Sedimenten entstehen so 85–300 Tg Methan pro Jahr (Conrad, 2009).

Methan ist der häufigste Kohlenwasserstoff in der Atmosphäre und spielt eine entscheidende Rolle in der atmosphärischen Energiebilanz. Aufgrund seiner Eigenschaft, Infrarotstrahlung zu absorbieren, ist Methan ein wichtiges Treibhausgas (Lacis et al., 1981; Ramanathan et al., 1985). Die durch Landwirtschaft und Förderung fossiler Energieträger freigesetzten Methanmengen tragen daher signifikant zur anthropogen bedingten globalen Klimaerwärmung bei. Die photochemische Oxidation von Methan und dessen Abbau durch Mikroorganismen begrenzen jedoch die Methankonzentration in der Atmosphäre. Methan wird von zahlreichen Mikroorganismen als alleiniges organisches Wachstumssubstrat verwertet, und zwar nicht nur aerob, sondern auch anaerob. Weil Methan als einfachster und stabilster Kohlenwasserstoff eine besonders niedrige chemische Reaktivität hat, erfordert dessen Verwertung besondere Aktivierungsmechanismen. Diese sind auch von angewandtem Interesse, da Methan industriell nur unter extremen Bedingungen aktiviert bzw. funktionalisiert werden kann (Arndtsen et al., 1995).

I.1. Methanogene Archaeen und Methanogenese

Methan ist ein Stoffwechselendprodukt einer metabolisch spezialisierten Gruppe von Mikroorganismen, die ihre Energie für das Wachstum obligat über die Bildung von Methan beziehen. Diese Mikroorganismen werden Methanogene genannt und gehören zum Phylum der Euryarchaeota innerhalb der Domäne Archaea. Methanogene lassen sich phylogenetisch (basierend auf dem 16S rRNA Gen) in 5 Ordnungen unterteilen: Methanobacteriales, Methanopyrales, Methanococcales, Methanomicrobiales und Methanosarcinales (Abb. 1).

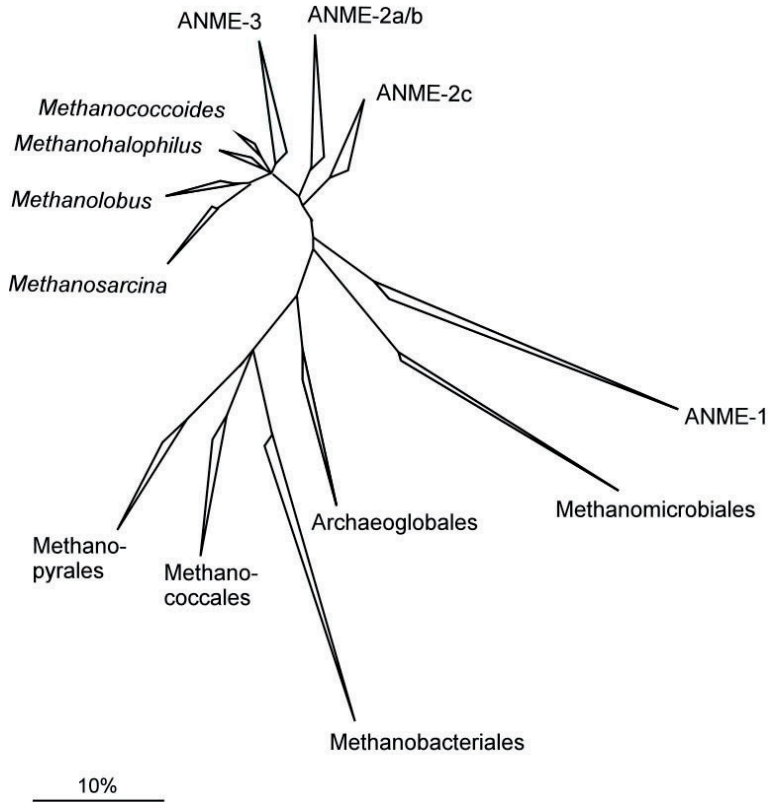

Abbildung 1. Phylogenie (Stammbaum) methanogener und methanotropher Archaeen basierend auf 16S rRNA Gen Sequenzierung. Der Balken entspricht 10% geschätzte Sequenzunterschiede (modifiziert nach Knittel & Boetius, 2009).

Methanogene Archaeen verwerten nur eine geringe Zahl von Substraten. Methan wird entweder durch Reduktion von Kohlendioxid oder aus Methylgruppen gebildet (Thauer et al., 2008). Einfache Elektronendonatoren wie Wasserstoff (H_2), Kohlenmonoxid (CO), Formiat ($HCOO^-$) und einige Alkohole (Ethanol, Isopropanol) werden oxidiert, um Kohlendioxid (CO_2, im neutralen Milieu überwiegend HCO_3^-) zu Methan zu reduzieren. Die Verwertung von H_2 zur Reduktion von CO_2 (hydrogenotrophe Methanogenese, (1)) ist der am weitesten verbreitete Stoffwechselweg innerhalb der Methanogenen und wird in Vertretern aller 5 Ordnungen gefunden:

$$4\ H_2 + HCO_3^- + H^+ \rightarrow CH_4 + 3\ H_2O;\ \Delta G° = -136\ \text{kJ mol}^{-1} \qquad (1).$$

Bei der acetotrophen (auch acetoklastischen) Methanogenese (2) wird Acetat (CH_3COO^-) disproportioniert:

$$CH_3COO^- + H_2O \rightarrow CH_4 + HCO_3^-;\ \Delta G° = -31\ \text{kJ mol}^{-1} \qquad (2).$$

Die Methylgruppe des Acetats wird zu CH_4 reduziert und die dafür notwendigen Elektronen werden durch die Oxidation der Carboxylgruppe zu CO_2 bereitgestellt. Das Schlüsselenzym ist ein Komplex aus Acetyl-CoA-Synthetase und Kohlenmonoxid-Dehydrogenase (Acs/CODH). Nach der ATP-abhängigen Anlagerung von Coenzym A an Acetat wird die Acetyl C-C Bindung durch Acs/CODH gespalten. Die Methylgruppe des Acetats wird dann auf Tetrahydrosarcinapterin (H_4SPT) übertragen und nachfolgend zu CH_4 reduziert (Hedderich & Whitman, 2006).

Im Gegensatz dazu wird bei der Verwertung von Methanol (CH_3OH, (3)), Methylaminen (CH_3NH_2) oder Dimethylsulfid ($(CH_3)_2S$) die Methylgruppe disproportioniert:

$$4\ CH_3OH \rightarrow 3\ CH_4 + HCO_3^- + H_2O + H^+;\ \Delta G° = -105\ kJ\ mol^{-1}\ CH_4 \qquad (3).$$

Entgegen der hydrogenotrophen Methanogenese ist die Verwertung von Methylgruppen auf wenige Vertreter der Ordnung Methanosarcinales beschränkt. Ausschließlich Angehörige dieser Ordnung sind zur acetotrophen CH_4-Produktion fähig. Ein Sonderfall bei der Verwertung von Methylgruppen ist *Methanosphaera* spp. aus der Ordnung Methanobacteriales. Dieser benötigen für die Reduktion von Methanol H_2 (Thauer et al., 2008):

$$CH_3OH + H_2 \rightarrow CH_4 + H_2O;\ \Delta G° = -112\ kJ\ mol^{-1} \qquad (4).$$

Aufgrund ihres eingeschränkten Substratspektrums sind Methanogene nicht in der Lage, tote Biomasse direkt in Methan zu überführen. Der Abbau von Biomasse zu Methan (und CO_2) ist ein komplexes Zusammenspiel von primären anaeroben Abbauern (Gärern), syntrophen Bakterien und methanogenen Archaeen. Dabei folgt die Umwandlung komplexer Biopolymere unter anoxischen Bedingungen einer trophischen Kaskade (Nahrungskette); Polymere wie Polysaccharide oder Proteine werden über Zucker bzw. Aminosäuren zu H_2, CO_2, Acetat, Propionat, Butyrat und Alkoholen (wie Ethanol) umgewandelt. H_2, CO_2 und Acetat werden direkt von methanogenen Archaeen verwertet. Die anderen Produkte werden durch sekundäre Fermentierer (syntrophe Bakterien) zu Acetat, H_2 und CO_2 umgesetzt und so für die methanogenen Archaeen zugänglich gemacht. Auch homoacetogene Bakterien können an diesem Kreislauf beteiligt sein, welche in der Lage sind aus H_2 und CO_2 Acetat zu bilden. Umgekehrt kann Acetat auch durch syntrophe Bakterien zu H_2 und CO_2 umgesetzt werden (Zinder, 1993; Schink, 1997; Abb. 2).

Unabhängig von ihrem Substrat nutzen alle methanogenen Archaeen das Schlüsselenzym Methyl-Coenzym M-Reduktase (MCR), um Methan freizusetzen. Die MCR katalysiert die exergone Umwandlung von Methyl-Coenzym M (CH_3–S–CoM) und

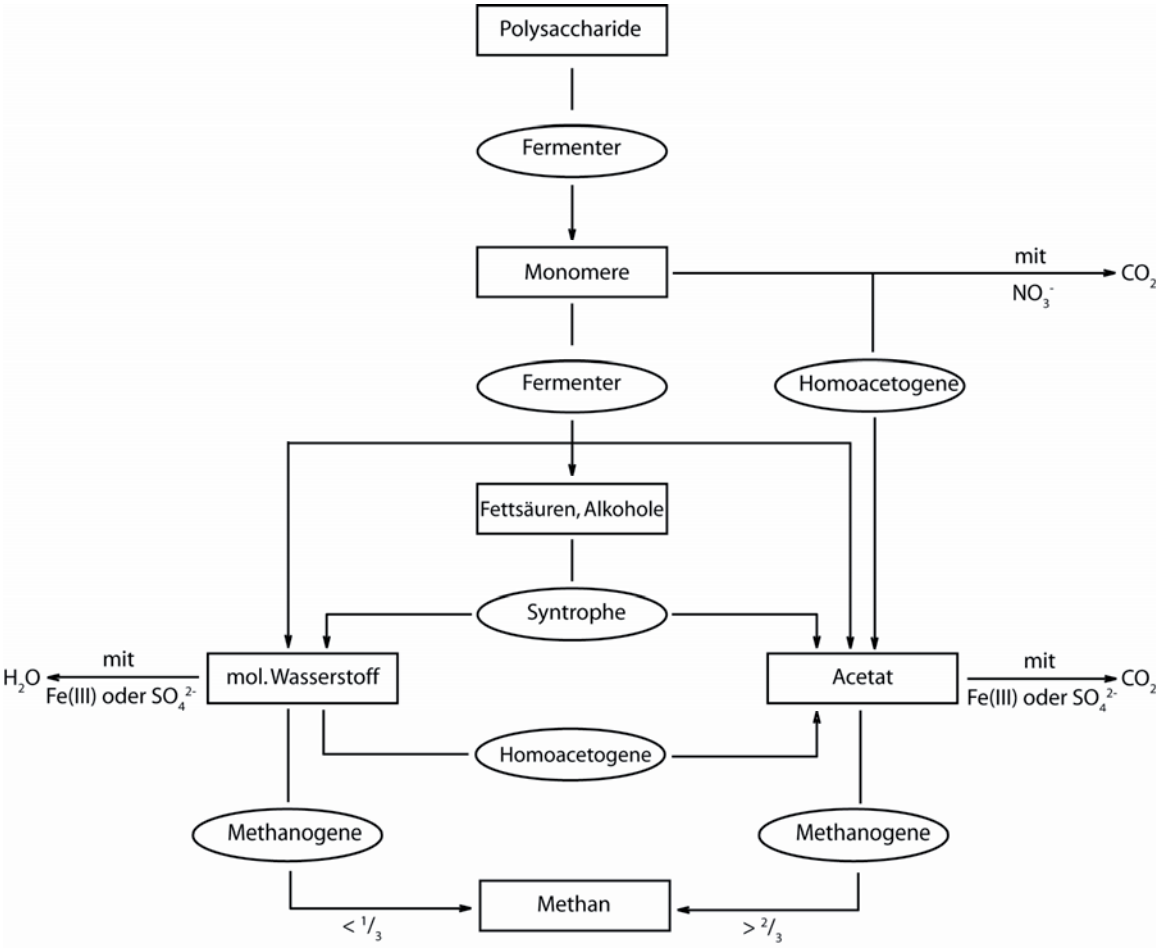

Abbildung 2. Mögliche Stoffwechselwege der anaeroben Oxidation komplexen organischen Materials bis zum Methan. Zwischenprodukte (Intermediate) in Vierecken, beteiligte Mikroorganismen in Ovalem (modifiziert nach Conrad, 2007).

Coenzym B (HS–CoB) zu Methan und dem Hetereodisulfid CoM–S–S–CoB (Hedderich & Whitman, 2006):

$$CH_3\text{–}S\text{–}CoM + HS\text{–}CoB \rightarrow CH_4 + CoM\text{–}S\text{–}S\text{–}CoB;\ \Delta G^\circ = -30\ \text{kJ mol}^{-1} \quad (5).$$

Die Energiekonservierung erfolgt durch Reduktion der Heterodisulfidbindung. Dabei unterscheiden sich methanogene Archaeen in der Form der Nutzung dieser Bindung. Methanosarcinales nutzen die Energie, indem mittels eines membranständigen Enzymkomplexes aus Heterodisulfid-Reduktase (HdrDE) und einer Hydrogenase (VhoACG) ein Ionengradient generiert wird. Die Reduktionsäquivalente aus der Oxidation des Wasserstoffs werden über Cytochrome auf ein redox-aktives Phenazin (Methanophenazin) übertragen. Methanophenazin ist dann der Elektrondonor für die Reduktion des Heterodisulfides (Hedderich et al., 1998). Methanogene der anderen vier Ordnungen besitzen

weder Cytochrome, Phenazine noch eine HdrDE. Die Reduktion des Disulfids erfolgt dabei mittels eines cytoplasmatischen Multienzymkomplexes bestehend aus einer Hydrogenase (MvhADG) und einer löslichen Heterodisulfid-Reduktase (HdrABC). Der Mechanismus der Regeneration reduziertem Ferredoxins könnte dabei einer Reaktion analog zum Butyryl-CoA-Dehydrogenase/Etf-Komplex-System aus *Clostridium kluyveri* folgen (Li et al., 2008; Thauer et al., 2008).

MCR kann auch als spezifisches Marker Gen zur phylogenetischen Charakterisierung der methanogenen Archaeen genutzt werden (neben dem 16S rRNA Genen, Abb.1). Das Gen, welches für die alpha-Untereinheit der MCR codiert (*mcrA*), ist hochgradig konserviert (Hallam et al., 2003). Vergleichende phylogenetische Studien haben gezeigt, dass Stammbaum-Topologien basierend auf 16S rRNA Genen und *mcrA* weitgehend konsistent sind (Springer et al., 1995; Lueders et al., 2001; vergleiche Abb. 1 & 3).

I.2 Methanotrophe Archaeen und anaerober Abbau von Methan

Erste Hinweise auf die anaerobe Oxidation von Methan mit Sulfat als terminalem Elektronenakzeptor (AOM) konnten mittels geochemischer Profile aus marinen Sedimenten gewonnen werden. Es wurde gezeigt, dass mit linearen Gradienten aus tieferen Sedimentschichten aufsteigendes Methan häufig in klar abgegrenzten Horizonten bei gleichzeitigem Umsatz von Sulfat aufgebraucht wurde (Methan-Sulfat-Übergangszonen) (Martens & Berner, 1974; Barnes & Goldberg, 1976; Reeburgh, 1976). Daraufhin wurde eine Kopplung der Methanoxidation an die Sulfatreduktion postuliert:

$$CH_4 + SO_4^{2-} \rightarrow HCO_3^- + HS^- + H_2O;\ \Delta G^\circ = -16{,}6\ \text{kJ mol}^{-1} \qquad (6).$$

Die Kopplung von Methanoxidation und Sulfatreduktion in einer 1:1 Stöchiometrie konnte durch Einsatz radioaktiver Isotopenmarkierung des Methans ($^{14}CH_4$) und Sulfats ($^{35}SO_4^{2-}$) bestätigt werden. In der Methan-Sulfat-Übergangszone zeigten die Raten der CH_4 -oxidation und der Sulfatreduktion distinkte Maxima (Reeburgh, 1980; Devol, 1983; Iversen & Jørgensen, 1985). Zehnder und Brock (1979, 1980) untersuchten AOM *in vitro,* indem sie verschiedene methanogene Kulturen und Sedimente mit $^{14}CH_4$ inkubierten und das gebildete $^{14}CO_2$ bestimmten. Dabei wurde ein Transfer von markiertem Kohlenstoff aus dem CH_4 in den CO_2-Pool nachgewiesen, jedoch machte dieser nur einen geringen Teil des gleichzeitig produzierten Methans aus. Es wurde keine Netto-AOM gefunden. Diesen Experimenten folgend wurde als Mechanismus der AOM eine syntrophe Kooperation von mindesten zwei

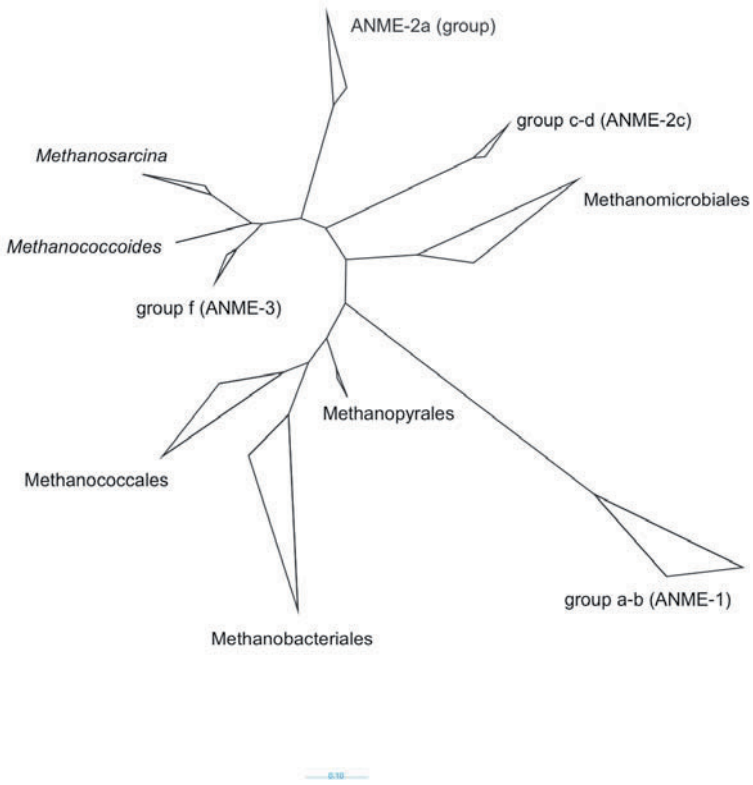

Abbildung 3. Phylogenie methanogener und methanotropher Archaeen basierend auf vergleichender *mcrA*-Sequenzanalyse (modifiziert nach Knittel & Boetius, 2009).

Mikroorganismen vorgeschlagen. Methanotrophe Archaeen aktivieren demnach das Methan und ein nicht näher bezeichnetes Intermediat dient den Sulfat-reduzierenden Bakterien als Elektronendonor. Weitere Untersuchungen von Hoehler et al. (1994) an marinen Sedimenten bekräftigten diese Theorie. Durch Zugabe eines spezifischen Inhibitors der Methanogenese (Bromoethansulfonat) konnte die Methanoxidation gehemmt werden, wohingegen die Zugabe von Sulfat AOM stimulierte. Als Intermediat zwischen den an der AOM beteiligten Organismen wurde molekularer Wasserstoff vorgeschlagen. Aufgrund der geringen freien Energie der AOM Reaktion ($\Delta G° = -16{,}6$ kJ mol^{-1} (6)) war jedoch unklar, ob die AOM-Aktivität das Wachstum beide Partner unterstützen kann. Aufgrund zunehmender geochemischer Indikatoren für die weltweite Verbreitung der AOM (zusammengefasst in Reeburgh, 2007), wurden Versuche zur Isolierung der methanotrophen Organismen unternommen, indem Methan als alleinige Energie- und Kohlenstoffquelle in anoxischen Inkubationen eingesetzt wurde (Valentine & Reeburgh, 2000), jedoch ohne Erfolg. Der erste direkte Hinweis für die Existenz anaerober methanotropher Organismen wurde durch Hinrichs et al. (1999) erbracht. Aus Methan emittierenden marinen Sedimenten des Eel River Beckens konnten Archaeen-spezifische Lipidbiomarker extrahiert werden. Die

Tetraetherlipide, Archaeol und sn-2-Hydroxyarchaeol, ähnelten denen aus anderen marinen anoxischen Methan-reichen Sedimenten (Elvert et al., 1999; Pancost et al., 2000) und waren strukturell identisch mit denen kultivierter Methanogener der Ordnung Methanosarcinales. Die archaeellen Lipide zeigten sehr leichte Kohlenstoffisotopien ($\delta^{13}C < -100‰$ vs. PDB). Nur die Nutzung von Methan, das am Standort ähnlich stark ^{13}C-abgereicherte Isotopiewerte (s. Abschnitt I.3) zeigte, kam als Kohlenstoffquelle für den Aufbau dieser Lipide in Frage. Eine parallele phylogenetische Analyse der 16S rRNA Gene aus Sedimentproben des Eel River Beckens zeigte das Vorkommen einer neuartigen archaeellen phylogenetischen Gruppe, nahe verwandt mit Methanogenen der Ordnungen Methanomicrobiales und Methanosarcinales. Es wurde daher vorgeschlagen, dass eine eigene, den methanogenen Archaeen verwandte Gruppe anaerob methanotropher Archaeen (ANME) die AOM katalysiert (Hinrichs et al., 1999; Abb.1). Der nächste Schritt zum Nachweis der Beteiligung von ANME an der AOM erfolgte durch deren visuelle Identifizierung *via* Mikroskopie und Fluoreszenz *in situ* Hybridisierung (FISH). Dazu wurden ANME-spezifische, an die rRNA bindende, Fluorochrom markierte Oligonukleotidsonden eingesetzt (Boetius et al., 2000). Es wurde gezeigt, dass in AOM-aktiven Sedimenten vom Hydratrücken (vor der Küste Oregons, Pazifischer Ozean) Aggregate aus ANME und Sulfat-reduzierenden Bakterien (SRB) dominieren. Die Zellen in den Konsortien repräsentierten >90% der gesamten mikrobiellen Gemeinschaft. Diese Ergebnisse stützten die Hypothese von Hoehler et al. (1994), nach der Methan syntroph in Kooperation von methanotrophen Archaeen und Sulfat-reduzierenden Bakterien abgebaut wird. *In vitro* Experimente mit solchen natürlichen ANME angereicherten Sedimenten konnten die Kopplung von Methanoxidation und Sulfatreduktion (gemäß Formel 6) bestätigen (Nauhaus et al., 2002). Der direkte Beweis für die Beteiligung der ANME Konsortien an der AOM erfolgte durch Kombination von FISH und Sekundärionen-Massenspektroskopie (SIMS). Es wurde gezeigt, dass die Biomasse der ANME/SRB-Konsortien extrem ^{13}C abgereichert war (Orphan et al., 2001, 2002). Dies ließ sich nur durch Inkorporation leichten Methans erklären und bestätigte vorherige Biomarkeranalysen von Hinrichs und Mitarbeitern (1999). Inzwischen konnten die ANME/SRB-Konsortien überall dort nachgewiesen werden, wo unter Ausschluss von Sauerstoff Methan und Sulfat gemeinsam vorkommen. Zu solchen Habitaten zählen kalte marine Methan-Quellen (cold seeps), Sulfat-Methan-Übergangszonen, hydrothermale Quellen, anaerobe Meerwasser-schichten und verschiedene terrestrische Habitate (Übersicht in Knittel & Boetius, 2009). Durch Visualisierung der AOM-Konsortien konnte gezeigt werden, dass diese entweder aus nur sehr wenigen Zellen bestehen (Orphan et al., 2002; Knittel et al., 2005; Schreiber et al.,

2010) oder auch zu eine der dichtesten und größten Zellakkumulationen heranwachsen können, die bisher in der Natur gefunden wurden (Michaelis et al., 2002). Drei distinkte Gruppen von ANME (ANME 1–3; Abb. 1) wurden aus marinen und terrestrischen Habitaten mittels 16S rRNA Gen-Charakterisierung identifiziert. ANME-1 ist entfernt verwandt mit Methanogenen der Ordnungen Methanomicrobiales und Methanosarcinales, während sich ANME-2 und ANME-3 deutlich den Methanosarcinales zuordnen lassen (Boetius et al., 2009). Eine vierte Gruppe („AOM-associated archaea“, AAA) wurde in AOM aktiven Frischwasser-Anreicherungen gefunden, welche Nitrat und Nitrit anstelle von Sulfat als finalen Elektronenakzeptor nutzten (Raghoebarsing et al., 2006). Es wurde jedoch kürzlich gezeigt, dass Nitrit-reduzierende Bakterien (NC10-Phylum) die AOM ohne Beteiligung der Archaeen katalysieren (Ettwig et al., 2008; Ettwig et al., 2009; Ettwig et al., 2010).

Weitere Unterstützung der phylogenetischen Zuordnung von ANME zu den methanogenen Archaeen lieferten molekularbiologische und biochemische Untersuchungen. Für ANME-1 konnte gezeigt werden, dass diese fast alle Gene der hydrogenotrophen Methanogenese in ihrem Genom tragen (Hallam et al., 2003; Hallam et al., 2004; Meyerdierks et al., 2005; Meyerdierks et al., 2010). Dies konnte kürzlich auch für ANME-2 bestätigt werden (Pernthaler et al., 2008). Allen ANME-Gruppen konnten jedoch bisher unbekannte *mcrA*-Sequenzen zugeordnet werden (Abschnitt I.1), welche auch als phylogenetischer Marker verwendet werden (Abb. 3). Das obligate Vorhandensein der MCR in allen bisher bekannten ANME bekräftigt die Vermutung, dass die Aktivierung des Methans in der sulfatabhängigen AOM eine Umkehrung des finalen Schrittes der Methanbildung ist und durch die MCR katalysiert wird. Biochemische Untersuchungen an hoch aktiven AOM-Biofilmen aus dem Schwarzen Meer unterstützen diese Vermutung (Krüger et al., 2003). Die Biofilme waren von ANME/SRB-Aggregaten dominiert und enthielten große Mengen eines MCR-ähnlichen Nickelproteins (Nickelprotein I), welches bis zu 7% des Gesamtproteins ausmachte. Das MCR-Homolog unterschied sich jedoch von dem methanogener Archaeen durch dessen größere Masse von 951 Da (anstelle von 905 Da; Krüger et al., 2003) und trägt als weitere Modifikation eine zusätzliche Methylthiolgruppe (Mayr et al., 2008). Es wurde spekuliert, dass diese Modifikationen eine Anpassung der MCR an AOM darstellt. Jedoch wurde ein weiteres abundantes MCR-Homolog aus den Schwarzmeermatten isoliert (Nickelprotein II, 3% des Gesamtproteins), welches diese Modifikationen nicht zeigte (Krüger et al., 2003). Dieses wurde den ANME-2 Archaeen zugeordnet (Thauer & Shima, 2008). Immunologische Studien mit Antikörpern gegen MCR an den AOM-aktiven Biofilmen aus dem Schwarzen Meer konnte die Expression der MCR in ANME-1 und ANME-2 Zellen

bestätigen (Heller et al., 2008; Milucká et al., in Vorbereitung). Es wurden gleiche Wirkmechanismen für die Methanaktivierung durch die MCR vorgeschlagen wie für deren Methanfreisetzung, lediglich die Richtung der Reaktion ist umgekehrt (Krüger et al., 2003). Dabei werden hauptsächlich zwei Mechanismen diskutiert: Ein Angriff des Thiylradikals (Coenzym B Radikal) direkt an CH_4 (Krüger et al., 2003), als auch eine Reaktion des Cofaktors F_{430} in seiner oxidierten Form mit Ni(III), welches stark elektrophil wirkend zu der Bildung eines Ni(III)-Methyl-Übergangszustands führt (Ragsdale, 2007; Shima & Thauer, 2005; Thauer & Shima, 2008, Abb. 4). In ihrer Funktion der Methanaktivierung sind jedoch beide Mechanismen aus energetischer Sicht problematisch. Daher wurde für den zweiten Mechanismus die weitere Beteiligung eines Ni(III)-Hydrids vorgeschlagen (Harmer et al., 2008), welches aus der anorganischen Chemie für die Aktivierung von Alkanen von Bedeutung ist (Shilov & Shul'pin, 1997).

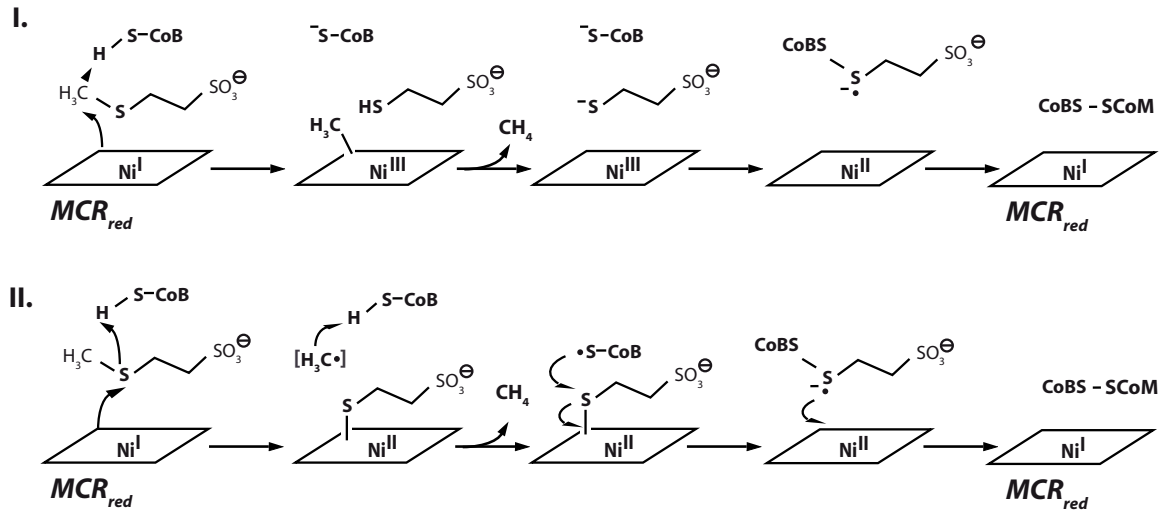

Abbildung 4. Vorgeschlagene Reaktionsmechanismen der Methyl-Coenzym M-Reduktase in der Aktivierung von Methan. In Mechanismus I. entsteht ein Methyl-Ni (III)-Intermediat, während bei Mechanismus II ein Methyl-Radikal entsteht. Modifiziert nach Ragsdale (2007).

Entgegen ihrer hohen Abundanz in natürlichen Habitaten zeigen ANME/SRB-Konsortien selbst unter optimierten Laborbedingungen ein sehr langsames Wachstum und die geringsten Wachstumserträge für mikrobielle Oxidation von organischen Substraten (Nauhaus et al., 2007). Die Wachstumserträge von SRB mit unterschiedlichsten organischen Substraten liegen zwischen 4 und 18 g Trockenbiomasse pro Mol Sulfat (Widdel, 1988; Rabus et al., 2000), abhängig vom jeweiligen Energiegehalt des Elektronendonors (Substrats). Bei der AOM hingegen betragen Wachstumserträge weniger als 1 g Trockenbiomasse pro Mol reduziertem Sulfat. Dies wird dadurch begründet, dass AOM einer der am wenigsten exergonen Prozesse ist (6), welches Leben noch aufrechterhalten kann (Nauhaus et al., 2007;

Wegener et al., 2008). Dieser energetische Aspekt kann Auswirkungen u.a auf enzymatische (katabole) Reversibilitäten und die Interpretation von Isotopenanalysen in AOM haben.

I.3 Fraktionierung stabiler Isotope

Isotopen-geochemische Untersuchungen haben bisher entscheidend zum Verständnis der Bildung und des Abbaus von Methan beigetragen. So können mithilfe der Kohlenstoff- und Wasserstoffisotopien ($^{13}C/^{12}C$, D/H) mikrobiell (biotisch) und thermogen (abiotisch) gebildetes Methan voneinander unterschieden werden. Solche Untersuchungen belegen eine überwiegend mikrobielle Herkunft des weltweiten Methans (Whiticar, 1999; Reeburgh, 2007; Conrad, 2009).

Isotopische Analysen basieren auf chemische-physikalischen Grundprinzipien: Atome gleicher Protonenzahl (Kernladungszahl) werden einem Element zugeordnet. Viele Elemente setzen sich jedoch aus Teilchen unterschiedlicher Atommassen zusammen, was in der Variabilität der Anzahl von Neutronen, den ungeladenen Kernbausteinen, begründet ist. Die unterschiedlichen Massen eines Atoms werden als Isotope bezeichnet (griech. iso topos; gleicher Ort [im Periodensystem der Elemente]). Die Isotope eines Elements können entweder stabil sein oder sich durch radioaktiven Zerfall in Tochterisotope verwandeln (Radioisotope). Stabile Isotope liegen in unserem Sonnensystem meist in sehr eng definiertem Verhältnis vor. Größere Unterschiede im Isotopenverhältnis lassen meist Rückschlüsse auf Herkunft außerhalb unseres Sonnensystems zu. Innerhalb eines abgegrenzten Systems verursachen die leichten Unterschiede in den physikalischen Eigenschaften der verschiedenen Isotope (u.a. Dampfdruck, Phasenübergängen, chemischen Reaktionskinetik), leichte Fraktionierungen (unterschiedliche Isotopenverhältnisse) in den verschiedenen Pools. Dieser Fraktionierungs-effekt wird genutzt, um Quellen oder Senken natürlich vorkommender Substanzen nachzuweisen und um chemische Umsätze von Molekülen nachzuvollziehen. Dabei wird der Umstand genutzt, dass schwerere Isotope eines Elements und die aus ihnen aufgebauten Moleküle reaktionsträger sind und langsamer diffusiv transportiert werden. So verbleiben bei einer chemischen Reaktion die schwereren Isotope sowie die aus ihnen aufgebauten Moleküle häufiger im Reaktanten-Pool oder in einem Mehrphasensystem häufiger in der Flüssig- als in der Gasphase. Besonders ausgeprägt ist der kinetische Isotopeneffekt in biologischen Reaktionen, die meist als eine Abfolge physikalischer und enzymatisch katalysierter chemischer Prozesse bei geringen Temperaturen ablaufen.

Das Verhältnis von schwerem zu leichtem Isotop in einem Element oder Molekül kann durch den Faktor *R* beschrieben werden (*R* = [schweres Isotop]/ [leichtes Isotop]). Da

die Schwankungen in der Isotopie eines Elements in verschiedenen Pools meist sehr gering sind, werden zur besseren Unterscheidbarkeit Delta-Notationen verwendet, welche die Abweichungen zu einem Standardisotopenverhältnis beschreiben:

$$\delta = (R_{Probe}/R_{Standard} - 1) \times 1000‰. \quad (7).$$

Für die meisten Elemente ist die Isotopenfraktionierung innerhalb einer Reaktion (R→P; Reaktant, Produkt) über den Fraktionierungsfaktor α definiert:

$$\alpha_{R/P} = R_R/R_P = (\delta_R + 1000‰) / (\delta_P + 1000‰) \quad (8).$$

Über α kann die isotopische Anreicherung in einem Substrat (Reaktant) oder auch die isotopische Veränderung im Reaktionsprodukt ermittelt werden. Da α meist sehr nahe an 1 liegt, wird neben α auch der Faktor ε ermittelt:

$$\varepsilon_{R/P} = (\alpha - 1) \times 1000‰. \quad (9).$$

Große Mengen stark ^{13}C-abgereicherten anorganischen Kohlenstoffs in marinen Porenwässern und authigenen Carbonaten zeigen die Bedeutung der anaeroben Oxidation von Methan im Kohlenstoffkreislauf sowohl heute sowie in der geologischen Geschichte der Erde auf (Whiticar, 1999; Reeburgh, 2007). Durch das Auffinden noch stärker ^{13}C-abgereicherter, der Gruppe der Archaeen zuzuordnender Membranlipide konnten die ANME-Organismen erstmals identifiziert werden (Elvert et al., 1999; Hinrichs et al., 1999, Abschnitt I.2).

Bei der aeroben Oxidation von Methan wie auch bei der Methanogenese, also dem der anaeroben Methanoxidation physiologisch nahestehendem Prozess, konnten Isotopenfraktionierungsfaktoren für verschiedene Substrate kalkuliert werden (indirekt wie auch direkt). Stets wurde eine bevorzugte Umsetzung der leichteren Moleküle ($^{12}CH_4$, $^{12}CO_2$, ^{12}C-Acetat etc. anstelle der ^{13}C-Isotopologe) gefunden. Die Untersuchung der Isotopenfraktionierungsfaktoren der anaeroben Methanoxidation beschränkte sich jedoch bisher auf indirekte Felduntersuchungen an marinen Porenwässern und die *in vitro* Fraktionierungsfaktoren der AOM waren vor dieser Arbeit nicht bekannt.

II. Zielsetzung der Arbeit und Ergebnisse im Überblick

II.1 Wissensstand und Zielsetzung

Die Aufgabe dieser Arbeit war die Optimierung von Anreicherungsmethoden und die Bereitstellung sedimentfreier Anreicherungen anaerober methanotropher Organismen. Diese sollte zur biochemischen Charakterisierung der anaeroben Oxidation von Methan genutzt werden, besonders hinsichtlich der Fraktionierungsfaktoren des Prozesses „*in vitro*".

Dabei wurden aus vorherigen Beobachtungen folgende Fragestellungen erarbeitet, die als Grundlage für diese Arbeit dienten:

- *An den bisher untersuchten AOM-Standorten werden unterschiedliche ANME-Gruppen festgestellt, jedoch konnte bisher keine Erklärung der Verteilungsmuster erarbeitet werden. Außerdem lag zu Beginn dieser Arbeit nur eine sedimentfreie AOM-Anreicherung vor.*

  Welche unterschiedlichen methanotrophen Stämme können von den unterschiedlichen Standorten angereichert werden und wie unterscheiden sich diese in ihren physiologischen Eigenschaften?

- *In AOM-dominierten Sedimenthorizonten zeigt das residuale Methan eine schwerere Isotopensignatur (Anreichung der Isotope ^{13}C und D gegenüber ^{12}C und H).*

  Welcher Isotopeneffekt im Kohlenstoff und Wasserstoff begleitet die anaerobe Oxidation des Methans unter Laborbedingungen – und kann dieser Isotopeneffekt die in marinen Sedimenten gefundenen Isotopen-fraktionierungen erklären?

- *In AOM-aktiven Sedimenthorizonten wurden mittels Tracerversuchen mehrfach parallele Produktion und Oxidation von radioaktiv markiertem Kohlenstoff des Methan bzw. Kohlendioxids beobachtet. Dies wurde bisher vor allem auf gleichzeitige Aktivität methanogener und methanotropher Populationen zurückgeführt. Dagegen zeigen Studien biologischer Reaktionen nahe dem thermodynamischen Gleichgewicht die Möglichkeit einer substantiellen enzymatischen Rückreaktion, welche ebenfalls Ursächlich für den Austausch von Produkt und Substrat-Pool seien kann.*

Kann während der anaeroben Oxidation von Methan und der begleitenden Sulfatreduktion ebenfalls ein Rückreaktionseffekt beobachtet werden? Welches Ausmaß hat diese Rückreaktion und welche Schlüsse lassen sich daraus auf natürliche Schwefel- und Kohlenstoffinventare AOM-dominierter Sedimenthorizonte ziehen?

- *Bisher konzentrierte sich die AOM-Forschung zumeist auf kalte methanreiche marine Standorte. Erste Untersuchungen von methanreichen terrestrisch Schlammvulkanen und eines marinen hydrothermalen Standortes ergaben Hinweise auf weitere Habitate mit mikrobieller anaeroben Oxidation von Methan.*

  Welche methanotrophen Mikroorganismen dominieren terrestrische Schlammvulkane und hydrothermale Quellen und unter welchen Bedingungen lassen sich diese Organismen anreichern?

II.2 Überblick der erzielten Ergebnisse

II.2.1 Kultivierung Detritus-freier Anreicherungen

Die Studien von Nauhaus und Kollegen (2002, 2005, 2007) zeigten erste Erfolge in der Kultivierung anaerober methanotropher Organismen. Im Verlauf dieser Arbeit wurde die Langzeitinkubation zur Anreicherung anaerober methanotropher Mikroorganismen verschiedener Standorten optimiert. Dazu wurden die Kulturen mit Methan und Sulfat als alleiniges Substrat inkubiert. Die Aktivität der Organismen wurde dabei über die Bestimmung der Sulfidkonzentration im überstehenden Medium vorgenommen. Bei erfolgreicher Aktivitätssteigerung wurde das Inokulum verdünnt und so eine stetige Anreicherung zu sedimentfreien Kulturen erzielt. Die Vorgehensweise ist in Abb. 5 skizziert. In diesen Studien wurden methanotrophe Organismen aller drei bisher bekannten Gruppen (ANME-1,-2,-3) von 8 verschiedenen Standorten (u.a. aus dem Mittelmeer, dem Schwarzen Meer, der Nordsee, arktischen Schlammvulkanen, hydrothermalen Quellen) teilweise bis zur Sedimentfreiheit angereichert. Beispielsweise nahm die Aktivität der Organismen aus hydrothermalen Sedimenten des Guaymas Beckens innerhalb von 7 Monaten von 3 auf 23 µmol $g_{Trockengewicht}^{-1}$ d^{-1} zu (Abb. 5 rechts). Für AOM-Konsortien verschiedener Standorte konnten Verdoppelungszeiten von 2 bis 8 Monaten ermittelt werden.

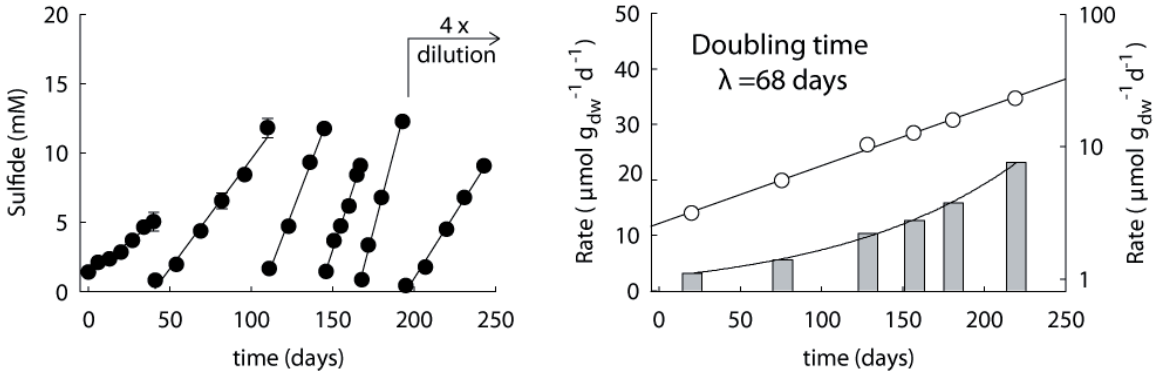

Abbildung 5. Links: Verlauf der Sulfidkonzentration in einer thermophilen (50 °C) AOM Anreicherung. Nach Anstieg der Sulfidkonzentration auf mehr als 10 mM wurde das Medium ausgetauscht. Nach 200 Tagen erfolgte eine Verdünnung um den Faktor 4.
Rechts: Anstieg der aus den Sulfidkonzentrationen berechneten Sulfatreduktionsraten über die Zeit (Balken); aus der halblogarithmischen Auftragung lässt sich die Verdopplungszeit der beteiligten Mikroorganismen kalkulieren (Kreise).

II.2.2 $^{13}C/^{12}C$ und D/H-Fraktionierung während der anaeroben Oxidation von Methan (AOM)

Auf der Auswertung von marinen Porenwasserprofilen und ersten Laborexperimenten basierenden Studien zeigten bisher widersprüchliche Isotopenfraktionierungen während der anaeroben Oxidation von Methan (Whiticar & Faber, 1986; Alperin et al., 1988; Martens et al., 1999; Seifert et al., 2006). In der vorliegenden Arbeit wurden mit den zuvor gewonnenen AOM-Anreicherungen Experimente zur Isotopenfraktionierung bei der AOM durchgeführt. In Batch-Experimenten wurden die Entwicklung der Methankonzentration und parallel die Isotopenverhältnisse des Kohlenstoffs ($^{13}C/^{12}C$) und Wasserstoffs (D/H) im residualen Methan gemessen (Abb. 6). Aus der Beziehung zwischen der Methanoxidation und der Isotopie des verbleibenden Methans ließen sich Fraktionierungsfaktoren für Kohlenstoff und Wasserstoff während der AOM für die verschiedenen AOM-Anreicherungen bestimmen (1.012–1.039 für $^{13}CH_4/^{12}CH_4$ und 1.109–1.315 für CDH_3/CH_4; ausführliche Erläuterungen in III.1). Diese waren signifikant größer als aus bisherigen Untersuchen von Isotopensignaturen aus marinen Porenwasserprofilen bekannt und zeigen mögliche Überlappung anderer Prozesse (u.a. Methanogenese) mit der AOM in natürlichen Systemen.

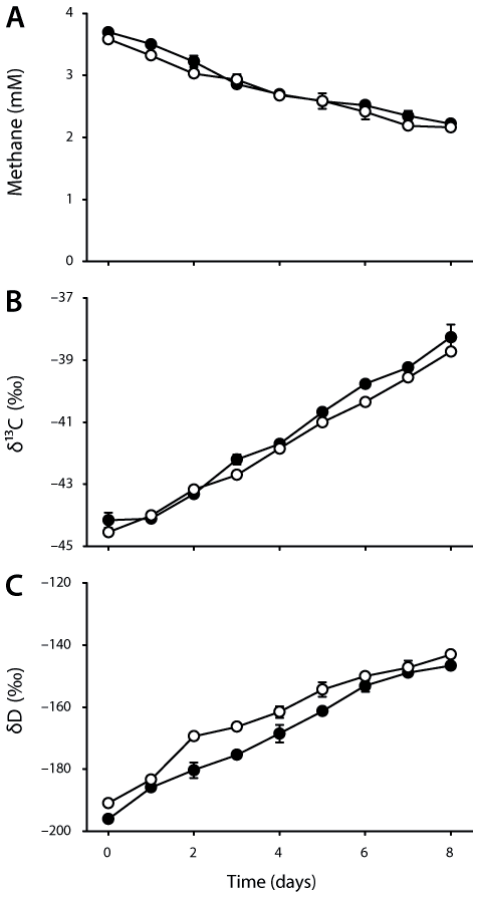

Abbildung 6. **A**. Zeitliche Entwicklung der Methankonzentration **B**. der Kohlenstoff- und **C**. der Wasserstoffisotopie im residualen Methan in einer AOM-Anreicherung vom Hydratrücken während einer achttägigen Inkubation.

II.2.3 Reversible Umsetzung von Kohlenstoff- und Schwefelverbindungen während der anaeroben Oxidation von Methan

Obwohl die anaerobe Oxidation von Methan zuerst direkt in marinen Habitaten entdeckt wurde, wurde diese experimentell in Kulturen methanogener Archaeen bestätigt, und zwar nicht als Nettoreaktion (Nettoumsatz von Methan), sondern als Nebenreaktion („Mini-AOM“, Rückreaktion) während der Methanogenese (Zehnder & Brock, 1979, 1980; Harder, 1997; Moran et al., 2005). Zur Überprüfung vorheriger Untersuchungen wurde in der vorliegenden Studie Versuche mit hoch aktiven AOM-Anreicherungskulturen unter Radioisotopen-markierung der Reaktionsprodukte (^{14}C-Carbonat und ^{35}S-Sulfid) durchgeführt. Nach unterschiedlichen Inkubationszeiten wurde die Veränderung der Konzentration (chemisch und radioaktiv) der Reaktanden und Produkte ermittelt. Aus den Verhältnissen der Pools zueinander konnten substantielle Rückreaktionen (Reversibilität) während der Oxidation des Methans als auch bei der gekoppelten Sulfatreduktion ermittelt werden, welche bis zu 13% der Nettoraten betrugen (Abb. 7). Die Rückreaktionen sind so ausgeprägt, dass diese in natürlichen Systemen zu einer signifikanten Durchmischung isotopischer Informationen von Produkt- und Reaktandenpools führen müssen und Auswirkungen auf die Interpretation solcher Messungen haben (ausführliche Erläuterungen in III.2).

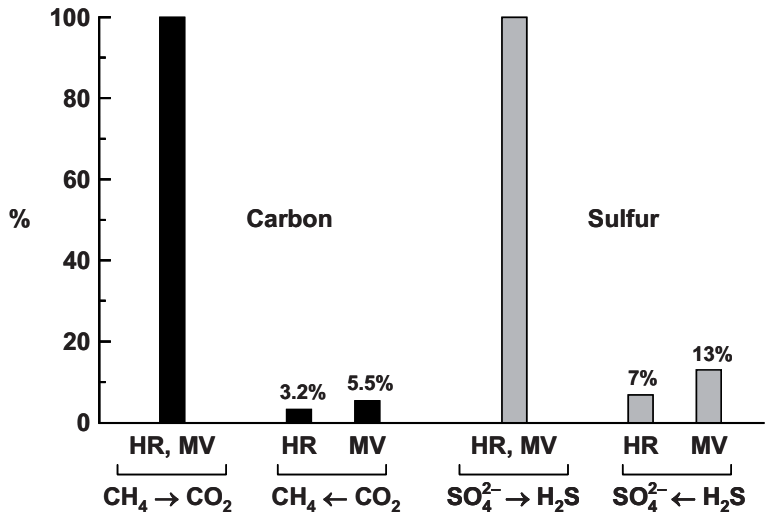

Abbildung 7. Verhältnis von Methanoxidations- und Sulfatreduktionsraten zu deren Rückreaktionen in den sedimentfreien Anreicherungen aus dem Hydratrücken (Hydrate Ridge, HR) und des Isis Schlammvulkans (MV).

II.2.4 Mikrobielle Untersuchungen der AOM an terrestrischen Methan-emittierenden Schlamm-Vulkanen

Bisher wurde die anaerobe Oxidation von Methan hauptsächlich in marinen Habitaten untersucht. In dieser Studie wurde an Sedimenten von Kohlenwasserstoff-emittierenden terrestrischen Schlammvulkanen (Paclele Mici, Karpaten, Rumänien) die anaerobe Oxidation von Methan, Methanogenese und methanabhängige Sulfatreduktion mittels Inkubation und Radioisotopenmarkierung nachgewiesen (Abb. 8). Untersuchungen der extrahierten und amplifizierten 16S rRNA Gene und Lipidanalysen zeigten zum ersten mal das Vorkommen von Mikroorganismen, die bis dahin nur in marinen Tiefseehabitaten zu finden waren und dort vermutlich als Konsortium die AOM katalysieren (ausführliche Erläuterungen in III.3). Dies war der erste Nachweis einer aktiven AOM-Gemeinschaft für ein nicht marines (terrestrisches) Habitat.

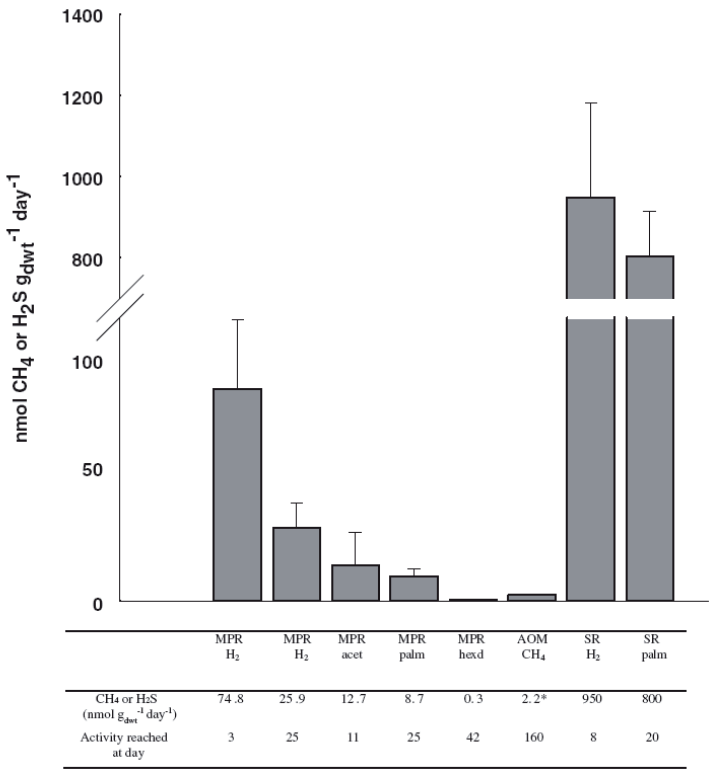

Abbildung 8. Mikrobielle Aktivität in Sedimenten eines terrestrischen Schlammvulkans ermittelt in Inkubationsexperimenten und mittels Radio-inkubationstechnik (*); Methanproduktion (MPR), anaerobe Methanotrophy (AOM) und Sulfatreduktion (SR).

II.2.5. Thermophile anaerobe Oxidation von Methan durch mikrobielle Konsortien

Die bisherigen Anreicherungen anaerober methanotropher Organismen wurden ausschließlich mit kalten marinen Sedimenten („cold seep sediments“, *in situ* Temperaturen von –1 bis 15 °C) begonnen. Dafür lag das Aktivitäts- und Wachstumsoptimum dieser AOM-Anreicherungen bei höchstens 20 °C. Ziel dieser Studie war die Anreicherung anaerober methanotropher Mikroorganismen bei höheren Temperaturen. Die hydrothermal geprägten Oberflächensedimente des Guaymas Beckens (Golf von Kalifornien) wurden schon mehrfach erfolgreich zur Anreicherung verschiedenener anaerober Mikroorganismen herangezogen (Kurr et al., 1991; Rueter et al., 1994; Khelifi et al., 2010). Wir konnten in diesen Sedimenten sulfatabhängige anaerobe methanotrophe Aktivität bis zu Temperaturen von 70 °C nachweisen (Abb. 9; ausführliche Erläuterungen in III.4).

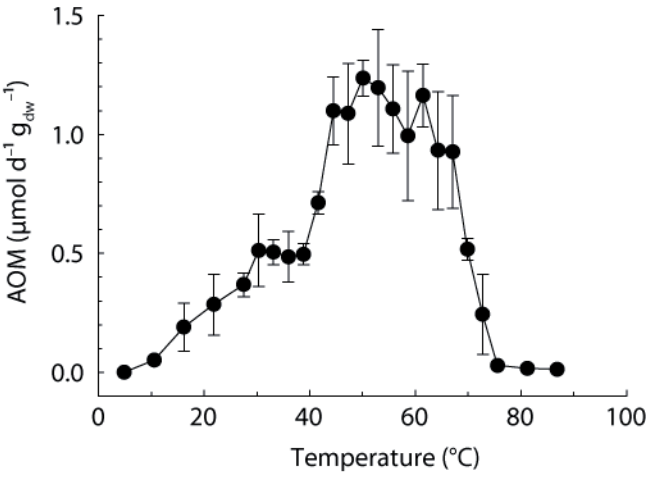

Abbildung 9. Raten der anaeroben Oxidation von Methan (AOM) in den Sedimenten des Guaymas Beckens innerhalb eines Temperaturgradienten von 4 bis 85 °C.

Eine optimale Anreicherung thermophiler AOM wurde bei 50 °C erziehlt. Die Anreicherungen wurden dominert von ANME-1 Archaeen und einem als Schwefel-reduzierenden bekannten verwandten bakteriellen Partnern. Dies ist die erste wachsende Anreicherung von Methanotrophen des ANME-1 Clusters. Die Ergebnisse dieser Studie lassen vermuten, dass die anaerobe Methanoxidation auch unter warmen bis heißen Bedingungen (bis 60 °C) in marinen Sedimenten eine entscheidende Senke von Methan darstellen kann.

II.3 Perspektiven weiterer AOM-Forschung

Die sulfatabhängige anaerobe Oxidation von Methan ist ein noch immer nicht vollständig verstandener Prozess. Die Interaktion der beteiligten Organismen konnte noch nicht aufgeklärt werden. Ein Schlüssel für das weitere Verständnis der AOM liegt in der Kultivierung und Isolierung der Methan-oxidierenden Archaeen und dem Sulfat-reduzierenden bakteriellen Partner. An solchen Kulturen könnten physiologische Experimente durchgeführt werden, die unter anderem die wechselseitige Beziehung der beteiligten Mikroorganismen aufzuklären helfen. Versuche zu Substratspektren des bakteriellen Partners könnten dabei das noch nicht identifizierte Intermediat (organisch/inorganisch) der vermeintlich syntrophen mikrobiellen Gemeinschaft identifizieren. Isolierungsstrategien könnten klassisch über Einzelzellentransfer (Verdünnungsserien nach Homogenisierung der Konsortien) oder über selektive Anreicherung („flow cytometry“) erfolgen.

In hoch angereicherten AOM-Kulturen, welche frei von Sedimentpartikeln sind und ausschließlich mit Methan und Sulfat als Substrate kultiviert werden, könnte mittels hochauflösender Mikroskopie die strukturelle Beziehung zwischen Archaeen und dem bakteriellen Partner untersucht werden. Ein zu klärender Aspekt ist u. a. das mögliche Vorhandensein von leitfähigen Strukturen (sog. nanowires), welche einen direkten Transfer von Reduktionsäquivalenten zwischen den Zellen vermitteln könnten. Dabei könnte auch die Untersuchung der Bedeutung von Cytochromen innerhalb der AOM-Konsortien von Bedeutung sein, da diese bei der direkten Übertragung von Elektronen eine wichtige Rolle übernehmen könnten.

Unklar ist auch noch der Umstand, warum alle bisherigen hochgradig angereicherten, sedimentfreien „cold seep“ AOM-Kulturen durch den Methanotrophen des Typs ANME-2 dominiert werden (mit Ausnahme einer ANME-3 dominierten Haakon Mosby Anreicherung; Holler, unveröffentlicht). Das Austesten der Methanaffinitäten (K_M-Wert für Methan) für verschiedene ANME (ANME 1–3) könnte helfen, die bisher ungeklärten Verteilungsmuster der verschiedenen Gruppen in marinen Sediment zu erklären und eine Korrelation zu den jeweiligen geochemischen Profilen verschiedener Habitate herzuleiten sowie weitere Isolierungsstrategien zu entwickeln.

Gelegentlich wird diskutiert, ob der Sulfat-reduzierende Partner der ANME-Archaeen durch Bakterien mit anderen Stoffwechselleistungen ersetzt werden kann. Das Austesten von alternativen Elektonenakzeptoren (u.a. Eisen(III), Mangan(IV bzw. III), div. Stickstoffspezies, halogene Verbindungen, verschiedene Schwefelverbindungen oder organische Säuren) und

die anschließende Kultivierung und Anreicherung der beteiligten Mikroorganismen könnten zum weiteren Verständnis der AOM beitragen.

Die AOM als eine, soweit bekannt, der am wenigsten exergonen katabolen Reaktionen ist ein idealer Modellprozess für das Austesten von enzymatischen Reversibilitäten. Wie in der vorliegenden Arbeit gezeigt werden konnte, ist die AOM von einem signifikanten „Rückfluss“ von markiertem Produkt zu seinem Substrat begleitet (CO_2 zu CH_4 und HS^- zu SO_4^{2-}). Ein solcher Austausch von Markierungen in verschiedene Pools sollte sich auch in anderen katabolen Reaktionen finden lassen, welche nahe dem thermodynamischen Gleichgewicht ablaufen. In marinen anoxischen Sedimenten sind viele mikrobiell katalysierte Prozesse substratlimitiert und somit thermodynamisch beinahe ausgeglichen. Auch solche Reaktionen sollten mit einer ausgeprägten Umkehrreaktion (Rückfluss) einhergehen. Diese Reversibilitäten sorgen für eine Durchmischung der verschiedenen Pools (Reaktanten und Produkte). Damit müsste auch die Isotopensignaturen der einzelnen Elemente durchmischt werden. Die Kenntnis der enzymatischen Reversibilitäten verschiedener metabolischer Prozesse (z.B. organoklastische Sulfatreduktion) kann klären, inwieweit diese Effekte in isotopenbasierten Bilanzierungen relevant sind und sich auf die Interpretation geochemischer Daten auswirkt.

Die Biomasse der hoch angereicherten sedimentfreien AOM aktiven -Anreicherungen kann genutzt werden, um mit metagenomischen, proteomischen und transkriptomischen Analysen die noch unbekannte Interaktion der beteiligten Mikroorganismen aufzuklären. Initiale Versuche zu proteomischen AOM-Analysen der Anreicherungen waren dabei vielversprechend, weil erstmalig reproduzierbar, und es konnte ein AOM-spezifisches Proteom erstellt werden, welches im Laufe der anstehenden Auswertung Inspiration für weitere physiologische Experimente seien kann.

Literatur

Alperin, M.J., Reeburgh, W.S., & Whiticar, M.J. (1988) Carbon and hydrogen isotope fractionation resulting from anaerobic methane oxidation. *Glob Biogeochem Cycles* **2**: 279–288.

Arndtsen, B.A., Bergman, R.G., Mobley, T.A., & Peterson, T.H. (1995) Selective intermolecular carbon-hydrogen bond activation by synthetic metal complexes in homogeneous solution. *Acc Chem Res* **28**: 154–162.

Barnes, R.O., & Goldberg, E.D. (1976) Methane production and consumption in anoxic marine sediments. *Geology* **4**: 297–300.

Boetius, A., Holler, T., Knittel, K., Felden, J., & Wenzhöfer, F. (2009) The seabed as natural laboratory: lessons from uncultivated methanotrophs. In *Microbiology Monographs: Uncultivated Microorganisms*. Epstein, S.S. (ed). Berlin: Springer, pp. 59–82.

Boetius, A., Ravenschlag, K., Schubert, C.J., Rickert, D., Widdel, F., Gieseke, A., Amann, R., Jørgensen, B.B., Witte, U., & Pfannkuche, O. (2000) A marine microbial consortium apparently mediating anaerobic oxidation of methane. *Nature* **407**: 623–626.

Conrad, R. (2007) Microbial ecology of methanogens and methanotrophs. *Adv Agron* **96**: 1–63.

Conrad, R. (2009) The global methane cycle: recent advances in understanding the microbial processes involved. *Environ Microbiol Rep* **1**: 285–292.

Devol, A. (1983) Methane oxidation rates in the anaerobic sediments of Saanich Inlet. *Limnol Oceanogr* **28**: 738–742.

Elvert, M., Suess, E., & Whiticar, M.J. (1999) Anaerobic methane oxidation associated with marine gas hydrates: superlight C-isotopes from saturated and unsaturated C_{20} and C_{25} irregular isoprenoids. *Naturwissenschaften* **86**: 295–300.

Ettwig, K.F., Shima, S., van de Pas-Schoonen, K.T., Kahnt, J., Medema, M.H., Op, C.H.J., Jetten, M.S., & Strous, M. (2008) Denitrifying bacteria anaerobically oxidize methane in the absence of *Archaea*. *Environ Microbiol* **10**: 3164–3173.

Ettwig, K., Van Alen, T., van de Pas-Schoonen, K., Jetten, M., & Strous, M. (2009) Enrichment and molecular detection of denitrifying methanotrophic bacteria of the NC10 phylum. *Appl Environ Microbiol* **75**: 3656–3662.

Ettwig, K.F., Butler, M.K., Le Paslier, D., Pelletier, E., Mangenot, S., Kuypers, M.M.M., Schreiber, F., Dutilh, B.E., Zedelius, J., de Beer, D., Gloerich, J., Wessels, H.J.C.T., van Alen, T., Luesken, F., Wu, M.L., van de Pas-Schoonen, K.T., Op den Camp, H.J.M., Janssen-Megens, E.M., Francoijs, K.-J., Stunnenberg, H., Weissenbach, J., Jetten,

M.S.M., & Strous, M. (2010) Nitrite-driven anaerobic methane oxidation by oxygenic bacteria. *Nature* **464**: 543–548.

Hallam, S.J., Girguis, P.R., Preston, C.M., Richardson, P.M., & DeLong, E.F. (2003) Identification of methyl coenzyme M reductase A (*mcrA*) genes associated with methane-oxidizing archaea. *Appl Environ Microbiol* **69**: 5483–5491.

Hallam, S.J., Putnam, N., Preston, C.M., Detter, J.C., Rokhsar, D., Richardson, P.M., & DeLong, E.F. (2004) Reverse methanogenesis: Testing the hypothesis with environmental genomics. *Science* **305**: 1457–1462.

Harder, J. (1997) Anaerobic methane oxidation by bacteria employing ^{14}C-methane uncontaminated with ^{14}C-carbon monoxide. *Mar Geology* **137**: 13–23.

Harmer, J., Finazzo, C., Piskorski, R., Ebner, S., Duin, E., Goenrich, M., Thauer, R., Reiher, M., Schweiger, A., & Hinderberger, D. (2008) A nickel hydride complex in the active site of methyl-coenzyme M reductase: Implications for the catalytic cycle. *J Am Chem Soc* **130**: 10907–10920.

Hedderich, R., & Whitman, W. (2006) Physiology and biochemistry of the methane-producing Archaea. In *The Prokaryotes*. Dworkin, M., Falkow, S., Rosenberg, E., Schleifer, K.-H., & Stackebrandt, E. (eds). New York: Springer pp. 1050–1079.

Hedderich, R., Klimmek, O., Kröger, A., Dirmeier, R., Keller, M., & Stetter, K.O. (1998) Anaerobic respiration with elemental sulfur and with disulfides. *FEMS Microbiol Rev* **22**: 353–381.

Heller, C., Hoppert, M., & Reitner, J. (2008) Immunological localization of coenzyme M reductase in anaerobic methane-oxidizing archaea of ANME 1 and ANME 2 type. *Geomicrobiol J* **25**: 149–156.

Hinrichs, K., Hayes, J., Sylva, S., Brewer, P., & DeLong, E.F. (1999) Methane-consuming archaebacteria in marine sediments. *Nature* **398**: 802–805.

Hoehler, T.M., Alperin, M.J., Albert, D.B., & Martens, C.S. (1994) Field and laboratory studies of methane oxidation in anoxic marine sediment: Evidence for a methanogenic-sulfate reducer consortium. *Glob Biogeochem Cycles* **8**: 451–463.

Iversen, N., & Jørgensen, B.B. (1985) Anaerobic methane oxidation rates at the sulfate-methane transition in marine sediments from Kattegat and Skagerrak (Denmark). *Limnol Oceanogr* **30**: 944–955.

Khelifi, N., Grossi, V., Hamdi, M., Dolla, A., Tholozan, J.-L., Ollivier B., & Hirschler-Réa, A. (2010). Anaerobic oxidation of fatty acids and alkenes by the hyperthermophilic sulfate-reducing archaeon *Archaeoglobus fulgidus*. *Appl Environ Microbiol* **76:** 3057–3060.

Knittel, K., & Boetius, A. (2009) Anaerobic oxidation of methane: Progress with an unknown process. *Annu Rev Microbiol* **63**: 311–334.

Knittel, K., Lösekann, T., Boetius, A., Kort, R., & Amann, R. (2005) Diversity and distribution of methanotrophic archaea at cold seeps. *Appl Environ Microbiol* **71**: 467–479.

Krüger, M., Meyerdierks, A., Glöckner, F.O., Amann, R., Widdel, F., Kube, M., Reinhardt, R., Kahnt, R., Bocher, R., Thauer, R.K., & Shima, S. (2003) A conspicuous nickel protein in microbial mats that oxidize methane anaerobically. *Nature* **426**: 878–881.

Kurr, M., Huber, R., König, H., Jannasch, H.W., Fricke, H., Trincone, A., Kristjansson, J.K., & Stetter, K.O. (1991). *Methanopyrus kandleri*, gen. and sp. nov. represents a novel group of hyperthermophilic methanogens, growing at 110°C. *Arch Microbiol* **156:** 239–247.

Lacis, A., Hansen, J., Lee, P., Mitchell, T., & Lebedeff, S. (1981) Greenhouse effect of trace gases, 1970-1980. *Geophys Res Lett* **8**: 1035–1038.

Li, F., Hinderberger, J., Seedorf, H., Zhang, J., Buckel, W., & Thauer, R.K. (2008) Coupled ferredoxin and crotonyl coenzyme A (CoA) reduction with NADH catalyzed by the butyryl-CoA dehydrogenase/Etf complex from *Clostridium kluyveri*. *J Bacteriol* **190**: 843–850.

Lueders, T., Chin, K.J., Conrad, R., & Friedrich, M. (2001) Molecular analyses of methyl-coenzyme M reductase alpha-subunit (*mcrA*) genes in rice field soil and enrichment cultures reveal the methanogenic phenotype of a novel archaeal lineage. *Environ Microbiol* **3**: 194–204.

Martens, C.S., Albert, D.B., & Alperin, M.J. (1999) Stable isotope tracing of anaerobic methane oxidation in the gassy sediments of Eckernförde Bay, German Baltic Sea. *Am J Sci* **299**: 589–610.

Martens, C.S., & Berner, R.A. (1974) Methane production in the interstitial waters of sulfate-depleted marine sediments. *Science* **185**: 1167–1169.

Mayr, S., Latkoczy, C., Krüger, M., Gunther, D., Shima, S., Thauer, R.K., Widdel, F., & Jaun, B. (2008) Structure of an F_{430} variant from archaea associated with anaerobic oxidation of methane. *J Am Chem Soc* **130**: 10758–10767.

Meyerdierks, A., Kube, M., Kostadinov, I., Teeling, H., Glöckner, F.O., Reinhardt, R., & Amann, R. (2010) Metagenome and mRNA expression analyses of anaerobic methanotrophic archaea of the ANME-1 group. *Environ Microbiol* **12**: 422–439.

Meyerdierks, A., Kube, M., Lombardot, T., Knittel, K., Bauer, M., Glöckner, F.O., Reinhardt, R., & Amann, R. (2005) Insights into the genomes of archaea mediating the anaerobic oxidation of methane. *Environ Microbiol* **7**: 1937–1951.

Michaelis, W., Seifert, R., Nauhaus, K., Treude, T., Thiel, V., Blumenberg, M., Knittel, K., Gieseke, A., Peterknecht, K., Pape, T., Boetius, A., Amann, R., Jørgensen, B.B., Widdel, F., Peckmann, J., Pimenov, N.V., & Gulin, M.B. (2002) Microbial reefs in the Black Sea fueled by anaerobic oxidation of methane. *Science* **297**: 1013–1015.

Moran, J.J., House, C.H., Freeman, K.H., & Ferry, J.G. (2005) Trace methane oxidation studied in several Euryarchaeota under diverse conditions. *Archaea* **1**: 303–309.

Nauhaus, K., Boetius, A., Krüger, M., & Widdel, F. (2002) *In vitro* demonstration of anaerobic oxidation of methane coupled to sulphate reduction in sediment from a marine gas hydrate area. *Environ Microbiol* **4**: 296–305.

Nauhaus, K., Treude, T., Boetius, A., & Krüger, M. (2005) Environmental regulation of the anaerobic oxidation of methane: A comparison of ANME-I and ANME-II communities. *Environ Microbiol* **7**: 98–106.

Nauhaus, K., Albrecht, M., Elvert, M., Boetius, A., & Widdel, F. (2007) *In vitro* cell growth of marine archaeal-bacterial consortia during anaerobic oxidation of methane with sulfate. *Environ Microbiol* **9**: 187–196.

Orphan, V.J., House, C.H., Hinrichs, K.-U., McKeegan, K.D., & DeLong, E.F. (2001) Methane-consuming archaea revealed by directly coupled isotopic and phylogenetic analysis. *Science* **293**: 484–487.

Orphan, V.J., House, C.H., Hinrichs, K.-U., McKeegan, K.D., & DeLong, E.F. (2002) Multiple archaeal groups mediate methane oxidation in anoxic cold seep sediments. *Proc Natl Acad Sci U S A* **99**: 7663–7668.

Pancost, R.D., Sinninghe Damsté, J.S., de Lint, S., van der Maarel, M.J.E.C., Gottschal, J.C., & The Medinaut Shipboard Scientific Party (2000) Biomarker evidence for widespread anaerobic methane oxidation in Mediterranean sediments by a consortium of methanogenic archaea and bacteria. *Appl Environ Microbiol* **66**: 1126–1132.

Pernthaler, A., Dekas, A.E., Brown, C.T., Goffredi, S.K., Embaye, T., & Orphan, V.J. (2008) Diverse syntrophic partnerships from deep-sea methane vents revealed by direct cell capture and metagenomics. *Proc Natl Acad Sci U S A* **105**: 7052–7057.

Rabus, R., Hansen, T., & Widdel, F. (2000) Dissimilatory sulfate- and sulfur reducing procaryotes. In *The Prokaryotes, electronic edition*. Dworkin, M., Falkow, S., Rosenberg,

E., Schleifer, K.-H., & Stackebrandt, E. (eds). New York: Fischer Verlag DOI: 10.1007/0-387-30742-7_22.

Raghoebarsing, A.A., Pol, A., van de Pas-Schoonen, K.T., Smolders, A.J.P., Ettwig, K.F., Rijpstra, W.I.C., Schouten, S., Damsté, J.S.S., Op den Camp, H.J.M., Jetten, M.S.M., & Strous, M. (2006) A microbial consortium couples anaerobic methane oxidation to denitrification. *Nature* **440**: 918–921.

Ragsdale, S.W. (2007) Nickel and the carbon cycle. *J Inorg Biochem* **101**: 1657–1666.

Ramanathan, V., Cicerone, R., Singh, H., & Kiehl, J. (1985) Trace gas trends and their potential role in climate change. *J Geophys Res* **90**: 5547–5566.

Reeburgh, W.S. (1976) Methane consumption in Cariaco Trench waters and sediments. *Earth Planet Sci Lett* **28**: 337–344.

Reeburgh, W.S. (1980) Anaerobic methane oxidation - Rate depth distributions in Skan Bay sediments. *Earth Planet Sci Lett* **47**: 345–352.

Reeburgh, W.S. (2007) Oceanic methane biogeochemistry. *Chem Rev* **107**: 486–513.

Rueter, P., Rabus, R., Wilkes, H., Aeckersberg, F., Rainey, F.A., Jannasch, H.W., & Widdel, F. (1994) Anaerobic oxidation of hydrocarbons in crude oil by new types of sulphate-reducing bacteria. *Nature* **372**: 455–458.

Schink, B. (1997) Energetics of syntrophic cooperation in methanogenic degradation. *Microbiol Mol Biol Rev* **61**: 262–280.

Schreiber, L., Holler, T., Knittel, K., Meyerdierks, A., & Amann, R. (2010) Identification of the dominant sulfate-reducing bacterial partner of anaerobic methanotrophs of the ANME-2 clade. *Environ Microbiol* **12**: 2327–2340.

Seifert, R., Nauhaus, K., Blumenberg, M., Krüger, M., & Michaelis, W. (2006) Methane dynamics in a microbial community of the Black Sea traced by stable carbon isotopes *in vitro*. *Org Geochem* **37**: 1411–1419.

Shilov, A.E., & Shul'pin, G.B. (1997) Activation of C–H bonds by metal complexes. *Chem Rev* **97**: 2879–2932.

Shima, S., & Thauer, R.K. (2005) Methyl-coenzyme M reductase and the anaerobic oxidation of methane in methanotrophic Archaea. *Curr Opin Microbiol* **8**: 643–648.

Springer, E., Sachs, M.S., Woese, C.R., & Boone, D.R. (1995) Partial gene sequences for the A subunit of methyl-coenzyme M reductase (*mcr*I) as a phylogenetic tool for the family *Methanosarcinaceae*. *Int J Syst Bacteriol* **45**: 554–559.

Thauer, R.K., & Shima, S. (2008) Methane as fuel for anaerobic microorganisms. *Ann NY Acad Sci* **1125**: 158–170.

Thauer, R.K., Kaster, A.-K., Seedorf, H., Buckel, W., & Hedderich, R. (2008) Methanogenic archaea: ecologically relevant differences in energy conservation. *Nat Rev Microbiol* **6**: 579–591.

Valentine, D.L., & Reeburgh, W.S. (2000) New perspectives on anaerobic methane oxidation. *Environ Microbiol* **2**: 477–484.

Wegener, G., Niemann, H., Elvert, M., Hinrichs, K.-U., & Boetius, A. (2008) Assimilation of methane and inorganic carbon by microbial communities mediating the anaerobic oxidation of methane. *Environ Microbiol* **10**: 2287–2298.

Whiticar, M.J. (1999) Carbon and hydrogen isotope systematics of bacterial formation and oxidation of methane. *Chem Geol* **161**: 291–314.

Whiticar, M.J., & Faber, E. (1986) Methane oxidation in sediment and water column environments - Isotope evidence. *Org Geochem* **10**: 759–768.

Widdel, F. (1988) Microbiology and ecology of sulfate- and sulfur-reducing bacteria. In *Biology of anaerobic microorganisms*. Zehnder, A.J.B. (ed). New York: John Wiley & Sons, pp. 469–585.

Zehnder, A.J.B., & Brock, T.D. (1979) Methane formation and methane oxidation by methanogenic bacteria. *J Bacteriol* **137**: 420–432.

Zehnder, A.J.B., & Brock, T.D. (1980) Anaerobic methane oxidation - occurrence and ecology. *Appl Environ Microbiol* **39**: 194–204.

Zinder, S.H. (1993) Physiological ecology of methanogens. In *Methanogenesis: Ecology, Physiology, Biochemistry & Genetics*. Ferry, J.G. (ed). New York: Chapman & Hall, pp. 128–26

III. Ergebnisse im Detail

Im Rahmen der Promotion wurden vier Manuskripte erarbeitet, welche Ergebnisse im Detail beschreiben und interpretieren. Die angefügten Erläuterungen zeigen den Anteil der beteiligten Autoren an den jeweiligen Arbeiten und erläutern die Arbeiten im Speziellen.

III.1 Substantial $^{13}C/^{12}C$ and D/H fractionation during anaerobic oxidation of methane by marine consortia enriched *in vitro*

Thomas Holler, Gunter Wegener, Katrin Knittel, Antje Boetius, Benjamin Brunner, Marcel M. M. Kuypers & Friedrich Widdel

Entwicklung des Konzepts in Zusammenarbeit von F.W., A.B. und T.H., Durchführung der Versuchsplanung, der Inkubationen, chemischen und phylogenetischen Analysen und Auswertung von T.H., G.W., K.K., B.B. und M.M.M.K., Erstellen des Manuskripts durch T.H., G.W. und F.W. in Zusammenarbeit mit allen Ko-Autoren.

Environmental Microbiology Reports 1 (5) (2009): 370–376

III.2 Carbon and sulfur back flux during anaerobic microbial oxidation of methane and coupled sulfate reduction

Thomas Holler, Gunter Wegener, Helge Niemann, Christian Deusner, Timothy G. Ferdelman, Antje Boetius, Benjamin Brunner & Friedrich Widdel

Entwicklung des Konzepts in Zusammenarbeit von F.W., T.H. und A.B., Durchführung der Versuchsplanung, der Inkubationen, chemischen Analysen und Auswertung von T.H., H.N., C.D., G.W., T.G.F. und B.B., Erstellen des Manuskripts durch T.H., G.W., B.B., T.G.F. und F.W. in Zusammenarbeit mit allen Ko-Autoren.

Manuskript in Vorbereitung

III.3 Microbiological investigation of methane- and hydrocarbon-discharging mud volcanoes in the Carpathian Mountains, Romania

Karine Alain, Thomas Holler, Florin Musat, Marcus Elvert, Tina Treude & Martin Krüger

Entwicklung des Konzepts von M.K. und F.M. in Zusammenarbeit mit K.A. und T.H., Durchführung der Versuchsplanung, Probenahme, Inkubationen, chemischen und phylogenetischen Analysen sowie Auswertung von K.A., T.H., F.M., M.E., T.T. und M.K., Erstellen des Manuskripts durch K.A. in Zusammenarbeit mit allen Ko-Autoren.

Environmental Microbiology 8 (4) (2006): 574–590

III.4 Thermophilic anaerobic oxidation of methane by marine microbial consortia

Thomas Holler, Friedrich Widdel, Katrin Knittel, Rudolf Amann, Matthias Y. Kellermann, Kai-Uwe Hinrichs, Andreas Teske, Antje Boetius & Gunter Wegener

Entwicklung des Konzepts von T.H. und G.W. in Zusammenarbeit mit F.W. und A.B., Durchführung der Versuchsplanung, Probenahme, Inkubationen, chemischen und phylogenetischen Analysen und Auswertung von T.H., G.W., K.K., R.A., M.Y.K., K-U.H. und A.T., Erstellen des Manuskripts durch T.H., G.W., F.W. und A.B. in Zusammenarbeit mit allen Ko-Autoren.

Manuskript eingereicht

III.1

Substantial $^{13}C/^{12}C$ and D/H fractionation during anaerobic oxidation of methane by marine consortia enriched *in vitro*

Thomas Holler,[1]* Gunter Wegener,[1] Katrin Knittel,[1] Antje Boetius,[1,2]
Benjamin Brunner,[1] Marcel M. M. Kuypers[1] and Friedrich Widdel[1]

Environmental Microbiology Reports 1 (5) (2009): 370–376

[1]Max Planck Institute for Marine Microbiology, Celsiusstr.1, 28359 Bremen, Germany
[2]Alfred Wegener Institute for Polar and Marine Research, 27515 Bremerhaven, Germany

*** Corresponding author**

Environmental Microbiology Reports (2009) **1**(5), 370–376 doi:10.1111/j.1758-2229.2009.00074.x

Substantial $^{13}C/^{12}C$ and D/H fractionation during anaerobic oxidation of methane by marine consortia enriched *in vitro*

Thomas Holler,[1]* Gunter Wegener,[1] Katrin Knittel,[1] Antje Boetius,[1,2] Benjamin Brunner,[1] Marcel M. M. Kuypers[1] and Friedrich Widdel[1]
[1]*Max Planck Institute for Marine Microbiology, Celsiusstraße 1, 28359 Bremen, Germany.*
[2]*Alfred Wegener Institute for Polar and Marine Research, 27515 Bremerhaven, Germany.*

Summary

The anaerobic oxidation of methane (AOM) by methanotrophic archaea and sulfate-reducing bacteria is the major sink of methane formed in marine sediments. The study of AOM as well as of methanogenesis in different habitats is essentially connected with the *in situ* analysis of stable isotope ($^{13}C/^{12}C$, D/H) signatures (δ-values). For their kinetic interpretation, experimental (cultivation-based) isotope fractionation factors (α-values) are richly available in the case of methanogenesis, but are scarce in the case of AOM. Here we used batch enrichment cultures with high AOM activity and without background methanogenesis from detrital remnants to determine $^{13}C/^{12}C$ and D/H fractionation factors. The enrichment cultures which originated from three marine habitats (Hydrate Ridge, NE Pacific; Amon Mud Volcano, Mediterranean Sea; NW shelf, Black Sea) were dominated by archaeal phylotypes of anaerobic methanotrophs (ANME-2 clade). Isotope fractionation factors calculated from the isotope signatures as a function of the residual proportion of methane were 1.012–1.039 for $^{13}CH_4/^{12}CH_4$ and 1.109–1.315 for CDH_3/CH_4. The present values from *in vitro* experiments were significantly higher than values previously estimated from isotope signature distributions in marine sediment porewater, in agreement with the overlap of other processes with AOM in the natural habitat.

Received 21 April, 2009; accepted 10 August, 2009. *For correspondence. E-mail tholler@mpi-bremen.de; Tel. (+49) 421 2028732; Fax (+49) 421 2028790.

Introduction

Stable isotope compositions (signatures) of chemical elements such as hydrogen, carbon, oxygen and sulfur in various natural compounds are widely used to track their source and to gain insights into the processes in which these compounds are involved. The use of isotope signatures as process indicators is based on the fact that physical processes (diffusive transport, phase transition) or chemical reactions (abiotic, biotic) alter the isotope composition of a compound derived from a source. In particular biotic net reactions discriminate against the heavier isotopes when substrate is not limiting. This so-called kinetic isotope effect is explained by the slightly stronger chemical bonds and lower diffusivity of the heavier isotopologues compared with the lighter ones, resulting in lower enzymatic rate constants of the former. Catabolic as well as biosynthetic products therefore usually exhibit lower fractions of the heavier isotopes than the substrate. The isotope composition of an element in its native or bound state may be expressed as isotope ratio, R = [Heavy]/[Light] (with brackets indicating molar concentrations or amounts in mol). For convenience, δ notations are commonly used; they are relative to a standard and defined as $\delta = (R_{Sample}/R_{Standard} - 1) \times 1000‰$. The key parameter describing isotope discrimination is the fractionation factor which for a particular reaction, S → P (S, substrate, reactant; P, product) is often defined as

$$\alpha_{S/P} = R_S/R_P = (\delta_S + 1000‰)/(\delta_P + 1000‰). \quad (1)$$

It relates the momentary isotope ratio of the substrate to that of the momentarily forming product. Because α-values usually deviate only slightly from 1, a convenient formalism is to express them as more distinctive enrichment factors, which are defined as $\varepsilon_{S/P} = (\alpha - 1) \times 1000‰$.

The biogeochemical understanding of methane formation and consumption in the environment has benefited greatly from stable isotope studies. Distinction of microbially from thermochemically produced methane in reservoirs and sediments is based on the stronger ^{13}C and D depletion of the former (Reeburgh, 2007, and literature therein). According to isotope signatures, most of the globally produced methane is of microbial origin. Stable isotope analysis also contributed an important piece of

evidence for the anaerobic microbial oxidation of methane (AOM); this was the finding of ^{13}C-depleted inorganic carbon (*c.* −15‰ below ambient inorganic carbon) in a distinct zone in anoxic sediments containing sulfate and biogenic methane (Reeburgh, 1982). Hints of the microorganisms involved in AOM again came from isotope analysis, the identification of ^{13}C-depleted and apparently methane-derived isoprenoic lipids in sediment horizons with AOM (Hinrichs *et al.*, 1999). These characteristic lipids were later assigned to archaeal cells living in tightly clustered consortia with *Deltaproteobacteria* (Boetius *et al.*, 2000; Orphan *et al.*, 2001). Today, AOM has become one of the most intensely investigated processes in anoxic marine habitats, motivated largely by its environmental significance as a process counteracting global methane emission (Knittel and Boetius, 2009, and literature therein).

The ^{13}C discrimination by biological methane formation in environments has been experimentally substantiated by numerous studies with active community samples and pure cultures (Valentine *et al.*, 2004; Conrad, 2005). Experiments permitted distinguishing between the carbon sources of methane, with a carbon fractionation factor of α_C ($\alpha^{13}C$) = 1.021–1.071 for CO_2 reduction and α_C = 1.007–1.027 for acetate cleavage (Conrad, 2005). Experimentally determined hydrogen isotope fractionation factors for methanogenesis were α_H (α_D, αD, α^2H) = 1.16–1.43 for CO_2 reduction and again less for acetate cleavage (Valentine *et al.*, 2004). In contrast, fractionation factors for AOM are scarce. Estimated α_C-values between 1.009 and 1.024 and α_H-values between 1.120 and 1.157 for AOM were obtained from models based on carbon species distribution in porewater depth profiles or in anoxic water columns (Whiticar and Faber, 1985; Alperin *et al.*, 1988; Martens *et al.*, 1999; Reeburgh *et al.*, 2006). However, the use of *in situ* isotope signatures for such estimates is critical because methanogenesis overlaps more or less with AOM (Orcutt *et al.*, 2005; Parkes *et al.*, 2007). Methanogenesis and AOM have opposite effects on the isotope signature of the methane pool ($^{12}CH_4$ is preferentially formed and consumed). The only experimental fractionation study of AOM reported so far employed microbial mats from methane seeps (Seifert *et al.*, 2006). Data led to the conclusion that significant methanogenesis, presumably from natural C_1-methyl compounds, occurred simultaneously with AOM, and that experimental fractionation data with such natural samples should be interpreted with caution despite high AOM activity. Here, we used enriched consortia that had performed AOM with methane and sulfate as the only added energy source over long incubation periods and no longer showed background methanogenesis if tested without methane addition. The high carbon and hydrogen isotope fractionation factors obtained here are thus very likely to result only from AOM.

Results and discussion

Enrichment of AOM activity and consortia

The microbial communities (consortia) used for the present experiments originated from sediment from Hydrate Ridge (NE Pacific) and Amon Mud Volcano (Eastern Mediterranean Sea), and from microbial mats covering methane seep chimneys in the Black Sea (NW region); detailed information about the sampling sites is given in Table S1 in *Supporting information*. Methane-dependent sulfide formation was observed with all three types of samples when incubated in artificial seawater medium (Nauhaus *et al.*, 2002). The AOM rate of the Hydrate Ridge (Nauhaus *et al.*, 2007) and Amon Mud Volcano samples increased gradually. Consecutive subincubations of aliquots over long periods (Hydrate Ridge, 80 months; Amon Mud Volcano, 26 months) resulted in detritus-free enrichments of loose flocks essentially composed of microbial cells. The Black Sea mat samples, which represented naturally enriched biomass in a loosely coherent matrix (Michaelis *et al.*, 2002), did not exhibit a significant increase in the AOM rate upon repeated transfer of the entire sample to new medium during the observation period (15 months). The specific AOM activities of the three types of culture material, which was used for the following experiments, are listed in Table 1. Background methanogenesis in the absence of methane was below the detection limit in our incubation experiments and thus must be below 0.05% of the AOM rate. Fluorescent hybridization targeting 16S rRNA revealed different proportions of archaeal phylotypes designated as ANME-2 (Table 1).

Measurement of carbon and hydrogen isotope fractionation

Experiments were based exclusively on the analysis of the three natural methane isotopologues, $^{12}CH_4$, $^{13}CH_4$ (abundance varying around 1.07%) and $^{12}CDH_3$ (abundance varying around 0.0115%); heavier isotopologues of methane are extremely rare and were therefore neglected. Because determination of the fractionation factor (according to Eq. 1) by isotope analysis of methane and the momentarily forming inorganic carbon is impracticable, we used a batch culture (closed system) incubation approach with mathematical treatment adopted from Rayleigh's considerations (1896) about gas mixture diffusion:

$$R_t/R_0 = (C_t/C_0)^{(1/\alpha)-1} \quad (2)$$

or

$$\ln(R_t/R_0) = [(1/\alpha)-1]\ln(C_t/C_0). \quad (3)$$

Table 1. Methane-oxidizing activity and abundance of apparent anaerobic methanotrophic (ANME) archaea in enrichment cultures used for isotope fractionation experiments.

Culture or sample, origin	Temperature optimum	Specific AOM activity[a] (mmol day^{-1} g^{-1})	Abundance (%) of detectable phylotypes among total cells[b,c]			
			ANME-2a	ANME-2c	ANME-3	ANME + DSS[d]
Sediment-free enrichment, Hydrate Ridge	12°C	0.3	17	64	1	> 99
Sediment-free enrichment, Amon Mud Volcano	20°C	2.0	20	49	5	98
Microbial mat, Black Sea	12°C	0.4	34	14	0	97

a. Related to dry mass (determined according to Nauhaus *et al.*, 2007).
b. ANME-1 was not detectable.
c. Phylotypes were identified and quantified by catalysed reporter deposition fluorescence *in situ* hybridization (CARD-FISH; Pernthaler *et al.*, 2002) using probes ANME-1-350, ANME-2a-647, ANME-2c-622 and ANME-3-1249 as described (Knittel and Boetius, 2009). Total cells were visualized by epifluorescence microscopy upon staining with 4′,6-diamidino-2-phenylindol (DAPI).
d. DSS, phylotypes related to *Desulfosarcina*/*Desulfococcus.*

R_0 and R_t are the isotope ratios of the substrate at the beginning and at a subsequent time point t, respectively, and C_0 and C_t the concentrations of the substrate also at the beginning and at the time point, t, respectively.

The enrichment cultures were incubated at their temperature optima (Table 1) in headspace-free bottles (250 ml) with anoxic medium containing methane (dissolved under overpressure before inoculation). To prevent local substrate limitation, the inoculum size was such that the predicted volumetric AOM rate did not exceed 0.2 mmol l^{-1} day^{-1}. Furthermore, cultures were continuously stirred with a magnet, and time-course measurements were not carried out below a methane concentration of 1.5 mmol l^{-1}. Samples were withdrawn with syringes while methane-free medium was simultaneously injected so as to keep the cultures headspace-free; concentrations were corrected for the resulting dilution. The methane concentration was followed by gas chromatography with flame ionization detection, and the isotopic composition ($^{13}C/^{12}C$, D/H) of residual methane was measured via gas chromatography combustion isotope ratio mass spectrometry (Table S3 *Supporting information*).

The decrease of the methane concentration during the incubation period was essentially linear (Hydrate Ridge enrichment in Fig. 1A; other enrichments in Fig. S1). Analysis of formed sulfide (not shown) confirmed the 1:1 stoichiometry of methane oxidized and sulfide formed, according to $CH_4 + SO_4^{2-} \rightarrow HCO_3^- + HS^- + H_2O$. The slight deviation from this stoichiometry due to the assimilated proportion of methane could not be revealed within the accuracy range of the analytical methods; previous studies showed that only around 1% of the consumed methane was assimilated into biomass of consortia (Nauhaus *et al.*, 2007; Wegener *et al.*, 2008). A methane-free control with inoculum did not show sulfide or methane formation, and a control without inoculum showed neither methane consumption nor sulfide formation.

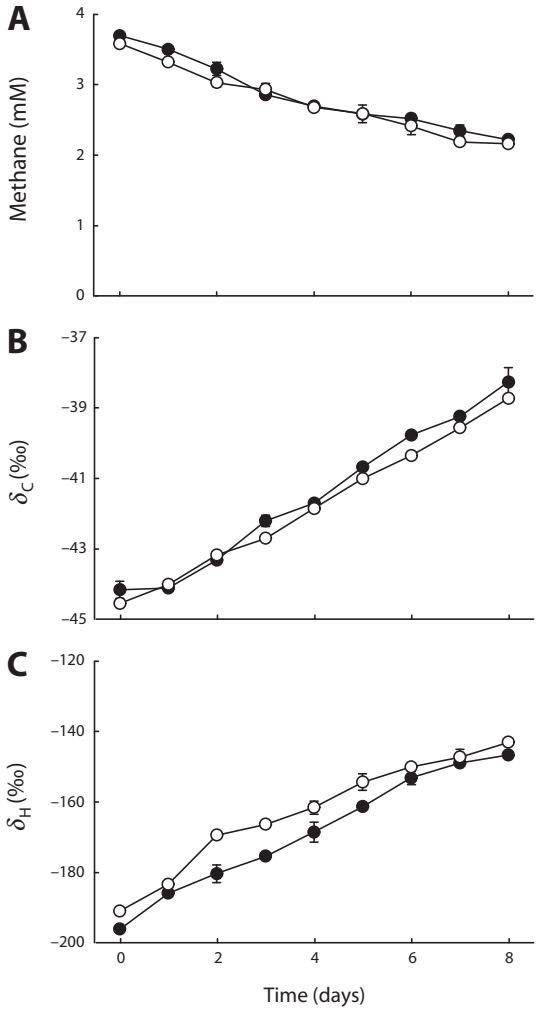

Fig. 1. Time-course of isotope enrichment in the methane pool during anaerobic oxidation of methane with sulfate in duplicate (● and ○) sediment-free enrichment cultures from Hydrate Ridge. The plot for determination of the fractionation factors from this experiment is shown in Fig. 2A and B. For time-courses of the other enrichment cultures see Fig. S1.
A. Decrease of the methane concentration in the aqueous phase.
B. Enrichment of $^{13}CH_4$ in residual methane.
C. Enrichment of CDH_3 in residual methane.

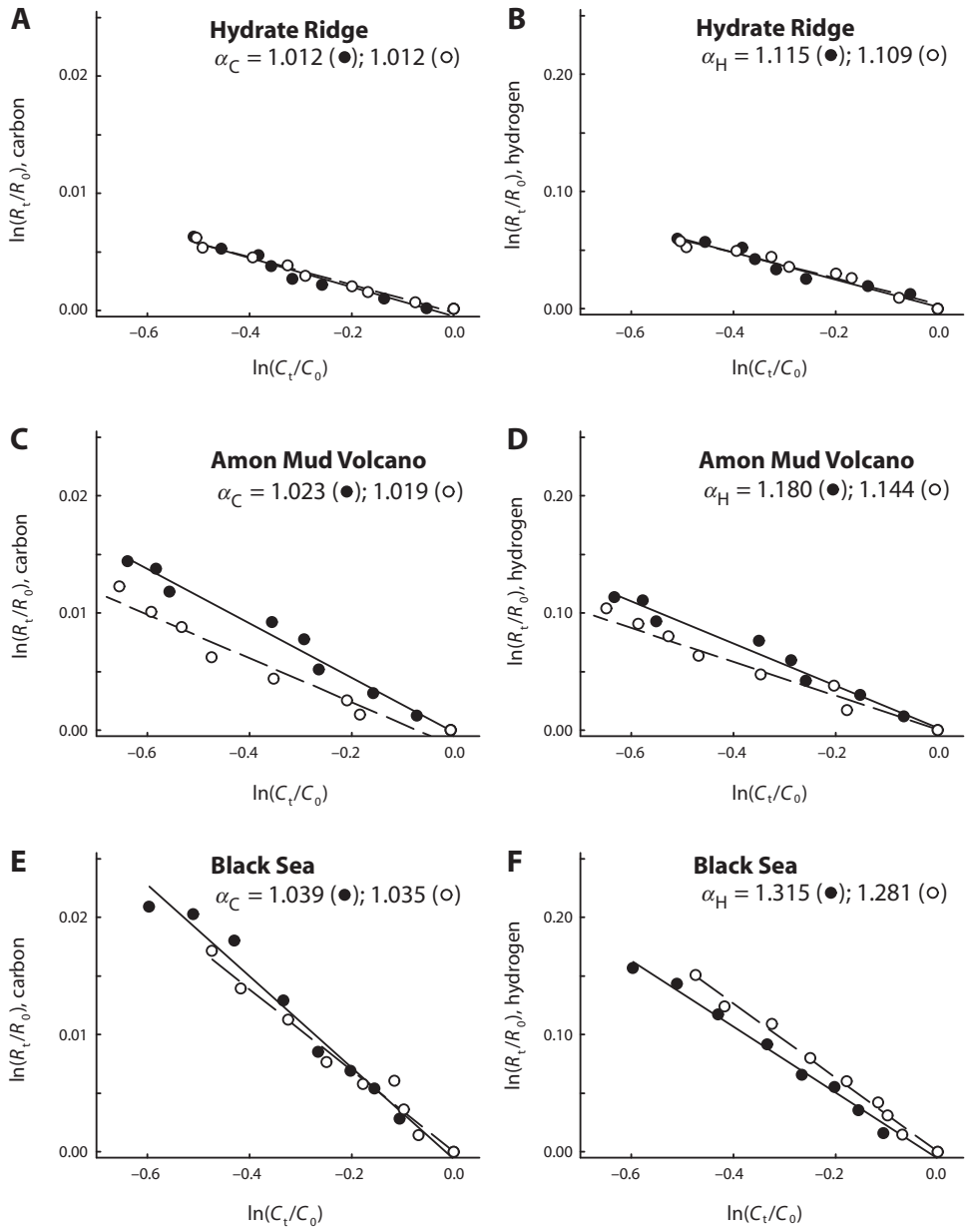

Fig. 2. Double logarithmic plots of the stable isotope compositions of carbon (A, C and E) and hydrogen (B, D and F; vertical scale 10-fold attenuated) in residual methane versus its residual proportion in anaerobic methanotrophic cultures from three habitats (● and ○ indicate duplicate experiments). For calculation of the regression line in the present approach, the impact of the zero point was the same as that of other points. $y = \ln(R_t/R_0)$; $x = \ln(C_t/C_0)$; $\alpha = 1/(\text{slope} + 1)$.
A and B. Sediment-free enrichment culture from Hydrate Ridge (experiment depicted in Fig. 1).
C and D. Sediment-free enrichment culture from Amon Mud Volcano (experiment depicted in Fig. S1).
E and F. Mat sample from Black Sea gas seep (experiment depicted in Fig. S1).

The remaining methane in the enrichment cultures always became enriched in ^{13}C-carbon and deuterium (δ_C- and δ_H-values increased; Fig. 1B and C; Fig. S1B, C, E and F). The double logarithmic plot of R_t/R_0 versus C_t/C_0 allowed straight-line fits with their slope (Eq. 3) yielding the depicted fractionation factors (α_C, α_H) (Fig. 2). Even though the fractionation factors varied within a relatively wide range between the cultures of different origin, they were very similar in replicates in cultures of the same origin. A plot of α_H versus α_C revealed an almost linear correlation (Fig. 3), with $^{12}CDH_3/^{12}CH_4$ fractionation in independent cultures being almost eightfold higher than $^{13}CH_4/^{12}CH_4$ fractionation. The linear correlation indicates that the reaction causing isotope fractionation is basically the same in the different cultures. Considering that the deuterated proportion of the presently used 'natural' (non-

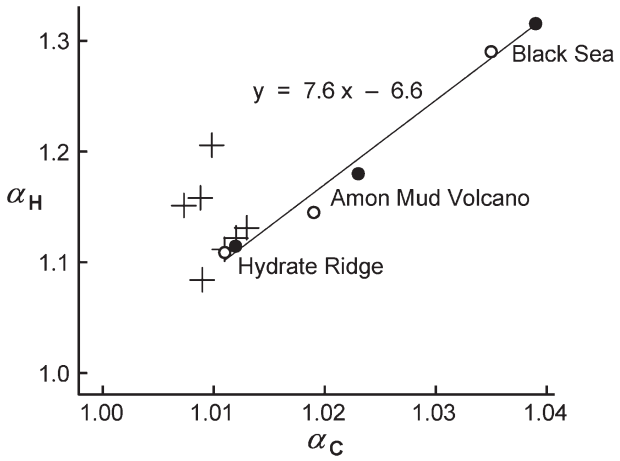

Fig. 3. Correlation between hydrogen and carbon isotope fractionation factors (α_H scale 10-fold attenuated) for the anaerobic oxidation of methane from the present batch experiments (●, ○) and from models based on isotope signatures (+) in environments with anaerobic oxidation of methane (from Alperin *et al.*, 1988; Martens *et al.*, 1999; Kessler *et al.*, 2006).

enriched) methane carries only one deuterium atom with a likeliness of 1/4 to react ($1/\leq 3$ in subsequent reactions), the isotopic effect of the ^{12}C–D bond in comparison with that of the ^{13}C–H bond during AOM is even more dramatic than seen in Fig. 3. This much stronger fractionation of the hydrogen isotopologues is in agreement with the expected differences in bond reactivity. Deuterium, due to its twofold higher atomic mass in comparison with the light isotope, has the highest kinetic effect of all isotopes (Cleland, 2005).

At present, there is no satisfying explanation for the variation of the fractionation factors between the cultures of different origin (α_C, 1.012–1.039; α_H, 1.109–1.315). An influence of background methanogenesis from residual detrital matter was excluded. The possible influence of mass transfer limitation on isotope patterns as discussed elsewhere for aerobic methanotrophs (Templeton *et al.*, 2006; Nihous, 2008) was examined in a one-dimensional diffusion and reaction model (for details see Appendix S1 in *Supporting information*). If the model was stressed by assuming a much faster ($\times 10^3$) methane consumption, lower ($\times 10^{-3}$) methane concentration or slower ($\times 10^{-5}$) diffusion in comparison with our *in vitro* conditions, the influence on isotope composition was negligible ($\Delta\delta < 0.1‰$). The observed variations are most likely due to kinetic factors. Besides variation of the incubation temperatures according to the optima of the cultures (Table 1), variation in the relative amounts of enzymes in the cells and their V_{max} (maximum specific activities) and K_M values may result in differences in the pool sizes of intermediates, thus influencing overall isotope fractionation. The deduced values are thus bulk fractionation factors rather than fractionation factors in the strict sense, which are those of single enzymatic reactions. A single enzymatic reaction at constant temperature is expected to always exhibit the same fractionation factor. Significant variation of fractionation factors has been also observed in different catabolic processes of C_1 compounds, methanogenesis from CO_2 and H_2 (α_C, 1.021–1.082) or acetate (α_C, 1.000–1.032) in archaeal cultures (Conrad, 2005), and the aerobic oxidation of methane to CO_2 in various bacterial cultures (α_C, 1.003–1.037; α_H, 1.156–1.319; Barker and Fritz, 1981; Coleman *et al.*, 1981; Reeburgh *et al.*, 1997; Kinnaman *et al.*, 2007).

A detailed understanding of *in situ* isotope signatures of methane is confronted with further complications, as indicated by the fractionation factors calculated from *in situ* depth profiles in comparison with those from our present experiments (Fig. 3). Except for the α_C-values from the Hydrate Ridge culture, the α_C-values from the other cultures were significantly higher than those from porewater studies. The *in situ* and experimental α_H-values were more similar. We are still far from a conclusive interpretation. Various types of anaerobic methanotrophs under different conditions may not only exhibit different bulk fractionation factors, as in the present study; there is also a simultaneous contribution from methanogenic horizons

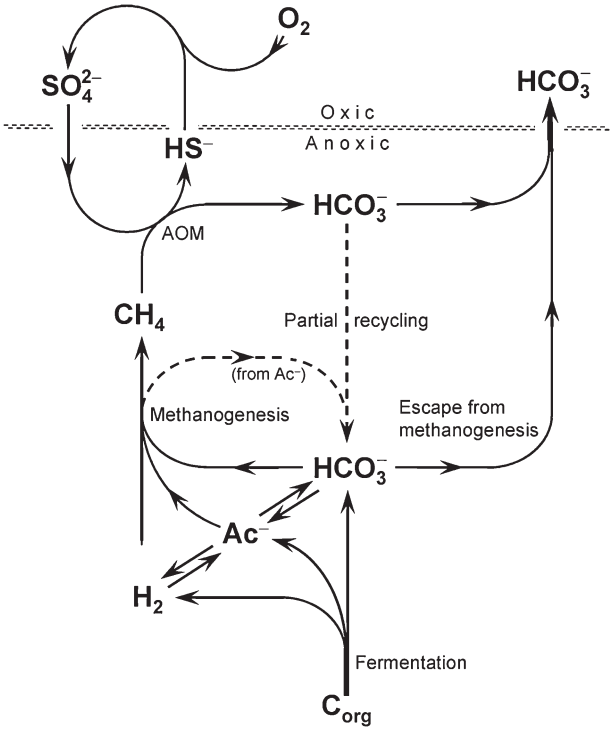

Fig. 4. Complexity of anaerobic processes associated *in situ* with anaerobic oxidation of methane (AOM). The scheme includes only the entering organic carbon that has been left from degradation with oxygen and sulfate. The content of $^{13}CH_4$ and CDH_3 in the methane pool is determined by isotope fractionation during methanogenesis from HCO_3^-, methanogenesis from acetate, and AOM.

overlapping with or adjacent to AOM zones (Orcutt *et al*., 2005; Parkes *et al*., 2007). Methanogenesis in turn may receive inorganic carbon not only from the microbial decay of organic carbon, but also from AOM, resulting in partial recycling of the carbon pool (Fig. 4). Further experimental investigations of isotope fractionation by consortia *in vitro* with stepwise variation of incubation parameters (temperature, AOM rate) for a single type of culture may help to understand the environmental factors that determine isotope fractionation.

Acknowledgements

We are indebted to the crews of the RV Sonne, RV Poseidon and the RV L'Atalante for their support on board. We thank Gabriele Klockgether for help during isotope analyses and two reviewers for helpful comments. This work was supported by the Max-Planck-Gesellschaft, the Bundesministerium für Bildung und Forschung (BMBF), and the Deutsche Forschungsgemeinschaft (DFG). This is publication No. GEOTECH-1294 of the R&D programme GEOTECHNOLOGIEN (BMBF and DFG) and project MUMM (Grants 03G0554A and 03G0608A, BMBF).

References

Alperin, M.J., Reeburgh, W.S., and Whiticar, M.J. (1988) Carbon and hydrogen isotope fractionation resulting from anaerobic methane oxidation. *Global Biogeochem Cycles* **2:** 279–288.

Barker, J.F., and Fritz, P. (1981) Carbon isotope fractionation during microbial methane oxidation. *Nature* **293:** 289–291.

Boetius, A., Ravenschlag, K., Schubert, C.J., Rickert, D., Widdel, F., Gieseke, A., *et al.* (2000) A marine microbial consortium apparently mediating anaerobic oxidation of methane. *Nature* **407:** 623–626.

Cleland, W.W. (2005) The use of isotopes to determine enzyme mechanisms. *Arch Biochem Biophys* **433:** 2–12.

Coleman, D.D., Risatti, J.B., and Schoell, M. (1981) Fractionation of carbon and hydrogen isotopes by methane-oxidizing bacteria. *Geochim Cosmochim Acta* **45:** 1033–1037.

Conrad, R. (2005) Quantification of methanogenic pathways using stable carbon isotopic signatures: a review and a proposal. *Org Geochem* **36:** 739–752.

Hinrichs, K.-U., Hayes, J., Sylva, S., Brewer, P., and DeLong, E. (1999) Methane-consuming archaebacteria in marine sediments. *Nature* **398:** 802–805.

Kessler, J.D., Reeburgh, W.S., and Tyler, S.C. (2006) Controls on methane concentration and stable isotope (δ^2H-CH_4 and δ^{13}C-CH4) distributions in the water columns of the Black Sea and Cariaco Basin. *Global Biogeochem Cycles* **20:** GB4004 (1–13).

Kinnaman, F.S., Valentine, D.L., and Tyler, S.C. (2007) Carbon and hydrogen isotope fractionation associated with the aerobic microbial oxidation of methane, ethane, propane and butane. *Geochim Cosmochim Acta* **71:** 271–283.

Knittel, K., and Boetius, A. (2009) Anaerobic oxidation of methane – progress with an unknown process. *Annu Rev Microbiol*, **63**, in press.

Martens, C.S., Albert, D.B., and Alperin, M.J. (1999) Stable isotope tracing of anaerobic methane oxidation in the gassy sediments of Eckernförde Bay, German Baltic Sea. *Am J Sci* **299:** 589–610.

Michaelis, W., Seifert, R., Nauhaus, K., Treude, T., Thiel, V., Blumenberg, M., *et al.* (2002) Microbial reefs in the Black Sea fueled by anaerobic oxidation of methane. *Science* **297:** 1013–1015.

Nauhaus, K., Boetius, A., Krüger, M., and Widdel, F. (2002) *In vitro* demonstration of anaerobic oxidation of methane coupled to sulphate reduction in sediment from a marine gas hydrate area. *Environ Microbiol* **4:** 296–305.

Nauhaus, K., Albrecht, M., Elvert, M., Boetius, A., and Widdel, F. (2007) *In vitro* cell growth of marine archaeal-bacterial consortia during anaerobic oxidation of methane with sulfate. *Environ Microbiol* **9:** 187–196.

Nihous, G.C. (2008) A quantitative interpretation of recent experimental results on stable carbon isotope fractionation by aerobic CH_4-oxidizing bacteria. *Geochim Cosmochim Acta* **72:** 4469–4475.

Orcutt, B., Boetius, A., Elvert, M., Samarkin, V., and Joye, S.B. (2005) Molecular biogeochemistry of sulfate reduction, methanogenesis and the anaerobic oxidation of methane at Gulf of Mexico cold seeps. *Geochim Cosmochim Acta* **69:** 4267–4281.

Orphan, V.J., House, C.H., Hinrichs, K.U., McKeegan, K.D., and DeLong, E.F. (2001) Methane-consuming archaea revealed by directly coupled isotopic and phylogenetic analysis. *Science* **293:** 484–487.

Parkes, R.J., Cragg, B.A., Banning, N., Brock, F., Webster, G., Fry, J.C., *et al.* (2007) Biogeochemistry and biodiversity of methane cycling in subsurface marine sediments (Skagerrak, Denmark). *Environ Microbiol* **9:** 1146–1161.

Pernthaler, A., Pernthaler, J., and Amann, R. (2002) Fluorescence *in situ* hybridization and catalyzed reporter deposition (CARD) for the identification of marine Bacteria. *Appl Environ Microbiol* **68:** 3094–3101.

Rayleigh, J.W.S. (1896) Theoretical considerations respecting the separation of gases by diffusion and similar processes. *Philos Mag* **42:** 493–498.

Reeburgh, W.S. (1982) A major sink and flux control for methane in marine sediments, anaerobic consumption. In *The Dynamic Environment of the Ocean Floor*. Fanning, K.A., and Manheim, F.T. (eds). Lahnham, MD, USA: Lexington Books, pp. 203–217.

Reeburgh, W.S. (2007) Oceanic methane biogeochemistry. *Chem Rev* **107:** 486–513.

Reeburgh, W.S., Hirsch, A.I., Sansone, F.J., Popp, B.N., and Rust, T.M. (1997) Carbon kinetic isotope effect accompanying microbial oxidation of methane in boreal forest soils. *Geochim Cosmochim Acta* **61:** 4761–4767.

Reeburgh, W.S., Tyler, S.C., and Carroll, J. (2006) Stable carbon and hydrogen isotope measurements on Black Sea water-column methane. *Deep Sea Res II* **53:** 1893–1900.

Seifert, R., Nauhaus, K., Blumenberg, M., Krüger, M., and Michaelis, W. (2006) Methane dynamics in a microbial community of the Black Sea traced by stable carbon isotopes *in vitro*. *Org Geochem* **37:** 1411–1419.

Templeton, A.S., Chu, K.-H., Alvarez-Cohen, L., and Conrad, M.E. (2006) Variable carbon isotope fractionation expressed by aerobic CH_4-oxidizing bacteria. *Geochim Cosmochim Acta* **70:** 1739–1752.

Valentine, D.L., Chidthaisong, A., Rice, A., Reeburgh, W.S., and Tyler, S.C. (2004) Carbon and hydrogen isotope fractionation by moderately thermophilic methanogens. *Geochim Cosmochim Acta* **68:** 1571–1590.

Wegener, G., Niemann, H., Elvert, M., Hinrichs, K.-U., and Boetius, A. (2008) Assimilation of methane and inorganic carbon by microbial communities mediating the anaerobic oxidation of methane. *Environ Microbiol* **10:** 2287–2298.

Whiticar, M.J., and Faber, E. (1985) Methane oxidation in sediment and water column environments – Isotope evidence. *Org Geochem* **10:** 759–768.

Supporting information

Additional Supporting Information may be found in the online version of this article:

Fig. S1. Stable isotope enrichment in the methane pool during anaerobic oxidation of methane with sulfate in sediment-free enrichment cultures from Amon Mud Volcano sediment and Black Sea mat.
Table S1. Origin of samples.
Table S2. Medium, incubation and sampling.
Table S3. Analytical methods.
Table S4. Phylogenetic assignment and quantification of microorganisms.
Appendix S1. Calculation of possible effect of mass transfer on isotope fractionation.

Please note: Wiley-Blackwell are not responsible for the content or functionality of any supporting materials supplied by the authors. Any queries (other than missing material) should be directed to the corresponding author for the article.

Supporting Information Holler *et al.* Substantial $^{13}C/^{12}C$ and D/H fractionation during anaerobic oxidation of methane by marine consortia enriched *in vitro*

Table S1. Origin of samples.

Site	Geographic location	Expedition
Hydrate Ridge (HR)	Cascadia Margin, NE Pacific 044° 34.2' N, 125° 08.7' W	RV Sonne, SO-148/1, August 2000
Amon Mud Volcano (AMV)	Eastern Mediterranean Sea 031° 42.6' N, 032° 22.2' E	RV L'Atalante, NAUTINIL, September 2003
Carbonate chimney in methane seep area of Black Sea (BS)	Dnyepr area, Black Sea 044° 46.4'N, 031° 58.2' E	RV Poseidon, POS-217/3, October 2004

Table S2. Medium, incubation, and sampling.

Medium	Artificial marine medium with 28 mM sulfate, 30 mM $NaHCO_3$, 1 mM Na_2S (details given by Widdel and Bak, 1992);
Incubation volume	250 ml (headspace-free)
Incubation temperatures	HR and BS, 12 °C; AMV, 20 °C
Sampling	Withdrawal of 6.5 ml (with simultaneous injection of medium), addition of conc. 0.05 ml $ZnCl_2$ (0.5 g ml^{-1}) for inactivation and absorption of sulfide

Table S3. Analytical methods.

Methane determination	GC 14 gas chromatograph (Shimadzu);Supel-Q Plot column, 30 m × 0.53 mm (Supelco), 110 °C;carrier gas, N_2; flame ionization detector
Sulfide determination	Colorimetric determination, methylene blue formation reaction in small assay (Aeckersberg *et al.*, 1991)
$^{13}C/^{12}C$ isotope analysis	Isotope ratio combustion mass spectrometry (IRC-MS): Separation of methane via G 1530A gas chromatography(Agilent Technology), hot injection, 200 °C; Supel-Q Plot column, 30 m × 0.53 mm (Supelco), 40 °C; carrier gas, He; Methane combustion at CuO-Ni-Pt catalyst (ThermoFinnigan), 940°C;(precision checked with methane standard)
D/H isotope analysis	Essentially as $^{13}C/^{12}C$ isotope analysis, but with pyrolysis at 1450 °C of methane to yield H_2

Table S4. Phylogenetic assignment and quantification of microorganisms.

Total cell counts	Cells on filters were stained with 4′,6-diamidino-2-phenylindol (DAPI)
Cell numbers in aggregates	Estimated assuming spherical cells (volume, 0.2 μm^3), occupying 74% of the aggregate volume (Lösekann *et al.*, 2007).
Phylotype quantification	Catalyzed reporter deposition fluorescence *in situ* hybridization (CARD-FISH; Pernthaler *et al*., 2002), targeting 16S rRNA: Probes ANME-2a-647, ANME-2c-622: Cell permeabilizationwith sodium dodecyl sulfate (50 mg ml^{-1}), 10 min, 22 °C (Knittel *at al*., 2005); Adjusted stringency: ANME-2a-647, 40% formamide; ANME-2c-622, 45% formamide Probe DSS658: Cell permeabilizationwith lysozyme (10 mg ml^{-1}), 15 min, 37 °C (Manz *et al*., 1998); Adjusted stringency: 60% formamide ProbeANME-1-350: Cell permeabilization with proteinase K (15 µg ml^{-1}), 2 min, 22 °C, Adjusted stringency: 40% formamide Oliogonucleotide probes were purchased from biomers.net (Ulm, Germany)

References

Aeckersberg, F., Bak, F., and Widdel, F. (1991) Anaerobic oxidation of saturated hydrocarbons to CO_2 by a new type of sulfate-reducing bacterium. *Arch Microbiol* **156:** 5–14.

Lösekann, T., Knittel, K., Nadalig, T., Fuchs, B., Niemann, H., Boetius, A., and Amann, R. (2007) Diversity and abundance of aerobic and anaerobic methane oxidizers at the Haakon Mosby Mud Volcano, Barents Sea. *Appl Environ Microbiol* **73:** 3348–3362.

Knittel, K., Lösekann, T., Boetius, A., Kort, R., and Amann, R. (2005) Diversity and distribution of methanotrophic archaea al cold seeps. *Appl Environ Microbiol* **71:**467–479.

Manz, W., Eisenbrecher, M., Neu, T.R., and Szewzyk, U. (1998) Abundance and spatial organization of Gram-negative sulfate-reducing bacteria in activated sludge investigated by *in situ* probing with specific 16S rRNA targeted oligonucleotides. *FEMS Microbiol Ecol* **25:** 43–61.

Pernthaler, A., Pernthaler, J., and Amann, R.(2002) Fluorescence *in situ* hybridization and catalyzed reporter deposition (CARD) for the identification of marine Bacteria. *Appl Environ Microbiol* **68:** 3094–3101.

Widdel, F., and Bak, F. (1992) Gram-negative mesophilic sulfate-reducing bacteria. In *The Prokaryotes*. Balows, A., Trüper, H.G., Dworkin, M., Harder, W., and Schleifer, K.-H. (eds). New York: Springer-Verlag, pp. 3352–3378.

Appendix S1

Calculation of possible effect of mass transfer on isotope fractionation

For convenience, we treated an assumed cell aggregate of 50 µm diameter as a one-dimensional system with bidirectional diffusion of methane and a cell-specific methane consumption rate of 3.8×10^{-16} mol cell^{-1} day^{-1}. The following diffusion coefficients (at 12°C) were used:

$^{12}CH_4$ (M_r = 12):	$^{13}CH_4$ or CDH_3 (M_r = 13):
$D = 1.32 \times 10^{-5}$ cm^2 s^{-1}	$D = (12/13)^{0.5} \times 1.32 \times 10^{-5} = 1.27 \times 10^{-5}$ cm^2 s^{-1}

With these values, the calculated concentration gradient was negligible and the isotope composition of methane did not change.

The model was stressed with (a) diffusion reduced by a factor of 10^5, (b) methane consumption increased by a factor of 10^3, or (c) a concentration of supplied methane of 10^{-6} M. These variations neither resulted in significant diffusion limitation nor in a significant of the isotope pattern ($\Delta\delta^{13}C$, $\Delta\delta^{2}H < 0.1$‰).

III.2

Carbon and sulfur back flux during anaerobic microbial oxidation of methane and coupled sulfate reduction

Thomas Holler,[1] Gunter Wegener,[1] Helge Niemann,[1,3] Christian Deusner,[1,4] Timothy G. Ferdelman,[1] Antje Boetius,[1,2] Benjamin Brunner[1] and Friedrich Widdel[1]*

Manuskript in Vorbereitung

---

[1]Max Planck Institute for Marine Microbiology, Bremen 28359, Germany

[2]Alfred Wegener Institute for Polar and Marine Research, Bremerhaven 27515, Germany

[3]Current address: Institute for Environmental Geosciences, University of Basel, Bernoullistrasse 30, Basel, Switzerland

[4]Current address: Leibniz Institute of Marine Sciences at the University of Kiel, Wischhofstrasse 1–3, Kiel 24148, Germany

***Corresponding author**

Abstract

Microbial degradation of substrates to terminal products is commonly understood as a unidirectional process. In individual enzymatic reactions, however, a certain reversibility (reverse reaction, product back flux) is common. Hence, it is also possible that entire pathways of microbial degradation are associated with back flux from the accumulating product pool via intracellular intermediates into the substrate pool. Here, we investigated carbon and sulfur back flux during the anaerobic oxidation of methane (AOM) with sulfate. AOM is one of the least exergonic microbial catabolic processes known to date. The involved enzymes must operate not far from the thermodynamic equilibrium, and such an energetic situation is likely to favor product back flux. Indeed, cultures of highly enriched archaeal-bacterial consortia, performing net AOM with unlabeled methane and sulfate, converted label from ^{14}C-bicarbonate and ^{35}S-sulfide to ^{14}C-methane and ^{35}S-sulfate, respectively. Back fluxes reached up to 5 and 13%, respectively, of the net AOM rate. The existence of catabolic back fluxes in the reverse direction (upstream) of net reactions has implications for biogeochemical isotope labeling and fractionation studies. In environments where biochemical processes are close to thermodynamic equilibrium, measured fluxes of labeled substrates to products are not equal to the microbial net rates. Detection of a reaction *in situ* by labeling may not even indicate a net reaction occurring in the direction of label conversion but may reflect the reverse component of a so far unrecognized net reaction. Furthermore, the natural isotopic composition of the substrate and product pool will be determined by both, the *in situ* forward and back flux rather than by an alleged unidirectional forward flux alone. This may have to be considered in the interpretation of stable isotope records.

Introduction

Microbial catabolic (degradation) rates in habitats and cultures are frequently quantified by isotope labeling of substrate and measuring the rate of label appearance in the product pool. Label flux is usually regarded as unidirectional and thus assumed to represent the net rate of substrate conversion. In enzyme kinetics, however, bi-directionality (reversibility) of biochemical reactions is a long-established feature (Haldane, 1930; Boyer, 1959; Cornish-Bowden, 2004; Bisswanger, 2008; Purich, 2010), as in chemical kinetics. If a substrate is converted to a product via an entire pathway and each reaction occurs with back reaction, some steady flux of the terminal product via intermediate pools back to the substrate pool should occur. Such back flux should be measurable by isotope labeling of the product, as in enzyme kinetics where measurement of such "isotope exchange" is an established method (references as above).

Concept of catabolic back flux and energy considerations

Catabolic processes can be portrayed as a cascade of enzymatically catalyzed steps. Viewed stochastically, only a fraction of enzyme molecules performs the forward reaction for any given enzymatic step. Simultaneously, another fraction performs the back reaction[1]. This concept of substrate and product flux (or forward- and back-flux) is illustrated in Fig. 1a for the reaction A $\rightarrow$ P. If reactions converting A to P are reversible, substrate output (v_{-1}) not only includes the part that never reached the product side ($^{\bullet}v_{-1}$) but also substrate derived from product ($^{*}v_{-1}$). In a steady state, the sum of the uptake rates must equal the sum of the release rates, i.e. $v_{+1} + v_{-n} = v_{-1} + v_{+n}$. Rearrangement yields the net rate, v:

$$v_{+1} - v_{-1} = v_{+n} - v_{-n} = v. \qquad \textbf{[1]}$$

The substrate output derived from product ($^{*}v_{-1}$) and the product output derived from substrate ($^{\bullet}v_{+n}$) are experimentally accessible by isotope labeling. For better distinction, we designate these rates $^{\bullet}v_{+n} = f_{+}$ and $^{*}v_{-1} = f_{-}$. The net rate can be expressed by f_{+} and f_{-}. Writing $v = v_{+1} - {}^{\bullet}v_{-1} - f_{-}$ (net disappearance of substrate) and considering mass conservation, $v_{+1} - {}^{\bullet}v_{-1} = f_{+}$, yields

[1] The existence of an enzyme catalyzing only one direction of an essentially reversible reaction (while not gaining energy from another source or not undergoing a permanent change) may be falsified as follows: If such an enzyme existed, its addition to a system in which concentrations of reactants (R) and products (P) have reached the thermodynamic equilibrium ($\Delta G = 0$ for R $\rightleftharpoons$ P) would cause a spontaneous shift away from the equilibrium. Such a "reaction valve" (a variant of "Maxwell's demon") would be in conflict with the second law of thermodynamics.

$$v = f_+ - f_-. \qquad [2]$$

Hence, for any catalytic system with reverse reactions in a steady state, the net rate is expressed by three pairs of rates (Eq. **1 and 2**; Fig. 1b), with f_+, f_- and v being experimentally

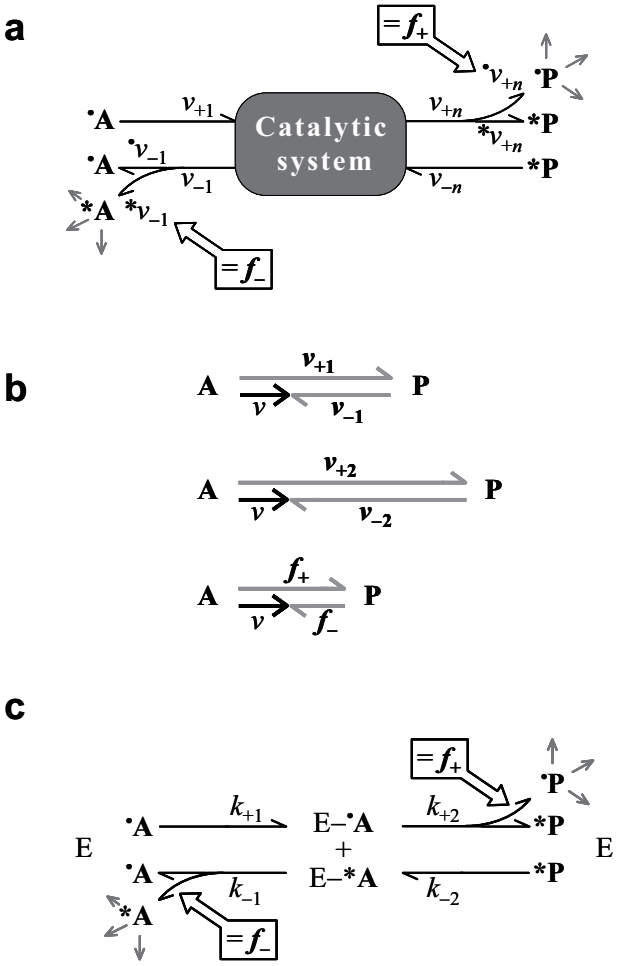

Fig. 1. Definition of forward and back flux during the net reaction A → P in a steady state catalytic system. Arrows indicate rates (velocities). The fate of substrate and product is followed by different label (A•, P*) of the initial pools. All reactions including uptake or binding and release are reversible. Forward (f_+) and back (f_-) flux are the concentrations (amounts per investigated volume) of P• and A* most recently derived per time from A• and P*, respectively. Hence, return to the side of their origin with progressing reaction is neglected by examining a short time interval (A* in A• and P• in P* remaining very dilute). **a** Catalytic system with reversible but otherwise unknown internal reactions. Release of A and P includes both, the returned fraction that never reached the other side, and the fraction directly derived from the other side. **b** "Vector" model of rates indicated by lengths or arrows. The same net rate (v) is the difference of uptake (binding) and release of substrate (v_{+1}, v_{-1}) and of product (v_{+2}, v_{-2}) as well as the difference between forward and back flux (f_+, f_-). The "vector" model was calculated (see text) for the enzymatic reaction using (in rate units): $v_{+1} = 6$, $v_{-1} = 4$, $v_{+2} = 9$, $v_{-2} = 7$; result: $v = 2$, $f_+ = 4.15$; $f_- = 2.15$. **c** Simple reversible enzyme (E) model. Forward and back flux are determined by stochastic decomposition of enzyme-substrate complex. The rate constants k_{+1}, k_{-1}, k_{+2}, k_{-2} correspond to v_{+1}, v_{-1}, v_{+2}, v_{-2}.

accessible. During net reaction A $\rightarrow$ P there are the inequalities

$$v_{+1},\ v_{+n} > f_{+} > v \text{ and } f_{+} > f_{-} . \qquad \textbf{[3]}$$

In chemical reactions the back flux becomes more significant the closer the net reaction approaches thermodynamic equilibrium. At equilibrium forward and back reactions are equivalent ($f_{-}/f_{+} = 1$) and no net reaction takes place ($v = 0$).

Thermodynamic values, such as free energy, are based on macroscopic time-independent equilibria, and cannot in principle predict reactions rates, which are determined by molecular mechanisms. Nevertheless, rates of forward and reverse reactions must be governed by substrate and product concentrations in such way that they yield a zero net rate at macroscopic equilibrium. This "thermodynamic constraint" is fundamental in enzyme kinetics (Haldane, 1930; Cleland, 1963; Cornish-Bowden, 2004; Bisswanger, 2008; Purich, 2010). In enzyme kinetics, the thermodynamic constraint of rates is most easily derived for a simple enzymatic reaction involving one substrate and product and formulated with a lumped enzyme-bound state, EA (Fig. 1c). As for a reversible two-step purely chemical reaction, formulation of equilibrium conditions (see Appendix A3) yields $k_{+1}k_{+2}/(k_{-1}k_{-2}) = [P]_e/[A]_e$ ($[P]_e$, $[A]_e$, concentrations at equilibrium). This is one form of the Haldane relationships. A more common formulation through multiplying nominator and denominator with $k_{-1} + k_{+2}$includes the experimentally accessible Michaelis (composite) constants, $(k_{-1} + k_{+2})/k_{+1} = K_{m+}$ and $(k_{-1} + k_{+2})/k_{-2} = K_{m-}$for the forward and reverse reaction, respectively. By designating $k_{+2} = k_{cat+}$ and $k_{-1} = k_{cat-}$ (catalytic constants for product and substrate formation, respectively) the Haldane relationship can be expressed as

$$\frac{k_{+1}k_{+2}}{k_{-1}k_{-2}} = \frac{k_{cat+}/K_{m+}}{k_{cat-}/K_{m-}} = \frac{[P]_e}{[A]_e} = K_e. \qquad \textbf{[4]}$$

The formulated equality of the kinetic equilibrium ratio $[P]_e/[A]_e$ with the thermodynamic equilibrium constant, K_e, treats concentrations (in kinetics) and activities (in thermodynamics) as numerically equivalent. (Strictly speaking, activity coefficients would have to be included.) Hence, as illustrated in Eq. **4**, kinetic constants of enzymes catalyzing the same reaction cannot vary independently of each other.

The thermodynamic equilibrium constant, K_e, is an exponential function of the standard free energy, $\Delta G°$ (see Appendix A3.1):

$$K_e = e^{-\Delta G°/(R\,T)} \qquad \textbf{[5]}$$

Thus, at equilibrium the rate constants k_{+1}, k_{+2}, k_{-1} and k_{-2} are connected to the experimentally accessible rates f_- and f_+ by the relationship (Appendix A3.2):

$$\frac{f_-}{f_+} = \frac{k_{-1}k_{-2}[\mathrm{P}]}{k_{+1}k_{+2}[\mathrm{A}]} = \frac{[\mathrm{P}]}{K_\mathrm{e}[\mathrm{A}]} = e^{\Delta G/(RT)} \qquad \textbf{[6]}$$

Under non-equilibrium condition, i.e. where the net flux is non-zero ($v \neq 0$ and $[\mathrm{A}]/[\mathrm{P}] \neq 1/K_\mathrm{e}$, $\Delta G \neq 0$) and where f_- relative to net rate $v = f_+ - f_-$, we can re-formulate Eq. **6** as

$$\frac{f_-}{v} = \frac{1}{K_e[\mathrm{A}]/[\mathrm{P}] - 1} = \frac{1}{e^{-\Delta G/(RT)} - 1} \qquad \textbf{[7]}$$

Eq. **7** shows that the back flux relative to the net rate must increase with decreasing "distance" from equilibrium. *Vice versa*, negligible back flux relative to the net rate can be only expected in case of strongly exergonic reactions (very negative ΔG, large denominator).

Back flux through weakly exergonic catabolism

Like enzymatically catalyzed reactions, one expects that back flux through the entire chain of catabolic reactions is more significant the less exergonic the overall reaction becomes. This follows from the “principal of detailed balancing”, which states that, at equilibrium, each step of an overall reaction must also be in equilibrium (Moore & Pearson, 1981). A weakly exergonic catabolism (energy metabolism) is common in strictly anaerobic microorganisms (e.g., Thauer et al., 1977; Thauer & Morris, 1984; Schink, 1997; Jackson & McInerney, 2002; Deppenmeier & Müller, 2008; Stams & Plugge, 2009). Still, the possibility of product back flux in anaerobes has been treated only in relatively few labeling studies. The probably best-known example is the conversion of added ^{14}C-methane to ^{14}C-carbon dioxide during net methane formation by various methanogenic archaea (Zehnder & Brock, 1979; Harder, 1997; Moran et al., 2005; Moran et al., 2007; Meulepas et al., 2010b). The key reaction of this back flux, the methyl carbon exchange between added $^{13}CH_4$ and its direct precursor, $^{12}CH_3$-coenzyme M, was recently quantified in an enzymatic assay with all reaction partners present at equilibrium concentrations, viz. without net methane formation or consumption (Scheller et al., 2010). Furthermore, conversion of added ^{35}S-sulfide to sulfate during its net reduction with lactate by *Desulfovibrio* has been observed (Trudinger & Chambers, 1973). The incorporation of added $^{14}CO_2$ into the carboxyl group of acetate during its oxidation via the Wood-Ljungdahl (carbon monoxide dehydrogenase) pathway in an anaerobe is an example of partial product back flux (Schauder et al., 1986; Spormann & Thauer, 1989).

Whereas these studies suggest reversibility of anaerobic processes close to thermodynamic equilibrium for specific substrate-product reactions, they do not demonstrate the reversibility of a catabolic pathway combining all substrates and products. Reversibility of a specific substrate-product combination does not provide evidence for the reversibility of an entire process.

A catabolic process where reversibility combining all substrates and products should be observable in AOM which is one of the least exergonic reactions sustaining life:

$$CH_4(g) + SO_4^{2-} + 2\ H^+ \rightarrow CO_2\ (g) + H_2S(aq) + 2\ H_2O \qquad \textbf{[8]}$$

$$\Delta G^\circ_{pH7} = -21\ \text{kJ mol}^{-1}$$

(ΔG *in situ* often between –20 and –40 kJ mol^{-1}; Knab et al., 2008; Alperin & Hoehler, 2009). It is of global relevance because it counteracts methane release from marine sediments into the oxic biosphere (Reeburgh, 2007; Knittel & Boetius, 2009; and references therein). AOM is catalyzed by consortia of phylogenetically distinct Euryarchaeota (anaerobic methanotrophs, ANME-groups) and associated Deltaproteobacteria (Hinrichs et al., 1999; Boetius et al., 2000; Knittel et al., 2003; Niemann et al., 2006; Schreiber et al., 2010) that are assumed to perform sulfate reduction. Labeling studies with natural sediment samples with AOM activity provided hints of $^{14}CO_2$ conversion to $^{14}CH_4$ during net AOM by the indigenous consortia (Treude et al., 2007; Orcutt et al., 2008). The mode of coupling, which appears not to involve conventional anaerobic intermediates such as H_2 or acetate, is a matter of discussion (Sørensen et al., 2001; Nauhaus et al., 2002; Orcutt & Meile, 2008; Alperin & Hoehler, 2009; Meulepas et al., 2010a).

Here we used essentially detritus-free, marine consortia that had been highly enriched *in vitro* with CH_4 and SO_4^{2-} to quantify the back flux of both, carbon and sulfur during AOM. To our knowledge, this is the first demonstration of "simultaneous" reversibility in a complete catabolic microbial system, coupled to low energy yields.

Materials and methods

Origin, enrichment and preparation of cultures for experiments

The investigated enrichment cultures originated from anoxic sediment of two marine methane seep areas, Hydrate Ridge (HR; Cascadia Margin, Oregon, NE-Pacific) and Isis Mud Volcano sediment (MV; Eastern Mediterranean Sea). Sediments had been sampled during the *R/V Sonne* (SO-148/1, 2000) *and R/V L'Atalante* (NAUTINIL, 2003) expeditions, respectively. Cell propagation in anoxic synthetic seawater medium (Widdel & Bak, 1992) with methane and sulfate as the only energy source has been described (Nauhaus et al., 2007; Holler et al., 2009).

Before the radiotracer studies, cultures were allowed to settle; the sedimented microorganisms were transferred to new medium with sulfate and sulfide concentrations. Aliquots were then transferred to culture tubes incubated at their temperature optima (HR, 12 °C; MV, 20 °C; Nauhaus et al., 2002; Holler et al., 2009).

Highly enriched consortia with their inherently slow growth (Nauhaus et al., 2007) were only available in limiting quantities and therefore used sparingly. Experiments with ^{14}C-bicarbonate and ^{35}S-sulfide labeling were carried out subsequently at different times, and the batches available at one time differed from that at another time with respect to cell density and volumetric activity, ranging from 70 to 120 μmol l^{-1} day^{-1} for HR and 50 to 190 μmol l^{-1} day^{-1} for MV. Within an experiment at a given time, however, the same enrichment batch was distributed equally so as to establish equal volumetric activities.

Incubation experiments with ^{14}C-label

Resuspended enrichments were distributed in amounts of 1 ml in 5 ml-tubes. Tubes were completely filled (headspace-free) with anoxic synthetic seawater medium saturated before with unlabeled CH_4 (under a gas phase of 150 kPa). Tubes were sealed with elastic butyl rubber. Controls were prepared with N_2 instead of CH_4 or without sulfate, or with sterilized (20 g formaldehyde l^{-1}) cultures. CH_4 oxidation and back flux were measured by injecting $^{14}CH_4$ (American Radiolabeled Chemicals) or ^{14}C-$NaHCO_3$ (Perkin Elmer), respectively, from aqueous solutions with high specific activity. Final specific activities in the medium were 6.5×10^8 Bq mol^{-1} for CH_4 (total concentration, 1.5×10^{-3} mol l^{-1}) and 4.5×10^8 Bq mol^{-1} for inorganic carbon (total concentration, 30×10^{-3} mol l^{-1}). After four days of incubation, the content of a tube was fixed by transfer to 25 ml NaOH (0.6 M) in a glass vial (50 ml). Radioactivity of carbonate or methane was determined after separating both fractions

as described (Treude et al., 2005). In brief, methane was stripped off with air, oxidized at 850 °C with CuO and trapped with 2-phenylethylamine base solution. Carbonate was subsequently acidified, and released CO_2 was again trapped. Trap solutions were mixed with Ultima Gold XR (Perkin Elmer) and analyzed in a 2900TR LSA liquid scintillation counter (Packard).

Incubation experiments with ^{35}S-label

To measure the sulfate reduction rate via labeling, a solution of ^{35}S-Na_2SO_4 (Amersham) was injected into a 5 ml culture tube (see above). The specific activity in the medium was 5.5×10^8 Bq mol^{-1} (total sulfate concentration, 28×10^{-3} mol l^{-1}). After 4 days, reduced sulfur was liberated with $CrCl_2$ and HCl and for analysis (see below) trapped in zinc acetate (Kallmeyer et al., 2004).

^{35}S-sulfide for labeling experiments was freshly generated from ^{35}S-Na_2SO_4 (see above) by bacterial reduction. *Desulfovibrio vulgaris* (DSM 2119) was incubated in a 20 ml tube containing 10 ml anoxic freshwater medium (Widdel and Bak, 1992), H_2 gas (with 20% CO_2; 150 kPa total pressure) as electron donor and 5×10^{-3} mol l^{-1} Na_2SO_4 with an adjusted label activity of 2.5×10^9 Bq mol^{-1}. After complete reduction of sulfate, the culture was mixed with anoxic H_3PO_4 (5 ml, 1 M). A slow N_2 stream was passed through the solution and headspace, further through anoxic citrate buffer (10 ml, 0.1 M, pH 4), and finally through a series of three anoxic solutions of $ZnCl_2$ (each 15 ml, 0.4 M) to trap sulfide. The collected ZnS suspension (75 ml) was acidified with H_3PO_4 (50 ml, 1 M) under an N_2 headspace in an anoxic 156 ml vial to release labeled sulfide. The preparation via a gas phase and citrate buffer avoided transfer of other sulfur species that may have been present as impurities in the *Desulfovibrio* culture.

Labeled H_2S gas in N_2 was withdrawn in portions of 0.2 ml (6 to 9 kBq), injected into the headspace of 16 ml culture tubes with 10 ml medium, and for 24 h equilibrated with the aqueous phase. Then, methane (200 kPa, overpressure) was injected, and samples were incubated on a rotary shaker. After 0, 3, 6, 8, 11, 15 and 19 days, four culture tubes (replicates) were sacrificed for analysis. Their content was mixed with an anoxic zinc acetate solution (0.25 M; 6 ml per tube) to fix sulfide. Total ^{35}S was determined in aliquots. $^{35}SO_4^{2-}$ was determined after thorough removal of ZnS by centrifugation (15 min, 2500 × *g*) and ultra-filtration (Anotop 25 membrane filter, 0.02 µm-pores; Whatman). Removal of ZnS was verified in filtrate aliquots by acidification with HCl (7 M; 0.5 ml per ml), purging with N_2, and scintillation counting (see above).

To analyze possible formation of ^{35}S-thiosulfate from labeled sulfide, unlabeled thiosulfate (final concentration, 1 mM) was added to filtrate aliquots. Sulfate and thiosulfate were separated by an ion chromatograph (Waters) equipped with an IC-Pak anion exchange column (50 × 4.6 mm) and conductivity detector. The eluent was isophthalic acid (1 mM, pH 4.5) in 10% aqueous methanol (10%, v/v; flow rate 1.0 ml min^{-1}). The separated fractions were checked for ^{35}S. However, ^{35}S-thiosulfate was not detectable.

Resulting samples with ^{35}S-label were mixed with LumaSafe Plus (Lumac LSC) and analyzed by liquid scintillation counting.

Other analyses

Total methane was determined using a 5890A gas chromatograph (Hewlett Packard) equipped with a stainless steel Porapak-Q column (183 m × 3.2 mm, 80/100 mesh; Agilent Technology) and flame ionization detector. Sulfide was determined colorimetrically using the methylene blue formation reaction in a miniaturized assay (Aeckersberg et al., 1991).

Determination of the reverse reaction rate

In catabolic conversion of substrate product with reversibility, A ⇌ P, forward and back flux (see introduction) are f_+ and f_- (moles volume^{-1} time^{-1}). When product label, P*, is added, appearance of A* reveals the back flux. If the label is a radioisotope with noticeable decay, error in label quantification is avoided by measuring radioactivity in all samples at the same time after the experiment; the specific isotope decay rate is independent of the chemical composition. The infinitesimal concentration d[A*] formed during an infinitesimal time dt depends on f_+ and f_-, heavy isotope discrimination in each direction (α_-, α_+; ≥1), and the proportion of label in total product and substrate (brackets indicate concentrations):

$$\mathrm{d[A^*]} = f_- \,\mathrm{d}t \frac{1}{\alpha_-} \frac{[\mathrm{P^*}]}{[\mathrm{P}]} - f_+ \,\mathrm{d}t \frac{1}{\alpha_+} \frac{[\mathrm{A^*}]}{[\mathrm{A}]} \qquad \textbf{[9]}$$

Treatment is simplified by assuming α_-, $\alpha_+ \approx 1$, and that the label proportion in the reactant pool remains very low ([A*]/[A] << [P*]/[P]) so that return by f_+ can be neglected. Eq. **9** then yields

$$\mathrm{d[A^*]} = f_- \,\mathrm{d}t \frac{[\mathrm{P^*}]}{[\mathrm{P}]} \qquad \textbf{[10]}$$

P* is increasingly diluted by steadily forming unlabeled P (Appendix A2 Fig. A2-1). If an increase Δ[A*] is measured after a short enough incubation time, Δ*t*, during which [P*]/[P] remains essentially constant, Eq. **10** can be simplified and rearranged to

$$f_{-} = \frac{\Delta[A^*]}{\Delta t}\frac{[P]}{[P^*]_0} = \frac{\Delta[A^*]}{\Delta t}\frac{[P]_0 + [P^*]_0}{[P^*]_0} \qquad \textbf{[11]}$$

$[P]_0$ is the initial product concentration and $[P^*]_0$ the initially label concentration. If $[P^*]_0 << [P]_0$, Eq. **11** is simplified to

$$f_{-} = \frac{\Delta[A^*]}{\Delta t}\frac{[P]_0}{[P^*]_0} \qquad \textbf{[12]}$$

Such treatment is similar as the common determination of substrate fluxes in habitats via labelling and measuring product label (Sorokin, 1962; Jørgensen, 1978). We applied Eq. **12** to evaluate ^{14}C back fluxes in the methane-bicarbonate system. Back flux of inorganic carbon during AOM was determined as $^{14}CH_4$ recovered from ^{14}C-bicarbonate after four days of incubation (end-point measurement) and applying Eq. **12** with $\Delta[A^*] = [^{14}CH_4]$, $[P]_0 = 0.031$ mol l^{-1}, and $[P^*] = [H^{14}CO_3]$ added (C_{inorg} calculated from added $NaHCO_3/CO_2$ buffer). A high concentration of C_{inorg} was initially added as $NaHCO_3$ (a common natural buffer for cultivation of AOM consortia and many other anaerobes). Based on the net AOM rate derived from methane-dependent sulfide formation, C_{inorg} increased during incubation from 30 (initial) to ≤30.4 mmol l^{-1}.

In contrast to the concentration of bicarbonate, that of sulfide was low at the beginning (<0.5 mM). This is advisable for cultivation anaerobes as sulfide can be inhibitory. However, now dilution of product label during AOM was significant and [P] in Eq. **10** is expressed as a function of time. Assuming that the net rate, *v*, of A → P is largely independent of [A] (zero-order behaviour, as common in many microbial batch incubations), and that cell growth is negligible during incubation the experimental data follow a straight-line fit with the slope f_{-}/v when displayed according to (for derivation see Appendix A2):

$$\ln\frac{[P^*]_0}{[P^*]_0 - [A^*]} = \frac{f_{-}}{v}\ln\frac{[P]}{[P]_0}. \qquad \textbf{[13]}$$

Assuming the aforementioned prerequisites (negligible isotope fractionation, concentration-independent rates, label concentration in the sulfate pool remaining low), we applied Eq. **13** with $[P^*]_0 = [H_2{}^{35}S]$ added, $[A^*] = [^{35}SO_4{}^{2-}]$, $[P] = [S_{red}]$ and $[P]_0 = [S_{red}]_0$ (S^{red}, chemically quantified sulfide).

Results

In the methane-consuming, sulfide-producing cultures enriched via repeated transfer (over some years) from sediment, loosely flocculating cell aggregates had been propagated while the sediment matrix with detritus had been diluted away. Consortia of archaea (ANME-2 groups) and Deltaproteobacteria were abundant (95 to 99% of detectable cells, according to DAPI and specific 16S rRNA probing; Nauhaus et al., 2007; Holler et al., 2009). Methane consumption and sulfide formation quantified chemically were always in accordance with Eq. **8**. The specific (dry mass related) activities of the HR and MV cultures were 0.3 and 2.0 mmol day^{-1} g^{-1}, respectively. Additional substrate labeling experiments with $^{14}CH_4$ and $^{35}SO_4^{2-}$ and product label quantification yielded a molar ratio between formed CO_2 and H_2S of 0.97/1 (HR) and 1.07/1 (MV), again in accordance with Eq. **8**[2].

Chemical analysis of incubations without methane revealed only marginal methane production (<0.05% of AOM rate). The rate of sulfide production without methane was <1% of the rate achieved in the presence of methane. This showed that background methanogenesis and sulfate reduction with endogenous compounds or dead cell carbon was essentially absent or very small, respectively. Cultures were therefore suitable to study the flux of labeled inorganic carbon and sulfide into the pools of methane and sulfate, respectively, when these were present as substrates.

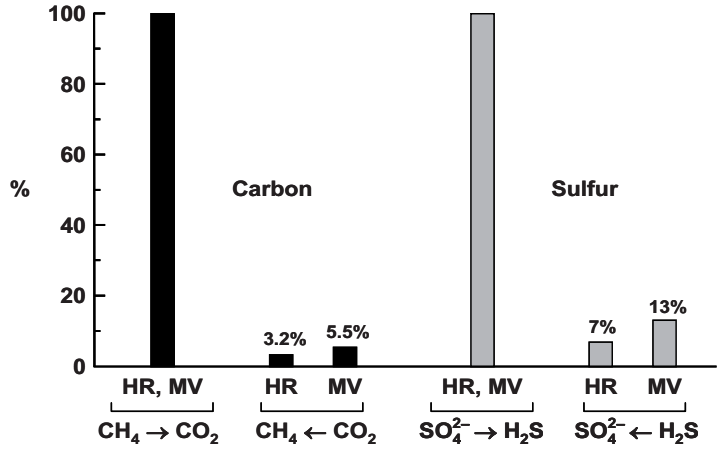

Fig. 2. Comparison of reverse (back flux) to net reactions (set to 100%) during the anaerobic oxidation of methane with sulfate by highly enriched consortia from Hydrate Ridge (HR) and Isis Mud Volcano (MV). The net reaction was measured by chemical quantification of product formation. (For data analysis underlying sulfur back flux see Fig. 3)

[2] Like chemical quantification (Nauhaus et al., 2002), such labeling experiments are not precise enough to reveal the proportion of methane-carbon channeled into biosynthesis as deviation from the 1:1 stoichiometry; only around 1% of consumed methane in assimilated (Nauhaus et al., 2007).

The rate of carbon back flux was 3.2 and 5.5% (HR, MV, respectively) of the net AOM rate determined by chemical quantification (Fig. 2). We also measured carbon isotope exchange while the net reaction was prevented by omission of sulfate in the presence of methane. Label from ^{14}C-inorganic carbon still appeared in the methane pool at rates of 2.4 and 2.3% (HR, MV, respectively) of the AOM rate with sulfate.

Every 2 to 3 days four replicates per series were sampled and fixed for analysis of sulfide concentrations, overall ^{35}S-content, formed $^{35}SO_4^{2-}$and other potentially labeled sulfur species. The time series yielded in methane dependent sulfate-reduction rates of 190 µmol l^{-1} day^{-1} (MV; Fig. 3) and 120 µmol l^{-1} day^{-1} (HR). While the overall ^{35}S activity was stable during the whole time series, increasing amounts of tracer were recovered in the $^{35}SO_4^{2-}$ pool of AOM-active samples. However, in contrast to constant sulfate reduction rates, label transfer from sulfide to sulfate pool decreased during the course of the experiment (as discussed in the previous section). The determined rates of sulfur back flux (Fig. 2 and 3) were 7 and 13% (HR, MV, respectively) of the AOM rate based on chemical quantification. The isotope exchange between the sulfide and sulfate pool was negligible when AOM was prevented by omission of methane, (<1% of AOM rate with methane and sulfate).

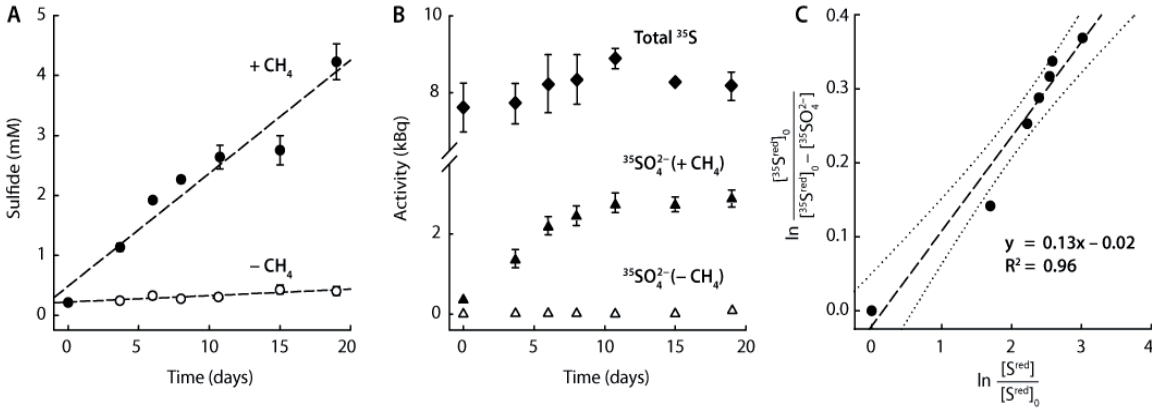

Fig. 3. Time course experiment with labeled sulfide (product) with highly enriched, detritus-free consortia from Isis Mud Volcano that perform anaerobic oxidation of methane. **A**. Developing sulfide concentrations in the presence (●) and absence (○) of methane. **B**. Development of ^{35}S-activity in the sulfate pool during incubation with (▲) and without (Δ) methane as electron donor. The total ^{35}S-activity (◆; sulfate + sulfide) is also indicated. The shown radiolabel was determined after incubation at the same time to eliminate the effect of decay. **C**. Double logarithmic plot according to Eq. **13** to calculate the reverse rate; dotted line marks the 95% confidence interval.

Discussion

A catabolic pathway within a single prokaryotic organism or at the community level (e.g. a consortium of organisms) represents a complex sequence of reactions involving more than one substrate and product. Still, the principles of microscopic reversibility and detailed balancing (Moore & Pearson, 1981) must be valid for an entire pathway. Therefore, the less exergonic the reaction becomes, or the closer to thermodynamic equilibrium, the more relevant becomes the back flux relative to the net rate. AOM is one of the least exergonic processes. Under the established conditions for cultivation and incubation provided in this study, the calculated (Nauhaus et al., 2002) free energy change is –25 to –35 kJ mol^{-1}. The range in habitats is often –20 to –40 kJ mol^{-1} (Knab et al., 2008; Alperin and Hoehler, 2009). The free energy actually dissipated by (driving) the *in vivo* catabolism is less negative than calculated values, due to coupling to energy conservation. Such coupling may be an important factor contributing to catabolic reversibility and back flux. Largely irreversible, energy-dissipating reactions during AOM are only expected in the anabolism (biosynthesis). As expected, both sulfate reduction and AOM were found to be reversible under these conditions in our experiments. The measured back flux of inorganic carbon (up to 5%) was at least one order of magnitude higher than methane-carbon back flux during true methanogenesis (Zehnder and Brock, 1979; Harder, 1997; Moran et al., 2005; Meulepas et al. 2010). The relative sulfur back flux during AOM was even higher (up to 13%). The results clearly demonstrate large fluxes of ^{35}S-labeled sulfide back to sulfate, and ^{14}C-labeled bicarbonate back to methane during the sulfate mediated oxidation of methane. These findings provide insights on the regulation of the catabolism of the coupled processes AOM and sulfate reduction and have consequences for the study of biochemical processes in habitats.

Implications for regulation of catabolism of coupled processes

Formulas connecting the kinetic behavior of isotope exchange with mechanistic enzyme models are usually complex (treatment for instance in Boyer, 1959; Britton, 1966; Britton & Dann, 1978; Cornish-Bowden, 2004; Purich, 2010). A quantitative explanation of the measured back flux in our experiments on the basis of enzyme mechanisms is impossible in view of the complexity of the system and lack of knowledge of reactions. While this concept holds for a general assessment of the likeliness that a process is reversible (small negative free energy change) and valid for a single reaction, it cannot be generalized and used for comparison of the reversibility of different catabolic pathways. Nevertheless, the general

relationship between free energy and relative rates of back to net flux as expressed for a simple reaction (Eq. **7**) is expected to hold for a given catabolic pathways.

Free energy change is only one parameter governing the product back flux in catabolic reactions and that kinetic factors are of importance. This is illustrated by the observed discrepancy between the back fluxes for the enrichment cultures from Hydrate Ridge and from Isis Mud Volcano despite identical incubation conditions. Such factors can be enzyme specific kinetics, coupling to energy conservation or regulation of enzyme expression. Interestingly, despite the differences in the absolute back fluxes, there is a similar ratio between the carbon and sulfur back flux for the Hydrate Ridge and Isis Mud Volcano enrichment cultures, with the sulfur back flux being slightly more than double the carbon back flux. This pattern may either imply that enzymes and transport in sulfate reduction is in general more reversible than methane oxidation in sulfate-reducing AOM consortia or that the energy yield for the sulfate reduction partner is smaller than for AOM partner in consortia. In this context, the mismatch between sulfide back flux compared to carbonate back flux is not surprising (Figure 2 and A1-1). Whereas there is a stoichiometric coupling between net sulfate consumption and net methane consumption, the reverse fluxes need not be coupled according to the stoichiometric ratios (Eq. **8**), analogous to an enzymatic reaction where the label of a transferable group can exchange independent of the reaction of the core molecule (Cornish-Bowden, 2004; Purich, 2010).

The importance of "regulation of enzyme expression" is observed in the experiments where either sulfate or methane was omitted. Many enzymes catalyze forth and back flux detectable by isotope exchange in the absence of a net reaction (Cornish-Bowden, 2004; Scheller et al., 2010; Eq. **12**). In a fully "catalytic" world, one would expect that back fluxes are maintained even if reactant of other half-reaction is absent. When net AOM was prevented by omission of sulfate while methane and inorganic carbon were present, carbon back flux was still observed, however to a lesser extent. This is explained by the continued function of, but down-regulation of enzymes and co-factors enabling methane conversion to inorganic carbon. When, *vice versa*, the net reaction of AOM was prevented by omission of methane while sulfate and sulfide were present, sulfur label exchange was not observed. One explanation for this observation could be that at low sulfide levels, sulfide back flux is a first order process, and therefore, little label was transferred. Another explanation could be that arrest of the net reaction results in the depletion or inactivation of a co-reactant or other component needed for an operative sulfur pathway. Forth and back fluxes through *in vivo* systems are certainly more delicate than through a single enzymatic reaction.

Consideration of product back flux in habitats

Many environmentally relevant and microbial-mediated chemical reactions occur close to equilibrium conditions. Our findings have implications for studies of environmental processes at low energy yields, for instance in anaerobic systems such as AOM environments, or the deep biosphere. Microbial catabolic activity in natural habitats is usually measured by examining the flux of added isotope label from substrate to product pool rather than by determining the net rate of product accumulation by chemical quantification. However, if back flux occurs, label flux from substrate is not identical with the microbial net rate. Precise net rate determination by isotope labeling would have to include both; forward and back flux measurement to yield the net rate ($v = f_+ - f_-$). Moreover, detection of a reaction *in situ* by labeling does not necessarily indicate a net reaction occurring in the direction of label conversion; it may represent the back flux during the opposite reaction and thus a "pseudo-reaction"; hence, dominance of the opposite reaction would have to be excluded, as extensively discussed for methanogenesis vs. AOM (Alperin & Hoehler, 2009). Nevertheless, as in biochemical studies of single enzyme reactions (Moore & Pearson, 1981; Scheller et al., 2010) isotope probing of back fluxes at near equilibrium conditions may provide means of probing catabolic mechanisms at the community level.

Finally, reverse reactions may be also important for the understanding of stable isotope fraction. So far, reversibility of individual catabolic reactions but not of the catabolism as a whole has been examined in isotope fractionation studies (e.g. Rees, 1973; Trudinger & Chambers, 1973; Brunner & Bernasconi, 2005; Johnston et al., 2007; Farquhar et al., 2008). Isotope fractionation between a reactant and product *in situ* may not be determined solely by unidirectional kinetic fractionation but in addition by fractionation in the reverse reaction direction. Furthermore, the isotope composition of methane and sulfate will depend on the isotope composition of their accumulating reaction products sulfide and bicarbonate in AOM environments. Refined measurements of isotope fractionations, which apparently depend on the type of microorganisms performing AOM cultures (Holler et al., 2009), would be needed to explore the significance of the reverse reaction for stable isotope signatures.

Acknowledgements

We thank G. Schüßler for help during isotope analyses. This work was supported by the Max-Planck-Gesellschaft, the Bundesministerium für Bildung und Forschung (BMBF), and the Deutsche Forschungsgemeinschaft (DFG). This is publication no. GEOTECH-XXXX of the R&D programme GEOTECHNOLOGIEN (BMBF and DFG) and project MUMM (Grants 03G0554A and 03G0608A, BMBF).

References

Aeckersberg, F., Bak, F., & Widdel, F. (1991) Anaerobic oxidation of saturated hydrocarbons to CO_2 by a new type of sulfate-reducing bacterium. *Arch Microbiol***156**: 5–14.

Alperin, M.J., & Hoehler, T.M. (2009) Anaerobic methane oxidation by archaea/sulfate-reducing bacteria aggregates: 1. Thermodynamic and physical constraints. *Am J Sci***309**: 869–957.

Bisswanger, H. (2008) *Enzyme kinetics: principles and methods*. Weinheim: Wiley-VCH.

Boetius, A., Ravenschlag, K., Schubert, C.J., Rickert, D., Widdel, F., Gieseke, A., Amann, R., Jørgensen, B.B., Witte, U., & Pfannkuche, O. (2000) A marine microbial consortium apparently mediating anaerobic oxidation of methane. *Nature***407**: 623–626.

Boyer, P.D. (1959) Uses and limitations of measurements of rates of isotopic exchange and incorporation in catalyzed reactions. *Arch Biochem Biophys***82**: 387–410.

Britton, H.G. (1966) The concept and use of flux measurements in enzyme studies. A theoretical analysis. *Arch Biochem Biophys***117**: 167–183.

Britton, H.G., & Dann, L.G. (1978) Use of flux ratio measurements for the determination of the order of addition of substrates and products in enzyme reactions. *Biochem J***169**: 29–37.

Brunner, B., & Bernasconi, S.M. (2005) A revised isotope fractionation model for dissimilatory sulfate reduction in sulfate reducing bacteria. *Geochim Cosmochim Acta***69**: 4759–4771.

Cleland, W.W. (1963) The kinetics of enzyme-catalyzed reactions with two or more substrates or products. I. Nomenclature and rate equations. *Biochim Biophys Acta***67**: 104–137.

Cornish-Bowden, A. (2004) *Fundamentals of enzyme kinetics*. London: Portland Press.

Deppenmeier, U., & Müller, V. (2008) Life close to the thermodynamic limit: How methanogenic archaea conserve energy. *Results Probl Cell Differ***45**: 123–152.

Farquhar, J., Canfield, D.E., Masterson, A., Bao, H., & Johnston, D.T. (2008) Sulfur and oxygen isotope study of sulfate reduction in experiments with natural populations from Fællestrand, Denmark. *Geochim Cosmochim Acta***72**: 2805–2821.

Haldane, J.B.S. (1930) *Enzymes*. London: Longmans, Green & Co.

Harder, J. (1997) Anaerobic methane oxidation by bacteria employing ^{14}C-methane uncontaminated with ^{14}C-carbon monoxide. *Mar Geology***137**: 13–23.

Hinrichs, K.-U., Hayes, J., Sylva, S., Brewer, P., & DeLong, E.F. (1999) Methane-consuming archaebacteria in marine sediments. *Nature***398**: 802–805.

Holler, T., Wegener, G., Knittel, K., Boetius, A., Brunner, B., Kuypers, M.M.M., & Widdel, F. (2009) Substantial ^{13}C/^{12}C and D/H fractionation during anaerobic oxidation of methane by marine consortia enriched *in vitro*. *Environ Microbiol Rep***1**: 370–376.

Jackson, B.E., & McInerney, M.J. (2002) Anaerobic microbial metabolism can proceed close to thermodynamic limits. *Nature***415**: 454–456.

Johnston, D.T., Farquhar, J., & Canfield, D.E. (2007) Sulfur isotope insights into microbial sulfate reduction: When microbes meet models. *Geochim Cosmochim Acta***71**: 3929–3947.

Jørgensen, B.B. (1978) A comparison of methods for the quantification of bacterial sulfate reduction in coastal marine sediments. 1. Measurement with radiotracer techniques. *Geomicrobiol J***1**: 11–27.

Kallmeyer, J., Ferdelman, T.G., Weber, A., Fossing, H., & Jørgensen, B.B. (2004) A cold chromium distillation procedure for radiolabeled sulfide applied to sulfate reduction measurements. *Limnol Oceanogr: Methods***2**: 171–180.

Knab, N.J., Dale, A.W., Lettmann, K., Fossing, H., & Jørgensen, B.B. (2008) Thermodynamic and kinetic control on anaerobic oxidation of methane in marine sediments. *Geochim Cosmochim Acta***72**: 3746–3757.

Knittel, K., & Boetius, A. (2009) Anaerobic oxidation of methane: progress with an unknown process. *Annu Rev Microbiol***63**: 311–334.

Knittel, K., Boetius, A., Lemke, A., Eilers, H., Lochte, K., Pfannkuche, O., Linke, P., & Amann, R. (2003) Activity, distribution, and diversity of sulfate reducers and other bacteria in sediments above gas hydrate (Cascadia Margin, Oregon). *Geomicrobiol J***20**: 269–294.

Meulepas, R.J.W., Jagersma, C.G., Khadem, A., Stams, A.J.M., & Lens, P.N.L. (2010a) Effect of methanogenic substrates on anaerobic oxidation of methane and sulfate

reduction by an anaerobic methanotrophic enrichment. *Appl Microbiol Biotechnol***87**: 1499–1506.

Meulepas, R.J.W., Jagersma, C.G., Zhang, Y., Petrillo, M., Cai, H., Buisman, C.J.N., Stams, A.J.M., & Lens, P.N.L. (2010b) Trace methane oxidation and the methane dependency of sulfate reduction in anaerobic granular sludge. *FEMS Microbiol Ecol***72**: 261–271.

Moore, J.W., & Pearson, R.G. (1981) *Kinetics and mechanism*. New York: John Wiley & Sons Inc.

Moran, J.J., House, C.H., Freeman, K.H., & Ferry, J.G. (2005) Trace methane oxidation studied in several Euryarchaeota under diverse conditions. *Archaea***1**: 303–309.

Moran, J.J., House, C.H., Thomas, B., & Freeman, K.H. (2007) Products of trace methane oxidation during nonmethyltrophic growth by *Methanosarcina*. *J Geophys Res***112**.

Nauhaus, K., Boetius, A., Krüger, M., & Widdel, F. (2002) *In vitro* demonstration of anaerobic oxidation of methane coupled to sulphate reduction in sediment from a marine gas hydrate area. *Environ Microbiol***4**: 296–305.

Nauhaus, K., Albrecht, M., Elvert, M., Boetius, A., & Widdel, F. (2007) *In vitro* cell growth of marine archaeal-bacterial consortia during anaerobic oxidation of methane with sulfate. *Environ Microbiol***9**: 187–196.

Niemann, H., Lösekann, T., de Beer, D., Elvert, M., Nadalig, T., Knittel, K., Amann, R., Sauter, E.J., Schluter, M., Klages, M., Foucher, J.P., & Boetius, A. (2006) Novel microbial communities of the Haakon Mosby mud volcano and their role as a methane sink. *Nature***443**: 854–858.

Orcutt, B., & Meile, C. (2008) Constraints on mechanisms and rates of anaerobic oxidation of methane by microbial consortia: process-based modeling of ANME-2 archaea and sulfate reducing bacteria interactions. *Biogeosciences***5**: 1587–1599.

Orcutt, B., Samarkin, V., Boetius, A., & Joye, S.B. (2008) On the relationship between methane production and oxidation by anaerobic methanotrophic communities from cold seeps of the Gulf of Mexico. *Environ Microbiol***10**: 1108–1117.

Purich, D.L. (2010) *Enzyme kinetics: catalysis & control: a reference of theory and best-practice methods*: Elsevier Sciense Ltd.

Reeburgh, W.S. (2007) Oceanic methane biogeochemistry. *Chem Rev***107**: 486–513.

Rees, C. (1973) A steady-state model for sulphur isotope fractionation in bacterial reduction processes. *Geochim Cosmochim Acta***37**: 1141–1162.

Schauder, R., Eikmanns, B., Thauer, R.K., Widdel, F., & Fuchs, G. (1986) Acetate oxidation to CO_2 in anaerobic bacteria via a novel pathway not involving reactions of the citric acid cycle. *Arch Microbiol***145**: 162–172.

Scheller, S., Goenrich, M., Boecher, R., Thauer, R.K., & Jaun, B. (2010) The key nickel enzyme of methanogenesis catalyses the anaerobic oxidation of methane. *Nature***465**: 606–608.

Schink, B. (1997) Energetics of syntrophic cooperation in methanogenic degradation. *Microbiol Mol Biol Rev***61**: 262–280.

Schreiber, L., Holler, T., Knittel, K., Meyerdierks, A., & Amann, R. (2010) Identification of the dominant sulfate-reducing bacterial partner of anaerobic methanotrophs of the ANME-2 clade. *Environ Microbiol***12**: 2327–2340.

Sørensen, K.B., Finster, K., & Ramsing, N.B. (2001) Thermodynamic and kinetic requirements in anaerobic methane oxidizing consortia exclude hydrogen, acetate, and methanol as possible electron shuttles. *Microb Ecol***42**: 1–10.

Sorokin, Y.I. (1962) Experimental investigation of bacterial sulfate reduction in the Black Sea using S^{35}. *Microbiol***31**: 329–335.

Spormann, A.M., & Thauer, R.K. (1989) Anaerobic acetate oxidation to CO_2 by *Desulfotomaculum acetoxidans*. Isotopic exchange between CO_2 and the carbonyl group of acetyl-CoA and topology of enzymes involved. *Arch Microbiol***152**: 189–195.

Stams, A.J.M., & Plugge, C.M. (2009) Electron transfer in syntrophic communities of anaerobic bacteria and archaea. *Nat Rev Microbiol***7**: 568–577.

Thauer, R.K., & Morris, J.G. (1984) Metabolism of chemotrophic anaerobes: Old views and new aspects. In *The microbe: Part II: Prokaryotes and eukaryotes.* . Kelly, D.P., & Carr, N.G. (eds): Society for General Microbiology Symposium 36. Cambridge Univ. Press., pp. 123–168.

Thauer, R.K., Jungerman, K., & Decker, K. (1977) Energy conservation in chemotrophic anaerobic bacteria. *Bacteriol Rev***41**: 100–180.

Treude, T., Krüger, M., Boetius, A., & Jørgensen, B.B. (2005) Environmental control on anaerobic oxidation of methane in the gassy sediments of Eckernförde Bay (German Baltic). *Limnol Oceanogr***50**: 1771–1786.

Treude, T., Orphan, V.J., Knittel, K., Gieseke, A., House, C.H., & Boetius, A. (2007) Consumption of methane and CO_2 by methanotrophic microbial mats from gas seeps of the anoxic Black Sea. *Appl Environ Microbiol***73**: 2271–2283.

Trudinger, P.A., & Chambers, L.A. (1973) Reversibility of bacterial sulfate reduction and its relevance to isotope fractionation. *Geochim Cosmochim Acta***37**: 1775–1778.

Widdel, F., & Bak, F. (1992) Gram-negative mesophilic sulfate-reducing bacteria. In *The Prokaryotes*. Balows, A., Trüper, H.G., Dworkin, M., Harder, W., & Schleifer, K.-H. (eds). New York: Springer, pp. 3352–3378.

Zehnder, A.J.B., & Brock, T.D. (1979) Methane formation and methane oxidation by methanogenic bacteria. *J Bacteriol***137**: 420–432.

Appendix

Carbon and sulfur back flux during anaerobic microbial oxidation of methane and coupled sulfate reduction

Thomas Holler, Gunter Wegener, Helge Niemann, Christian Deusner, Timothy G. Ferdelman, Antje Boetius, Benjamin Brunner and Friedrich Widdel

Content

A1. AOM as enzymatically catalyzed system

The anaerobic oxidation of methane (AOM) is presently understood as two stoichiometrically coupled enzymatic reactions sequences, methane oxidation that may essentially represent a reversal of methanogenesis, and dissimilatory sulfate reduction possibly via the known bacterial pathway. If carbon and sulfur are processed throughout as C_1- and S_1-intermediates (viz. without C_2-, S_2- or higher compounds), the involved enzymatic reactions in a steady state (no change of cellular pools) must take place at the same net rate (Fig. A1-1, full black arrows), according to the 1:1 stoichiometry $CH_4 + SO_4^{2-} \rightarrow HCO_3^- + HS^- + H_2O$. In contrast, the extent of forward and back fluxes can differ among reactions. If the product is isotopically labeled, the label migrates "upstream" (arrows, ←) via the intermediate pools. Label concentration in an intermediate decreases with its "distance" from the product pool. Hence, label back flux via an individual reaction must be greater than the revealed total catabolic back flux.

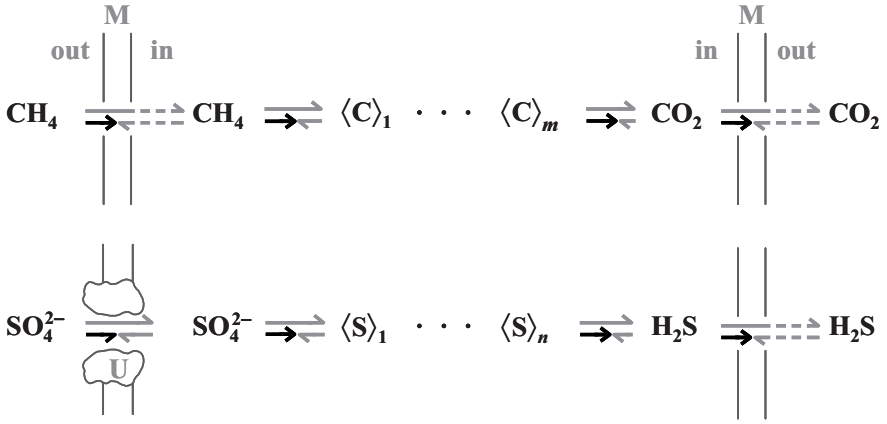

Fig. A1-1. Schematic illustration of forward flux (→), back flux (←) and net rate (→) during anaerobic oxidation of methane (with *m* and *n* enzymatic steps for methane oxidation and sulfate reduction, respectively). SO_4^{2-} enters the cell via an uptake system (U), while CH_4, CO_2 and H_2S are assumed to diffuse rapidly through the cytoplasmic membrane (M) and other layers. ⟨C⟩ and ⟨S⟩ are assumed C_1-carbon and S_1-sulfur intermediates, respectively. Co-reactants (such as coenzymes), and coupling between oxidation and reduction (transfer of reducing equivalents) are not depicted. The rates are indicated by the lengths and directions of the arrows ("one-dimensional vectors"). A dynamic steady state (time-constant intermediate pools) inside the cell is assumed. In the assumed linear pathways, the net rate is the same for every reaction whereas the forward and reverse fluxes can differ.

A2. Calculation of the reverse reaction rate

In the catabolic reversible conversion of a substrate to a product, A ⇌ P, the forward and the back flux (see Fig. 1, main text) are f_+ and f_- (moles volume^{-1} time^{-1}). When product label, P*, is added, appearance of A* reveals the back flux. If the label is a radioisotope with noticeable decay, error in label quantification is avoided by measuring radioactivity in all samples at the same time after the experiment; the specific isotope decay rate is independent of the chemical composition. The infinitesimal concentration d[A*] formed during an infinitesimal time span dt depends on f_+ and f_-, heavy isotope discrimination in each direction (factors, α_-, $\alpha_+ \geq 1$), and the proportion of label in total product and substrate (brackets indicate concentrations):

$$\mathrm{d[A^*]} = f_- \,\mathrm{d}t \frac{1}{\alpha_-} \frac{[\mathrm{P^*}]}{[\mathrm{P}]} - f_+ \,\mathrm{d}t \frac{1}{\alpha_+} \frac{[\mathrm{A^*}]}{[\mathrm{A}]} \qquad \textbf{[A2-1]}$$

Treatment is simplified by assuming α_-, $\alpha_+ \approx 1$, and that the label proportion in the reactant pool remains very low ([A*]/[A] << [P*]/[P]) so that return by f_+ can be neglected. Eq. **A2-1** then yields

$$\mathrm{d[A^*]} = f_- \,\mathrm{d}t \frac{[\mathrm{P^*}]}{[\mathrm{P}]} \qquad \textbf{[A2-2]}$$

P* is increasingly diluted by steadily forming unlabeled P (Fig. A2-1 with P* as ^{35}S). If an increase Δ[A*] is measured after a short enough incubation time, Δt, during which [P*]/[P] remains essentially constant, Eq. **A2-2** can be simplified and rearranged to

$$f_- = \frac{\Delta[\mathrm{A^*}]}{\Delta t} \frac{[\mathrm{P}]}{[\mathrm{P^*}]_0} = \frac{\Delta[\mathrm{A^*}]}{\Delta t} \frac{[\mathrm{P}]_0 + [\mathrm{P^*}]_0}{[\mathrm{P^*}]_0}. \qquad \textbf{[A2-3]}$$

$[\mathrm{P}]_0$ is the initial product concentration and $[\mathrm{P^*}]_0$ the initially label concentration. If $[\mathrm{P^*}]_0 << [\mathrm{P}]_0$, Eq. **A2-3** is further simplified to

$$f_- = \frac{\Delta[\mathrm{A^*}]}{\Delta t} \frac{[\mathrm{P}]_0}{[\mathrm{P^*}]_0}. \qquad \textbf{[A2-4]}$$

Such treatment is similar as the common determination of substrate fluxes in habitats via labeling and measuring product label (Sorokin, 1962; Jørgensen, 1978). We applied Eq. **A2-4**, which corresponds to Eq. **12** (main text) to evaluate ^{14}C back fluxes in the methane-bicarbonate system.

If, however, label dilution is significant, as with the product sulfide, [P] in Eq. **A2-2** is expressed as a function of time. We assume that the net rate, v, of A $\rightarrow$ P is largely independent of [A] (zero-order behaviour, as common in many microbial batch incubations), and that cell growth is negligible during incubation. Then, v is constant and product increases according to $[P] = [P]_0 + [P^*]_0 + v\,t$, or with $[P^*]_0 << [P]_0$ according to

$$[P] = [P]_0 + v\,t\,. \qquad \textbf{[A2-5]}$$

The needed variable [A*] (Eq. **A2-2**) is introduced via $[P^*] = [P^*]_0 - [A^*]$ (mass conservation) leading to

$$\frac{1}{[P^*]_0 - [A^*]}\,\mathrm{d}[A^*] = f_- \frac{1}{v\,t + [P]_0}\,\mathrm{d}t\,. \qquad \textbf{[A2-6]}$$

Integration with [A*] = 0 at $t = 0$ yields

$$\ln\frac{[P^*]_0}{[P^*]_0 - [A^*]} = \frac{f_-}{v}\ln\frac{[P]_0 + v\,t}{[P]_0} \qquad \textbf{[A2-7]}$$

or with resubstition (Eq. **A2-3**)

$$\ln\frac{[P^*]_0}{[P^*]_0 - [A^*]} = \frac{f_-}{v}\ln\frac{[P]}{[P]_0}\,. \qquad \textbf{[A2-8]}$$

Experimental data displayed in a plot of the left versus the right argument are thus expected to follow a straight-line fit with the slope f_-/v.

In the absence of a net reaction ($v = 0$), direct application of Eq. **A2-7** and Eq. **A2-8** is meaningless. Rather, Eq. **A2-6** must be applied with $v = 0$. Integration yields

$$\ln\frac{[P^*]_0}{[P^*]_0 - [A^*]} = f_-\frac{t}{[P]_0} \qquad \textbf{[A2-9]}$$

for obtaining f_- (= f_+) via a graphic plot, again only as long as label return [A*] $\rightarrow$ [P*] is negligible. Solving Eq. **A2-9** for [A*] = [A*](t) shows the "saturating" function, $[A^*] = [P^*]_0\,(1 - e^{-(f_-/[P]_0)t})$, again valid as long as label return [A*] $\rightarrow$ [P*] is insignificant.

For proof of consistency, Eq. **A2-9** is also derived by transforming the right side of Eq. **A2-7** according to

$$\ln\left(1 + \frac{v\,t}{[P]_0}\right)^{\frac{f_-}{v}} = \ln\left(1 + \frac{1}{[P]_0/v\,t}\right)^{\frac{[P]_0}{v\,t}\cdot\frac{v\,t}{[P]_0}\cdot\frac{f_-}{v}} = \ln\left(1 + \frac{1}{[P]_0/v\,t}\right)^{\frac{[P]_0}{v\,t}\cdot\frac{t\,f_-}{[P]_0}}\,. \qquad \textbf{[A2-10]}$$

Then the limit of the argument is formed for $v \to 0$, which is $[P]_0/(v\,t) \to \infty$:

$$\lim_{[P]_0/(v\,t)\to\infty} \left(1+\frac{1}{[P]_0/v\,t}\right)^{\frac{[P]_0}{v\,t}\cdot\frac{t\,f_-}{[P]_0}} = e^{\frac{t\,f_-}{[P]_0}}. \qquad \textbf{[A2-11]}$$

With this Eq. **A2-7** is written as

$$\ln\frac{[P^*]_0}{[P^*]_0-[A^*]} = \ln e^{\frac{t\,f_-}{[P]_0}} = f_-\frac{t}{[P]_0}, \qquad \textbf{[A2-12]}$$

which is identical to Eq. **A2-9**.

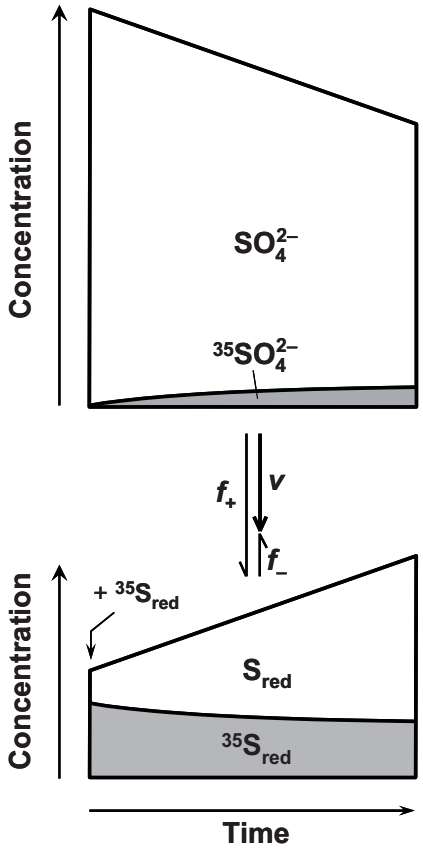

Fig. A2-1. Schematic illustration of transfer of added sulfide ($^{35}S_{red}$) label (grey) to the sulfate pool by back flux (f_-) during sulfate reduction with constant net rate. The net rate is $v = f_+ - f_-$. Label flux decreases due to label dilution by steadily forming product.

A3. Thermodynamics and kinetics in catabolism

A3.1 Actual free energy, standard free energy, and equilibrium constant

We consider the reaction

$$a\,\mathrm{A} + b\,\mathrm{B} \rightarrow p\,\mathrm{P} + q\,\mathrm{Q} \qquad \textbf{[A3-1]}$$

where A, B are reactants, and P and Q are products. Symbols a, b, p, q are stoichiometric factors. The free energy of this reaction depends on activities:

$$\Delta G = \Delta G^\circ + RT \ln \frac{\{\mathrm{P}\}^p \{\mathrm{Q}\}^q}{\{\mathrm{A}\}^a \{\mathrm{B}\}^b}. \qquad \textbf{[A3-2]}$$

At equilibrium, $\Delta G = 0$, so that

$$\Delta G^\circ = -RT \ln \frac{\{\mathrm{P}\}_\mathrm{e}^p \{\mathrm{Q}\}_\mathrm{e}^q}{\{\mathrm{A}\}_\mathrm{e}^a \{\mathrm{B}\}_\mathrm{e}^b} = -RT \ln K_\mathrm{e}, \qquad \textbf{[A3-3]}$$

with index e indicating activity at equilibrium. Eq. **A3-3** can be rewritten as

$$K_\mathrm{e} = e^{-\Delta G^\circ/(RT)} = 10^{-\Delta G^\circ/(RT \ln 10)}, \qquad \textbf{[A3-4]}$$

with $R = 8.314$ J K^{-1} mol^{-1} $= 8.314 \cdot 10^{-3}$ kJ K^{-1} mol^{-1}, and ln 10 = 2.303.

A3.2 Actual concentrations, equilibrium constant, and actual free energy

For convenience, we now consider a reaction with only one reactant and one product:

$$\mathrm{A} \rightarrow \mathrm{P}. \qquad \textbf{[A3-5]}$$

The free energy of this reaction is

$$\Delta G = \Delta G^\circ + \mathrm{RT} \ln \frac{\{\mathrm{P}\}}{\{\mathrm{A}\}}, \qquad \textbf{[A3-6]}$$

which can be divided by RT:

$$\frac{-\Delta G}{RT} = \frac{-\Delta G^\circ}{RT} + \ln \frac{\{\mathrm{A}\}}{\{\mathrm{P}\}}. \qquad \textbf{[A3-7]}$$

Eq. **A3-7** is brought to an exponential form,

$$e^{-\Delta G/(RT)} = e^{-\Delta G^\circ/(RT) + \ln\{\mathrm{A}\}/\{\mathrm{B}\}}, \qquad \textbf{[A3-8]}$$

which is the same as

$$e^{-\Delta G/(RT)} = e^{-\Delta G^\circ/(RT)} \frac{\{A\}}{\{P\}} \ . \qquad \textbf{[A3-9]}$$

Using Eq. **A3-4** introduces K_e in Eq. **A3-9**, yielding

$$e^{-\Delta G/(RT)} = K_e \frac{\{A\}}{\{P\}} \ . \qquad \textbf{[A3-10]}$$

or

$$e^{\Delta G/(RT)} = \frac{\{P\}}{K_e\{A\}} \ . \qquad \textbf{[A3-11]}$$

With activities ≈ concentrations and the connection between the equilibrium constant and the four enzymatic rate constants, $K_e = k_{+1}\, k_{+2}/(k_{-1}\, k_{-2})$, explained in A3.3, we obtain

$$e^{\Delta G/(RT)} = \frac{[P]}{K_e[A]} = \frac{k_{-1}\, k_{-2}\, [P]}{k_{+1}\, k_{+2}\, [A]} \ , \qquad \textbf{[A3-12]}$$

which is used in Eq. **6** in the main text (Discussion).

A3.3 Kinetic rate constants, equilibrium, and Haldane relationship

We consider reaction **A3-5** as being enzymatically catalyzed, with E indicating the enzyme and EA the enzyme-substrate complex (Fig. A3-1).

$$E + A \underset{k_{-1}}{\overset{k_{+1}}{\rightleftharpoons}} EA \underset{k_{-2}}{\overset{k_{+2}}{\rightleftharpoons}} E + P$$

Fig. A3-1. Simple enzymatic reaction with lumped state (EA) of enzyme-bound substrate.

Equilibrium conditions (no net reactions, index e indicating equilibrium) are characterized by the equalities

$$k_{+1}[E]_e\, [A]_e = k_{-1}[EA]_e \qquad \textbf{[A3-13]}$$

and

$$k_{-2}[E]_e\, [P]_e = k_{+2}[EA]_e \ . \qquad \textbf{[A3-14]}$$

Division of Eq. **A3-13** by **A3-14** eliminates $[E]_e$ and $[EA]_e$:

$$\frac{k_{+1}[\mathrm{A}]_\mathrm{e}}{k_{-2}[\mathrm{P}]_\mathrm{e}} = \frac{k_{-1}}{k_{+2}}. \qquad \textbf{[A3-15]}$$

Assuming numerical equality between thermodynamic equilibrium constant (Eq. **A3-3**, **A3-4**) and $[\mathrm{P}]_\mathrm{e}/[\mathrm{A}]_\mathrm{e}$ yields

$$\frac{k_{+1}k_{+2}}{k_{-1}k_{-2}} = \frac{[\mathrm{P}]_\mathrm{e}}{[\mathrm{A}]_\mathrm{e}} = K_\mathrm{e}. \qquad \textbf{[A3-16]}$$

Strictly speaking, activity coefficients would have to be included. Nominator and denominator are then multiplied with $(k_{-1} + k_{+2})$:

$$\frac{k_{+1}k_{+2}(k_{-1}+k_{+2})}{k_{-1}k_{-2}(k_{-1}+k_{+2})} = \frac{k_{+2}(k_{-1}+k_{+2})/k_{-2}}{k_{-1}(k_{-1}+k_{+2})/k_{+1}} = \frac{[\mathrm{P}]_\mathrm{e}}{[\mathrm{A}]_\mathrm{e}}. \qquad \textbf{[A3-17]}$$

With $(k_{-1} + k_{+2})/k_{-2} = K_{\mathrm{m}-}$ and $(k_{-1} + k_{+2})/k_{+1} = K_{\mathrm{m}+}$, the Michaelis constants of the back and forward reaction, and $k_{+2} = k_{\mathrm{cat}+}$ and $k_{-1} = k_{\mathrm{cat}-}$ (catalytic constants for product and substrate formation, respectively) Eq. **A3-17** is written as

$$\frac{k_{\mathrm{cat}+}K_{\mathrm{m}-}}{k_{\mathrm{cat}-}K_{\mathrm{m}+}} = \frac{k_{\mathrm{cat}+}/K_{\mathrm{m}+}}{k_{\mathrm{cat}-}/K_{\mathrm{m}-}} = \frac{[\mathrm{P}]_\mathrm{e}}{[\mathrm{A}]_\mathrm{e}}, \qquad \textbf{[A3-18]}$$

the Haldane relationship. This is usually derived in a different manner by applying the equation for the net rate, v, of a reversible reaction and setting $v = 0$ (Bisswanger, 2008; Cornish-Bowden, 2004).

A3.4 Forward and back flux resulting from enzymatic binding and release reactions

We consider a reaction where substrate and product are distinguishable by labeling at the start of the reaction, according to Fig. A3-2.

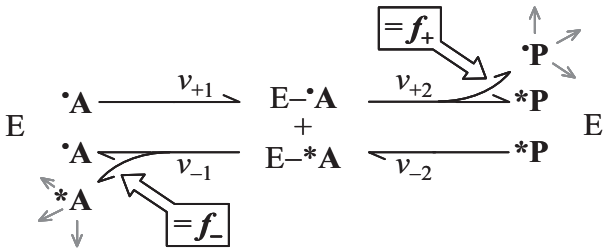

Fig. A3-2. Simple enzymatic reaction with lumped state (EA) of enzyme-bound substrate. For real or theoretical distinction, the product pool is labeled (P*). Label gradually appears in the substrate pool that was originally unlabeled (A•).

The enzyme-substrate complex is partly derived from the starting unlabeled substrate designated as $A^{\bullet}$, and partly from the starting labeled product, designated as P*. During an "infinitesimal" time span, newly formed A* and $P^{\bullet}$ are diluted in the pools of $A^{\bullet}$ and P*, respectively, so that return to the side of origin can be neglected. Assuming a steady state with constant concentrations of enzyme substrate complex, the rate of formation of $EA^{\bullet}$ equals the rates of its decomposition. Decomposition to $A^{\bullet}$ and $P^{\bullet}$ occurs stochastically to both sides, the velocities depending on the proportion of $EA^{\bullet}$ among total enzyme-substrate complex, $EA^{\bullet} + EA^*$:

$$v_{+1} = v_{-1}\frac{[EA^{\bullet}]}{[EA^{\bullet}]+[EA^*]} + v_{+2}\frac{[EA^{\bullet}]}{[EA^{\bullet}]+[EA^*]}. \qquad \textbf{[A3-19]}$$

Eq. **A3-19** is rearranged to

$$\frac{v_{+1}}{v_{-1}+v_{+2}} = \frac{[EA^{\bullet}]}{[EA^{\bullet}]+[EA^*]}. \qquad \textbf{[A3-20]}$$

Partition of the flux f_+ in v_{+2} equals partition of $EA^{\bullet}$ in $EA^{\bullet} + EA^*$:

$$\frac{f_+}{v_{+2}} = \frac{[EA^{\bullet}]}{[EA^{\bullet}]+[EA^*]}. \qquad \textbf{[A3-21]}$$

This is expressed with Eq. **A3-20** as

$$\frac{f_+}{v_{+2}} = \frac{v_{+1}}{v_{-1}+v_{+2}}. \qquad \textbf{[A3-22]}$$

Because of steady state, $v_{-1} + v_{+2} = v_{+1} + v_{-2}$ (formation of total complex occurs at the same rate as its decomposition), Eq. **A3-22** can be converted to

$$f_+ = \frac{v_{+1}v_{+2}}{v_{+1}+v_{-2}}. \qquad \textbf{[A3-23]}$$

An analogous calculation with EP* and f_- yields

$$f_- = \frac{v_{-1}v_{-2}}{v_{+1}+v_{-2}}. \qquad \textbf{[A3-24]}$$

A3.5 Forward and back flux expressed by rate constants of an enzyme

The rates in Eq. **A3-23** can be expressed via the corresponding rate constants and concentrations of the respective species :

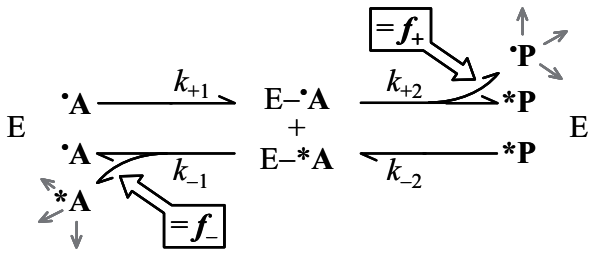

Furthermore, $[EA^{\bullet}] + [EA^*] = [EA]$ (total enzyme-substrate complex), so that Eq. **A3-23** yields

$$f_+ = \frac{k_{+1}[A^{\bullet}]\ k_{+2}[EA]}{k_{+1}[A^{\bullet}] + k_{-2}[P^*]}. \qquad \textbf{[A3-25]}$$

In an analogous manner Eq. **A3-24** yields

$$f_- = \frac{k_{-1}[EA]\ k_{-2}[P^*]}{k_{+1}[A^{\bullet}] + k_{-2}[P^*]}. \qquad \textbf{[A3-26]}$$

Because these fluxes also occur (unnoticed) if there is no label, the signs (*,•) used for initial distinction can be omitted. The ratio f_-/f_+ is then written as

$$\frac{f_-}{f_+} = \frac{k_{-1}k_{-2}[P]}{k_{+1}k_{+2}[A]} \qquad \textbf{[A3-27]}$$

which according to Eq. **A3-16** is

$$\frac{f_-}{f_+} = \frac{[P]}{K_e[A]}. \qquad \textbf{[A3-28]}$$

This equation and Eq. **A3-12** yield Eq. **7** in the main text. Back flux f_- can be also related to the net rate ($v = f_+ - f_-$) via substituting $f_+ = v + f_-$:

$$\frac{f_-}{v} = \frac{1}{K_e[A]/[P] - 1} \quad (\text{for } v \neq 0,\ [A]/[P] \neq 1/K_e)\ . \qquad \textbf{[A3-29]}$$

To express f_+ and f_- via the concentration of total enzyme, $[E_0] = [E] + [EA]$, the steady-state equation depicted in Fig. A3-2 is formulated in the common manner (Bisswanger, 2008):

$$k_{+1}[E][A^{\bullet}] + k_{-2}[E][P^*] = k_{-1}[EA] + k_{+2}[EA] \qquad \textbf{[A3-30]}$$

$$\Rightarrow [E](k_{+1}[A^{\bullet}] + k_{-2}[P^*]) = (k_{-1} + k_{+2})[EA]. \qquad \textbf{[A3-31]}$$

Omitting again label sign included for initial distinction and substituting $[E] = [E_0] - [EA]$ and solving for [EA] yields

$$[EA] = \frac{[E_0](k_{+1}[A] + k_{-2}[P])}{(k_{-1} + k_{+2} + k_{+1}[A] + k_{-2}[P])}. \qquad \textbf{[A3-32]}$$

Expressing then [EA] in Eq. **A3-25** by Eq. **A3-32** yields for the forward flux

$$f_+ = \frac{k_{+1}[A]k_{+2}[E_0](k_{+1}[A] + k_{-2}[P])}{(k_{+1}[A] + k_{-2}[P])(k_{-1} + k_{+2} + k_{+1}[A] + k_{-2}[P])}. \qquad \textbf{[A3-33]}$$

Multiplying nominator and denominator by $(k_{-1} + k_{+2})/k_{+1}k_{-2}$ introduces the composite constants $(k_{-1} + k_{+2})/k_{+1} = K_{m+}$ and $(k_{-1} + k_{+2})/k_{-2} = K_{m-}$, the Michaelis constants for the forward and reverse reaction, respectively:

$$f_+ = \frac{k_{+1}[A]k_{+2}[E_0](K_{m-}[A] + K_{m+}[P])}{(k_{+1}[A] + k_{-2}[P])(K_{m+}K_{m-} + K_{m-}[A] + K_{m+}[P])}. \qquad \textbf{[A3-34]}$$

Multiplying nominator and denominator again in the same way and introducing $k_{+2} = k_{cat+}$, the catalytic constant (Cornish-Bowden, 2004) for the forward reaction, yields

$$f_+ = \frac{K_{m-}[A]k_{cat+}[E_0](K_{m-}[A] + K_{m+}[P])}{(K_{m-}[A] + K_{m+}[P])(K_{m+}K_{m-} + K_{m-}[A] + K_{m+}[P])}. \qquad \textbf{[A3-35]}$$

Enzyme kinetics also often uses $k_{cat+}[E_0] = v_{max+}$, the maximum forward rate that would be achieved under saturation, viz. when all E_0 is present as enzyme-substrate complex, and when there is no product causing reverse reaction. In an analogous manner we obtain for the back flux

$$f_- = \frac{K_{m+}[P]k_{cat-}[E_0](K_{m-}[A] + K_{m+}[P])}{(K_{m-}[A] + K_{m+}[P])(K_{m+}K_{m-} + K_{m-}[A] + K_{m+}[P])}. \qquad \textbf{[A3-36]}$$

In an analogous manner as above, $k_{cat-}[E_0] = v_{max-}$ may be used, the maximum back rate that would be achieved in the absence of substrate (no forward reaction) and if all E_0 would be present as enzyme-substrate complex.

For proof of consistency, the net rate can be formed by $v = f_+ - f_-$ and using Eq. **A3-35** and Eq. **A3-36**. This yields

$$v = \frac{(K_{m-}[A]k_{cat+} - K_{m+}[P]k_{cat-})[E_0]}{K_{m+}K_{m-} + K_{m-}[A] + K_{m+}[P]}, \qquad \textbf{[A3-37]}$$

the classic rate equation of a reversible enzyme reaction with one substrate and one product (Bisswanger, 2008; Cornish-Bowden, 2004). As long as there is no product, viz. [P] = 0, and thus no back reaction, Eq. **A3-37** yields

$$v = \frac{k_{\mathrm{cat}+}[\mathrm{E}_0][\mathrm{A}]}{K_{\mathrm{m}+} + [\mathrm{A}]} = \frac{v_{\mathrm{max}+}[\mathrm{A}]}{K_{\mathrm{m}+} + [\mathrm{A}]} \qquad \textbf{[A3-38]}$$

the well-known rate equation for a unidirectional enzymatic reaction, $\mathrm{A} \rightarrow \mathrm{P}$.

References

Sorokin, Y.I. (1962) Experimental investigation of bacterial sulfate reduction in the Black Sea using S^{35}. *Microbiol* 31:329–335.

Jørgensen, B.B. (1978) A comparison of methods for the quantification of bacterial sulfate reduction in coastal marine sediments. 1. Measurement with radiotracer techniques. *Geomicrobiol J* 1:11–27.

Bisswanger, H. (2008) *Enzyme kinetics: principles and methods* (Wiley-VCH, Weinheim).

Cornish-Bowden, A. (2004) *Fundamentals of enzyme kinetics* (Portland Press, London).

III.3

Microbiological investigation of methane- and hydrocarbon-discharging mud volcanoes in the Carpathian Mountains, Romania

Karine Alain,[1]* Thomas Holler,[1] Florin Musat,[1] Marcus Elvert,[2] Tina Treude[1] and Martin Krüger[1,3]

Environmental Microbiology 8 (4) (2006): 574–590

[1]Max Planck Institute for Marine Microbiology, Celsiusstr.1, 28359 Bremen, Germany

[2]Research Center Ocean Margins, University of Bremen, Leobener Str., D-28359 Bremen, Germany

[3]Geomicrobiology, Federal Institute for Geosciences and Resources, D-30655 Hannover, Germany.

*** Corresponding author**

Environmental Microbiology (2006) **8**(4), 574–590 doi:10.1111/j.1462-2920.2005.00922.x

Microbiological investigation of methane- and hydrocarbon-discharging mud volcanoes in the Carpathian Mountains, Romania

Karine Alain,[1*] Thomas Holler,[1] Florin Musat,[1] Marcus Elvert,[2] Tina Treude[1] and Martin Krüger[1,3]
[1]*Max Planck Institute for Marine Microbiology, Celsiusstr. 1, D-28359 Bremen, Germany.*
[2]*Research Center Ocean Margins, University of Bremen, Leobener Str., D-28359 Bremen, Germany.*
[3]*Geomicrobiology, Federal Institute for Geosciences and Resources (BGR), Stilleweg 2, D-30655 Hannover, Germany.*

Summary

Paclele Mici is a terrestrial mud volcano field located in the Carpathian Mountains (Romania), where thermal alteration of sedimentary organic compounds leads to methane, higher hydrocarbons and other petroleum compounds that are continuously released into the environment. The hydrocarbons represent potential substrates for microorganisms. We studied lipid biomarkers, stable isotope ratios, the effect of substrate (methane, other organic compounds) addition and 16S rRNA genes to gain insights into the hitherto unknown microbial community at this site. Quantitative real-time polymerase chain reaction analysis demonstrated that bacteria were much more abundant than archaea. Phylogenetic analyses of 16S rDNA clone sequences indicated the presence of bacterial and archaeal lineages generally associated with the methane cycle (methanogens, aerobic and anaerobic methanotrophs), the sulfur cycle (sulfate reducers), and groups linked to the anaerobic degradation of alkanes or aromatic hydrocarbons. The presence of sulfate reducers, methanogens and methanotrophs in this habitat was also confirmed by concurrent surveys of lipid biomarkers and their isotopic signatures. Incubation experiments with several common and complex substrates revealed the potential of the indigenous microbial community for sulfate reduction, methanogenesis and aerobic methanotrophy. Additionally, consistently to the detection of methane-oxidizing archaea (ANME) and ^{13}C-depleted archaeal lipids, a weak but significant activity of anaerobic methane oxidation was measured by radiotracer techniques and *in vitro*. This survey is the first to report the presence and activity of ANME in a terrestrial environment.

Received 12 May, 2005; accepted 16 August, 2005. *For correspondence. E-mail kalain@mpi-bremen.de; Tel. (+49) 421 20 28 746; Fax (+49) 421 20 28 790.

Introduction

Mud volcanoes are remarkable geological structures formed by the emission of semi-liquid argillaceous and gas-enriched mud matrices, so-called mud breccia (or mud *ejecta*), from deep sediment layers. These particular features are observed in terrestrial and marine areas worldwide. The geographical occurrence of mud volcanoes is strongly controlled by the geological settings, the majority of them being localized in areas of recent tectonic activity, particularly in zones of compression (Dimitrov, 2002; Kopf, 2002). Often, zones with mud volcanoes are also hydrocarbon-rich, suggesting a relationship between the formation of these geological structures and hydrocarbon generation (Dimitrov, 2002). Recent studies pointed out that methane emissions from terrestrial mud volcanoes constitute a significant input to the atmosphere during both the quiescent and eruptive stages (Dimitrov, 2002; Kopf, 2002; Milkov *et al*., 2003; Etiope *et al*., 2004). They may thus contribute significantly to the global methane budget and, hence, to the greenhouse effect.

The largest areas of terrestrial mud volcanoes in Europe are located in the Carpathian Mountains in eastern Romania. Among these volcanoes, the natural reserve Paclele Mici mud volcano (PMMV) field hosts breccia structures with significant activity. Calculations based on gas flux measurements have estimated the total methane output of the 65 vents of the PMMV field to approximately 383 t year^{-1} (Etiope *et al*., 2004).

During the last three decades, extensive scientific efforts have been directed towards understanding the nature, the mode of formation and the dynamics of marine mud volcanoes. Concurrently with geological, geophysical and biogeochemical investigations, surveys also included in several cases an analysis of the biological and microbial community structures (e.g. Milkov *et al*., 2004; Heijs *et al*., 2005). In the case of terrestrial mud volcanoes (e.g. Hov-

land *et al*., 1997), however, only few studies investigated the composition and functions of their microbial communities (Yakimov *et al*., 2002).

The aim of the present work was to study the microbial community of a terrestrial mud volcano that has been characterized recently with respect to geological settings (Etiope *et al*., 2004). We investigated the composition and metabolic potentials of the microbial communities of one representative mud volcano of the PMMV field using a combination of culture-based investigations, lipid biomarker analyses, 16S rDNA and functional-gene phylogenetic surveys and radiotracer experiments. Also, analyses of the actual chemical composition of the mud breccia and released gas were included.

Results

Site description and biogeochemical characterization

The PMMV field is located in the Carpathian Mountains above a sediment nappe of marine origin consisting of sediments of the Miocene epoch (23.8–5.32 million years ago). In May 2004, the main mud volcano and its dozens of flanking vents (so-called gryphons) and satellite mud pools (so-called salses) were in a quiescent stage (Fig. 1A). At the time of the observation, the majority of the mud cones showed no overflow but exhibited liquid breccia deep in their craters. Periodic deep bubbling sounds indicated ongoing activity inside most of the cones. Large and small gas bubbles were breaking the surface of the salses with a relatively high frequency (Fig. 1B). At the surface of some mud pools adjacent to the central dome, oil leakage was visible (Fig. 1B). We focused our investigations on the mud pool neighbouring the central crater.

Analyses of the gaseous hydrocarbons showed that gas bubbles were mainly composed of methane (74.7%, $n = 3$). Traces (< 1%) of other hydrocarbons, including ethane, propane, *iso*-butane and *n*-butane, were also detected. Measurements of the δ^{13}C-values of the released CH_4 gave a mean value of –30.7‰ in the mud pool closest to the central dome ($n = 3$ samples), and a value of -28.9 ± 4.0‰ for the volcano field ($n = 6$ samples from 3 vents).

The sediment of the upper 20 cm of the mud pool was characterized by a temperature of 12°C and a pH of 7.8. The salinity was around 40‰. Elemental analyses of particle-free pore waters revealed low concentrations of calcium (2.3 mM), potassium (7–10 mM) and magnesium (6–10 mM), but high concentrations of sodium (665–895 mM) and strontium (0.8–1.0 mM) in comparison with marine environments (Table 1). The sulfate concentration of 1.5–2 mM was also much lower than in a marine environment. Dissolved sulfide could not be detected. An estimation of the content of dissolved carbonate and bicarbonate was deduced from the excess of anions versus the sum of measured cations with consideration of pH. It varied in the central part of the mud pool and in the outflow (data not shown); the central part was characterized by an alkalinity of 270 mM while the content of dissolved carbonate and bicarbonate in the outflow was close to zero.

The content of total inorganic carbon (TIC) in the mud was close to 1.3% dry weight (dwt) (Table 1). The total organic carbon (TOC) was between 1.3% and 1.4% dwt (Table 1). Analyses of total sulfur (TS) and total nitrogen (TN) revealed 0.2–0.4% and 0.1% dwt respectively. As became evident during lipid biomarker analyses, the mud volcano samples contained high amounts of oil components. Considering the presence of an unresolved com-

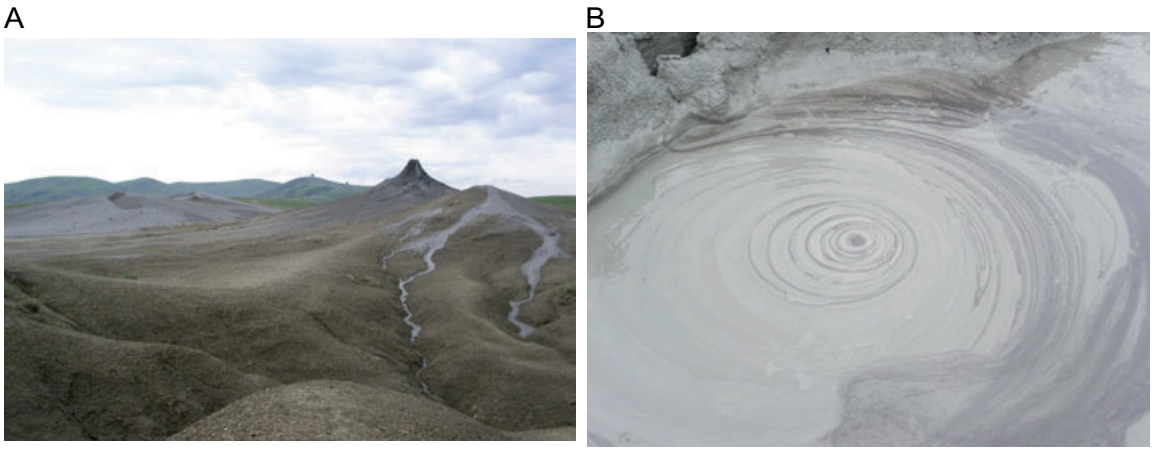

Fig. 1. Photographic images of mud volcano craters of the Paclele Mici field.
A. The central crater is the highest cone on the right, in the back.
B. Bubbling salse with oil leakage.

Table 1. Geochemical composition of Paclele Mici salse 1 mud breccia (A, pore waters; B mud).

A		Concentration (mM) of							
	Sample	Li^+	Na^+	K^+	Mg^{2+}	Ca^{2+}	Sr^{2+}	Cl^-	SO_4^{2-}
	Centre of salse	1.6	895	10.6	10.6	2.3	1.0	662	2.0
	Outflow	1.2	665	7.4	6.1	2.3	0.8	714	1.5

B		Content (%dwt) of			
	Sample	TIC	TOC	TS	TN
	Centre of salse	1.28	1.29	0.21	0.11
	Outflow	1.30	1.40	0.36	0.11

TIC, total inorganic carbon; TOC, total organic carbon; TS, total sulfur; TN, total nitrogen.

plex mixture (UCM) in all fractions analysed, oil obviously represents the major part of the organic carbon at the study site. Hydrocarbon fractions showed a variety of polyaromatic hydrocarbons, including fluorene, phenanthrenes, pyrenes and chrysenes.

Microbial abundance

16S rDNA gene copy numbers of Bacteria and Archaea were calculated by quantitative real-time polymerase chain reaction (PCR) and converted to cell numbers as described elsewhere (Klappenbach *et al.*, 2001). Based on these calculations, the respective abundances of Bacteria and Archaea were estimated to be $3.4–6.1 \times 10^8$ and $0.25–1.6 \times 10^6$ cells per gram dry weight (g_{dwt}) of mud.

Microbial activities

Potential *in situ* rates of methanogenesis and sulfate reduction were measured directly in the original samples over a period of 125 days after collection. The activities of sulfate reduction and methanogenesis were found to be 330 ± 20 nmol g_{dwt}^{-1} day^{-1} ($\pm$ SD, $n = 3$) and 34 ± 10 nmol g_{dwt}^{-1} day^{-1} ($\pm$ SD, $n = 3$) respectively.

Microbial activities were also measured by monitoring product formation upon addition of possible natural substrates and compared with negative controls without supportive substrates. High activity of sulfate reduction was measured with hydrogen and palmitate but not with acetate (which yielded methane) (Fig. 2). The rates measured in the presence of hydrogen and palmitate were 950 ± 220 nmol H_2S g_{dwt}^{-1} day^{-1} ($\pm$ SD, $n = 3$) and 800 ± 110 nmol H_2S g_{dwt}^{-1} day^{-1} ($\pm$ SD, $n = 3$) respectively. The response of the sulfate-reducing community to H_2/CO_2 was rapid: a high activity was measured from the eighth day of incubation (Fig. 2). In contrast, no sulfide production was detected with gaseous hydrocarbons (ethane, butane, propane) or crude oil when sulfate was used as terminal electron acceptor.

The range of substrates for methanogenesis was much wider. Methanogenic activity ($\pm$ SD, $n = 3$) was measured with hydrogen (74.8 ± 24.4 nmol CH_4 g_{dwt}^{-1} day^{-1}), formate (25.9 ± 7.6 nmol CH_4 g_{dwt}^{-1} day^{-1}), acetate (12.7 ± 8.6 nmol CH_4 g_{dwt}^{-1} day^{-1}), palmitate (8.7 ± 2.6 nmol CH_4 g_{dwt}^{-1} day^{-1}) and hexadecane (0.33 ± 0.01 nmol CH_4 g_{dwt}^{-1} day^{-1}) (Fig. 2). When hydrogen or acetate was added, production of methane was significant by the third (H_2) or eleventh (acetate) day of incubation. The production of methane from less-easily degradable organic matter, like hexadecane and crude oil, also started rapidly after addition of the respective substrates (Fig. 2).

Besides methanogenesis, other microbial processes related to the methane cycle were detected. Methane was consumed rapidly in oxic incubations, indicating that aerobic methanotrophy is significant. Furthermore, radiotracer experiments revealed anaerobic oxidation of methane (AOM) in anoxic incubations. The measured rate of AOM was 2.1 ± 0.3 nmol g_{dwt}^{-1} day^{-1} ($\pm$ SD, $n = 10$) with 2 mM SO_4^{2-} (concentration *in situ*) and 4.4 ± 0.6 nmol g_{dwt}^{-1} day^{-1} ($\pm$ SD, $n = 10$) with 12 mM SO_4^{2-}. After 160 days, AOM activity was also detectable through sulfide production under high methane pressure incubations. Radiotracer experiments showed that the sulfate-reduction rate was on average higher in incubations performed with 0.5 mM CH_4 [360 ± 7 nmol g_{dwt}^{-1} day^{-1} ($\pm$ SD, $n = 5$)] than in incubations performed without methane [333 ± 19 nmol g_{dwt}^{-1} day^{-1} ($\pm$ SD, $n = 3$)].

Enrichment and isolation of microorganisms

A culture-based approach gave the first information on the microbial community composition. Strains of sulfate-reducing microorganisms were isolated from enrichment cultures during successive dilution series. Two chemolithoautrophic strains, PMMV-str.A18 and PMMV-str.AE16, were isolated at 20°C with H_2 as the energy source, CO_2 as the carbon source (+acetate for strain A18) and SO_4^{2-} as the terminal electron acceptor. Phylo-

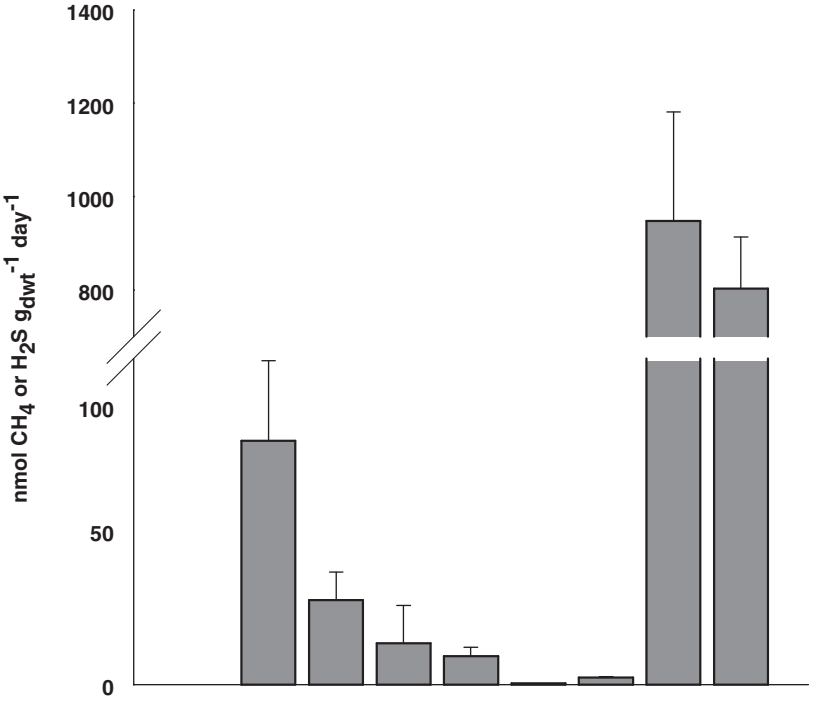

	MPR H_2	MPR H_2	MPR acet	MPR palm	MPR hexd	AOM CH_4	SR H_2	SR palm
CH_4 or H_2S (nmol g_{dwt}^{-1} day^{-1})	74.8	25.9	12.7	8.7	0.3	2.2*	950	800
Activity reached at day	3	25	11	25	42	160	8	20

* rate measured with radiotracers

Fig. 2. Microbial activities measured in culture-based incubation experiments, without and with radiotracer techniques, under anoxic conditions (mean ± standard deviation, $n = 3$). The type of measured metabolic process is indicated under each bar, and the energetic substrate that was added is indicated just below. MPR, methane production (methanogenesis); AOM, anaerobic oxidation of methane (SO_4^{2-} was added as a terminal electron acceptor); SR, sulfate reduction; form, formate; acet, acetate; palm, palmitate; hexd, hexadecane.

genetic analyses of the 16S rRNA gene sequences of these isolates assigned them to the families Desulfovibrionaceae and Desulfobulbaceae within the *Deltaproteobacteria* (Fig. 5). PMMV-str.A18 was very closely related to the marine hydrogen-scavenging *Desulfovibrio* sp. HS2 (Dinh *et al*., 2004), sharing 98.7% 16S rRNA gene sequence similarity. PMMV-str.AE16 was closely affiliated to *Desulfobacterium catecholicum* (which has to be reclassified in another genus) (96% 16S rDNA similarity), a complete oxidizer able to grow on a wide range of non-hydrocarbon aromatic compounds (Szewzyk and Pfennig, 1987).

Chemotaxonomic and isotopic analysis of lipid biomarkers

Insights into the composition of the microbial community were gained from lipid biomarker analyses. The main components of archaeal origin were archaeol and hydroxyarchaeol (Koga *et al*., 1993; 1998). Values of $\delta^{13}C$ for the archaeol clustered around –22‰ whereas those of hydroxyarchaeol were around –52‰. The dominant bacterial biomarkers were diplopterol and a suite of fatty acids. The δ-value of diplopterol was –30‰. Analysis of the fatty acid fractions revealed a significant part of *iso*- and *anteiso*-methyl branched chain fatty acids, such as $iC_{15:0}$ and $aiC_{15:0}$. Unfortunately, because of the presence of a high UCM relative to the fatty acids, carbon isotopic compositions of these lipids could not be determined. Also, the relative abundance of the fatty acids could only be determined by monitoring a fragment ion at *m*/*z* 117 which is characteristic of trimethylsilyl-esters fatty acids. The *iso*- and *anteiso*-methyl branched fatty acids are common constituents of diverse Gram-positive and Gram-negative bacteria (Findlay and Dobbs, 1993). Finally, several lipid biomarkers typically encountered within sulfate-reducing bacteria (SRB) were detected. They consisted in high amounts of saturated and unsaturated *iso*- and *anteiso*-C17 fatty acids, generally associated with *Deltaproteobacteria*, and of $10MeC_{16:0}$, diagnostic for the family Desulfobacteraceae (Kuever *et al*., 2001).

Phylogenetic analyses of 16S rRNA genes and rarefaction curves

To estimate the overall microbial diversity, bacterial and archaeal 16S rRNA gene libraries were constructed. A

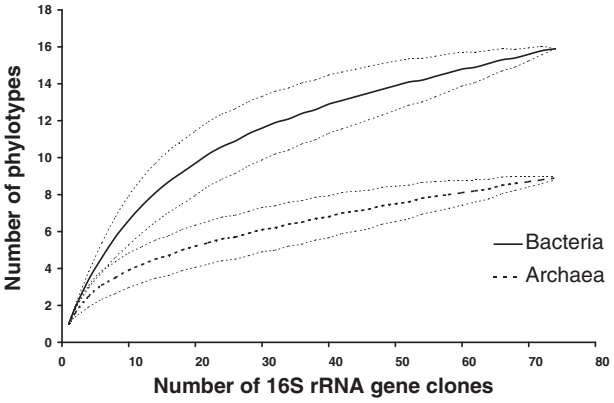

Fig. 3. Rarefaction curves of the diversity detected in the bacterial and in the archaeal libraries. The number of phylotypes (sequences sharing more than 99% 16S rRNA gene sequence similarity were grouped within one phylotype) is plotted versus the number of 16S rRNA gene clones. The dotted lines represent 95% confidence intervals.

total of 76 archaeal clones and 75 bacterial clones were screened.

A rarefaction analysis was performed to estimate the degree of coverage of the natural microbial diversity by the bacterial and archaeal clone libraries (Fig. 3). This survey indicated that these libraries did not completely cover the diversity of the natural habitat. Nevertheless, both rarefaction curves were close to the saturation limit, assuring that the major part of the microbial diversity was detected.

Phylogenetic analyses clustered the archaeal 16S rRNA gene sequences into eight phylotypes (cut-off 99% 16S rDNA similarity) (Fig. 4). These phylotypes were all affiliated to the phylum *Euryarchaeota*. Sequences related to the order *Methanosarcinales* and more precisely to the ANME-2 group (e.g. Hinrichs *et al*., 1999; Knittel *et al*., 2005) dominated the library. This group possesses no pure representative in culture and is likely to be involved in the anaerobic oxidation of methane. ANME-2 sequences accounted for 89% ($n = 68$ sequences) of all archaeal clone sequences. Within the ANME-2 group, five distinct phylotypes were identified. Independent of the phylogenetic reconstruction method applied, representative sequences of the ANME-2 group always formed a monophyletic cluster related to the ANME-2a subgroup. Representative sequences of this group shared some sequence signatures with ANME-2a sequences but also displayed differences. In addition, some sequences were assigned to a phylotype related to ANME-1 (Michaelis *et al*., 2002; Orphan *et al*., 2002; Knittel *et al*., 2005), a second putative methane-oxidizing group distantly related to the *Methanosarcinales* and *Methanomicrobiales*. These sequences, accounting for 3% of archaeal sequences, formed a deep branch within this group. PMMV-Arc186, the representative sequence of this group, was most closely related to sequences from methane hydrate-bearing sediments (Hydrate Ridge, Cascadia margin off Oregon) and also from microbial mats enclosing carbonate reefs (Black Sea), sharing a maximum of 94% 16S rDNA similarity with them. The presence of methanogenic groups was supported by the detection of a phylotype affiliated to the *Methanomicrobiales*. Sequences of this group accounted for 1.5% of all archaeal sequences. Remaining archaeal sequences (5%) were only distantly related to known Archaea; their phylogenetic affiliation could not be clarified.

Compared with the archaeal diversity, the bacterial diversity was relatively large. Phylogenetic analyses grouped the sequences into 16 different phylotypes (Fig. 5). The majority of the sequences, accounting for 40% of all bacterial sequences, were assigned to the *Deltaproteobacteria*, a subdivision mainly constituted of SRB (Widdel and Bak, 1992). Within this subdivision, sequences related to PMMV-Bac228 were the most frequently recovered, representing 26.7% of the bacterial clones. They were very closely related (97% similarity) to the clone sequence HMMVPog-4 detected from the marine mud volcano Haakon Mosby (T. Lösekann *et al*., in preparation). The other phylotypes of *Deltaproteobacteria*, PMMV-Bac226 and PMMV-Bac44, representing 8% and 5.3% of all bacterial sequences, respectively, were affiliated to the family Desulfobacteraceae. Sequences related to the *Gammaproteobacteria* were also represented within the library, accounting for 9.4% of the bacterial sequences. Within the *Gammaproteobacteria*, few sequences were closely related to halophilic bacteria of the family Halomonadaceae. The larger part of the *Gammaproteobacteria* (8%) was closely affiliated to sequences recovered from the marine mud volcano Haakon Mosby (96–97% similarity) (T. Lösekann *et al*., in preparation), and more distantly to other methylotrophic strains (~93% similarity). A significant part of the sequences (12%) was assigned to the *Bacteroides-Cytophaga* group. Numerous sequences were affiliated to the phylum Firmicutes (12%). Interestingly, many sequences grouping into this phylum (10.7%) were closely affiliated to uncultivated microorganisms detected in diverse marine methane-rich habitats (Lanoil *et al*., 2001; Knittel *et al*., 2003). The phylotypes PMMV-Bac19 (6.7%) and PMMV-Bac225 (12%), belonging to the phylum '*Planctomyces* and relatives' and to a novel non-described division, respectively, were also abundant in the clone library. Again, their closest relatives were environmental sequences recovered from methane-seeping habitats (Lanoil *et al*., 2001). Three more rarely retrieved phylotypes were affiliated to the taxonomic divisions '*Chloroflexaceae* and relatives' (1.3%), Green-non-sulfur Bacteria (5.4%) and the candidate division WS6 (1.3%) (Dojka *et al*., 2000).

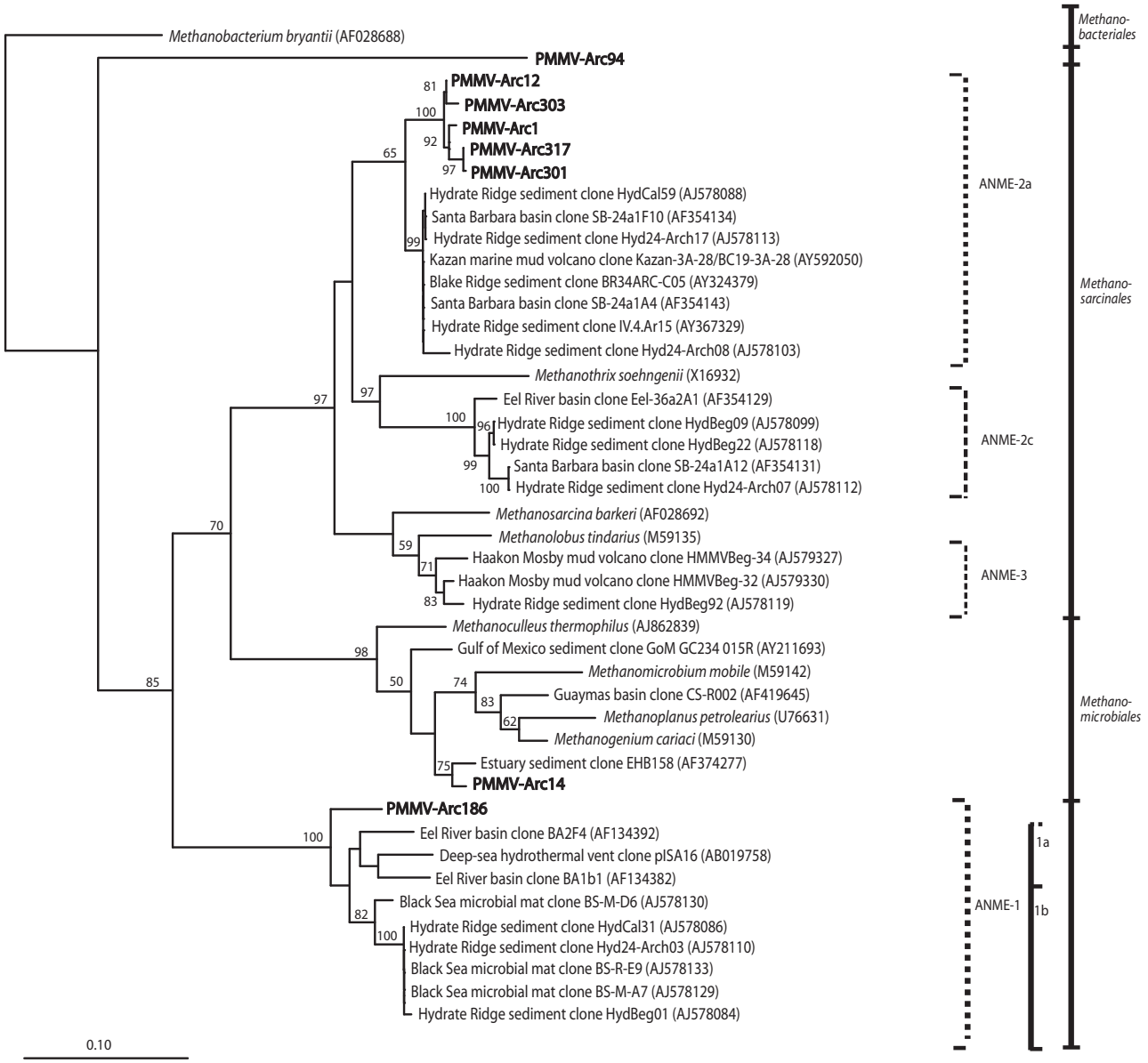

Fig. 4. Phylogenetic reconstruction showing the affiliations of the 16S rRNA gene sequences of the clones from the archaeal clone library from the Paclele Mici mud volcano (PMMV) with selected reference sequences of the domain Archaea. Sequences from this study are given in bold. The tree topology shown was obtained by the maximum likelihood algorithm, with 100 bootstrap replicates. The scale bar indicates 10% estimated sequence divergence.

Phylogeny and conservation of active-site amino-acids in mcrA *genes*

In order to confirm the phylogenetic affiliation of the 16S rDNA sequences to ANME groups, clone libraries targeting genes coding for a conserved region of the alpha subunit of the methyl-coenzyme M reductase (*mcrA*) were constructed; indeed, recent surveys led to the suggestion that *mcrA* genes could substitute for 16S rRNA in determining phylogenetic relationships among methanogens (Luton *et al*., 2002). Of 30 screened clones, all were found to belong to the McrA group e. This group is associated with ANME-2 (Hallam *et al*., 2003; Inagaki *et al*., 2004) (Fig. 6). In order to estimate the potential for catalytic activity of the detected McrA, the deduced amino acid sequences were aligned with representative sequences of ANME-1 and ANME-2 McrA, and with the McrA sequences of *Methanothermobacter thermoautotrophicus* and *Methanosarcina barkeri* as references, as described before by Hallam and colleagues (2003). This analysis showed that the active sites encoded by this region of the gene were conserved, suggesting that the McrA of ANME-2 from this habitat may be capable of catalytic activity.

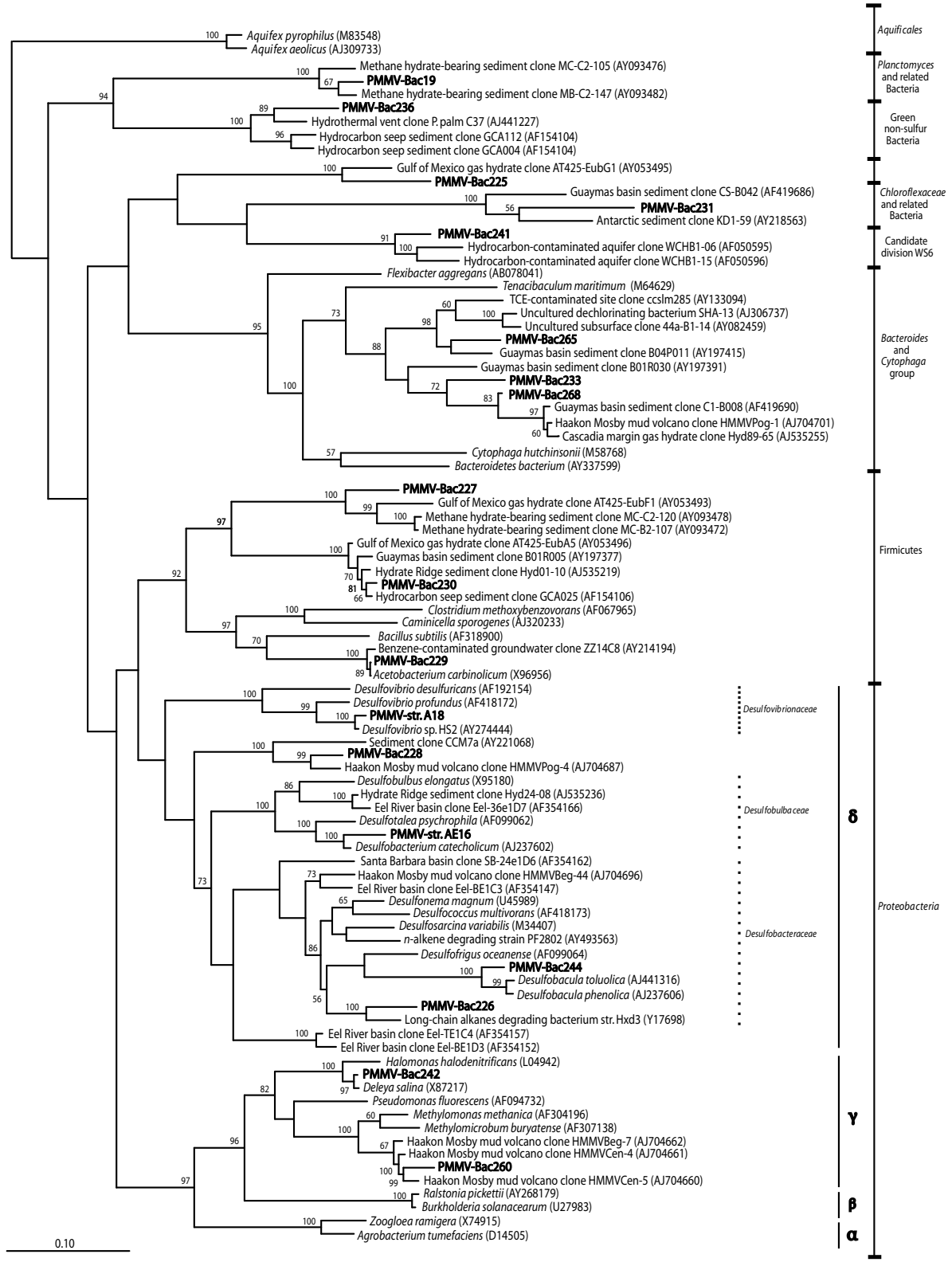

Fig. 5. Phylogenetic reconstruction showing the affiliations of the 16S rRNA gene sequences of the isolates and clones from the bacterial clone library from the Paclele Mici mud volcano (PMMV) with selected reference sequences of the domain Bacteria. Sequences from this study are given in bold. The tree topology shown was obtained by the maximum likelihood algorithm, with 100 bootstrap replicates. The scale bar indicates 10% estimated sequence divergence.

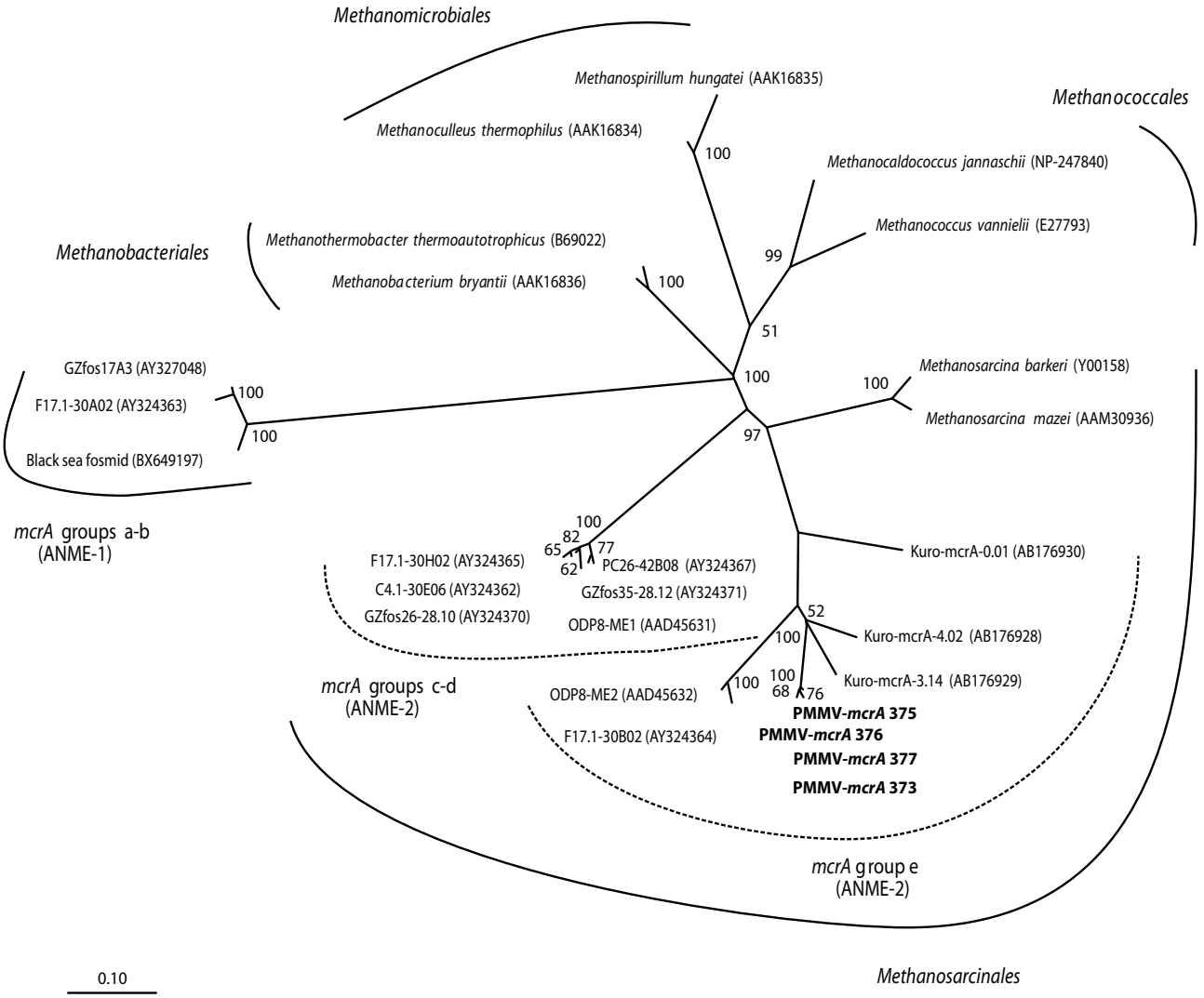

Fig. 6. Phylogenetic tree based on partial amino acid sequences deduced from *mcrA* gene sequences in comparison with selected reference sequences from environmental clones and methanogens. Sequences from this study are given in bold. The tree topology shown was obtained by the Neighbour-joining algorithm, with 100 bootstrap replicates. The scale bar indicates 10% estimated sequence divergence.

Discussion

Biogeochemical setting

Mud volcanism in the Carpathian Mountains is caused by tectonic compression events, and results in the extrusion of mud breccias and gas bubbles strongly charged with methane. As demonstrated by gas analyses, gas bubbles were mostly composed of methane (~75%). Prior measurements demonstrated that carbon dioxide, nitrogen and helium were also present (Etiope *et al.*, 2004), probably accounting for the other 25%. The $\delta^{13}C$ value of the released CH_4 of –30.7‰ indicates a thermogenic and likely kerogenic origin (Whiticar, 1999). Gas bubbles, which break the surface of the pool with quite high frequency, may favour the penetration of oxygen in local micro niches of the top part of the mud pool.

The chemical composition of the mud breccias extruded in the PMMV field is atypical for terrestrial sources, suggesting that they may have been derived from the mixing of former marine sediments (or brines) with groundwater sources or resulting from ion exchanges. Their high salinity (40‰) supports the hypothesis of a brine origin.

The ratios between sodium and calcium, magnesium or potassium in the pore waters suggest a depletion of calcium and magnesium in comparison with seawater, while the sodium–potassium ratio is close to seawater composition. This chemical anomaly could be the result of ion exchanges during fluid–sediment or fluid–rock interactions. The high concentration of strontium in the pore waters indicates an intense dissolution and re-precipitation of carbonates (Morse and Mackenzie, 1990). The sulfate concentration of 1.5–2 mM is much lower than

in a marine environment but obviously high enough to allow significant microbial sulfate reduction and establishment of diverse SRB. Methane, carbon dioxide plus hydrogen and ethane, propane, *iso*-butane and butane together with the high concentrations of petroleum hydrocarbons in the mud breccia may serve as important energy and carbon sources for the indigenous microorganisms.

Microbial diversity and functions

The top 20 cm of the mud breccias contained relatively few microorganisms in comparison with eutrophic environments. Lipid biomarker and quantitative PCR analyses indicate a predominance of Bacteria, accounting for 10^8 cells per g_{dwt}, while Archaea represent only 10^5–10^6 cells per g_{dwt}. The active venting observed in the area where the samples were collected might explain the relatively low microbial abundance by preventing the settlement of a stable microbial biocoenosis in this zone. Alternatively, while this habitat is *a priori* not limited in organic carbon, considering the high amounts of aromatic hydrocarbons that were detected, the nature of this carbon might have selected for a specialized microflora. However, although the total microbial biomass is rather low, the bacterial diversity is quite high. This was demonstrated both by the detection of a complex suite of bacterial lipid biomarkers and by the recovery of 16 different phylogenetic bacterial groups (Fig. 5). The detection of a restricted number of archaeal lipid biomarkers and of few 16S rDNA phylotypes indicates that the archaeal diversity is more limited.

In accordance with the presumed marine origin of this mud volcano, the sulfate-reducing population is likely to be a relevant component of the indigenous microbial community of this mud volcano. Several membrane components characteristic of SRB were found. These included high amounts of $10MeC_{16:0}$, typically encountered within the family Desulfobacteraceae (Kuever *et al*., 2001). This indicates that Desulfobacteraceae or other related $10MeC_{16:0}$-producing species are abundant in this habitat. Saturated and unsaturated *iso*- and *anteiso*-C_{17} fatty acids were also abundant. These are commonly described as diagnostic markers for the mesophilic, Gram-negative SRB of the δ-subclass of *Proteobacteria* (Boschker and Middelburg, 2002). These fatty acids can be encountered in species of the genera *Desulfobacter* (Taylor and Parkes, 1983) and *Desulfobacula* (Kuever *et al*., 2001), or among species of the genera *Desulfobulbus* (Taylor and Parkes, 1983; Knoblauch *et al*., 1999), *Desulforhabdus* and *Desulforhopalus* (Knoblauch *et al*., 1999; Rütters *et al*., 2001) respectively. Consistently with the results of the chemotaxonomic study, the major part of the bacterial 16S rRNA gene sequences affiliated with the *Deltaproteobacteria*. This subdivision encompasses mesophilic and metabolically versatile microorganisms sharing the capability to perform dissimilatory sulfate reduction. However, some *Deltaproteobacteria* are able to ferment substrates or to use alternative electron acceptors such iron(III), nitrate or sulfur compounds (Widdel and Bak, 1992). Within this subdivision, most of the sequences are related to sequences from marine methane-rich habitats. In addition, two phylotypes are affiliated to the family Desulfobacteraceae, confirming the results of the chemotaxonomic analysis. Microbial activity measurements support the assumption that SRB play a significant role within the microbial community. Activity measurements showed that *in situ* sulfate-reduction rates were high. High rates were also measured when substrates such as H_2/CO_2 or palmitate were added. Significant activity was measured promptly after addition of H_2/CO_2, indicating either a good adaptation to this substrate or the presence of a high number of cells able to utilize it. Furthermore, two representatives of the sulfate-reducing community, affiliated to the Desulfovibrionaceae and to the Desulfobulbaceae, were isolated using H_2 as the electron donor.

No sulfate reduction could be measured in incubations with the gaseous hydrocarbons ethane, butane and propane, which had been detected in small concentrations in gas bubbles. This indicates that if there is a biological conversion of these compounds *in situ*, it is not likely to rely on sulfate reduction as a terminal process. Interestingly, the two phylotypes of the clone library belonging to the Desulfobacteraceae are very closely related to sequences of sulfate reducers able to degrade long-chain alkanes or aromatic compounds (Bak and Widdel, 1986; Aeckersberg *et al*., 1998; So and Young, 1999; Kuever *et al*., 2001). This suggests that microorganisms able to degrade some of the oily compounds expelled by the volcano are present, although no activity under sulfate-reducing conditions was observed with the few tested substrates.

Different lines of evidence indicate that the methanogenic community of this particular habitat represents a second active microbial guild. One of the main lipid biomarker is the archaeal lipid archaeol (Koga *et al*., 1993; 1998). The determination of its stable carbon isotope ratio indicated a value of around −22‰, suggesting a possible synthesis by methanogenic microorganisms (Hinrichs *et al*., 2003). Results gained from microbial activity measurements showed that the range of substrates for methanogenic microorganisms and their syntrophic partners is quite wide. Methanogenic activity was measured with common substrates such as hydrogen, formate and acetate. Hydrogenotrophic and acetoclastic methanogenesis are likely to be active *in situ*, as significant methane production was measured in short-term incubations. In addition, palmitate and hexadecane, which may be part of the oil fraction, were also degraded under methanogenic conditions. The presence of methanogenic groups at the

PMMV, which was already evident after methane-production rate measurements and structural and isotopic analyses of biomarkers, is further supported by the detection of a phylotype affiliated to the *Methanomicrobiales*. Furthermore, one sequence affiliated to the Firmicutes, PMMV-Bac229, is very closely related (> 99% similarity) to the sequence of the homoacetogen *Acetobacterium carbinolicum* (Willems and Collins, 1996), indicating the potential presence of microorganisms able to grow through acetogenesis.

Independent analyses indicate that the aerobic methanotrophic/methylotrophic community is active and abundant in PMMV sediments. Among the lipid biomarkers derived from bacterial sources, the hopanoid diplopterol was found to be quantitatively important. Diplopterol is synthesized *de novo* by various aerobic bacteria, including nitrate-reducers or cyanobacteria, but it is especially a major membrane component of aerobic methylotrophic bacteria (Rohmer *et al*., 1984). Its δ-value near −30‰ points to a partial methanotrophic origin, although contributions by other bacteria can not be ruled out. In addition, several sequences of the bacterial library are affiliated to sequences recovered from the marine mud volcano Haakon Mosby and more distantly to methylotrophic strains of the γ-subclass of *Proteobacteria*. This community is likely to be active *in situ* as aerobic methanotrophy was detected in oxic incubations with methane. Aerobic methanotrophy is obviously restricted to the uppermost centimetres of the mud pool and to zones where the active venting of gas creates local turbulences that may favour oxygen penetration.

Phylogenetic analyses indicate the presence of bacterial groups which are likely to be decomposers involved in the aerobic and anaerobic degradation of the organic matter. Many of the sequences can be assigned to the *Bacteroides-Cytophaga* group, a phylum comprising aerobic, microaerophilic and anaerobic chemo-organoheterotrophs especially proficient in the degradation of polymers. Sequences affiliated to the Firmicutes also represent a large fraction of the library. This phylum encompasses metabolically versatile microorganisms and, especially, a high proportion of fermentative microorganisms. Finally, many sequences belonging to the phylum '*Planctomyces* and relatives' were recovered. *Planctomyces* are typically facultative aerobic chemoorganotrophs that grow by fermentation or respiration of sugars. Interestingly, a similar survey of the bacterial communities inhabiting a saline terrestrial petroleum-discharging mud volcano in Italy reported also the presence of decomposers. However, in that case, the community was dominated by highly specialized hydrocarbonoclastic bacteria of the genera *Alcanivorax* and *Marinobacter* that were not detected here (Yakimov *et al*., 2002).

Finally, several data indicate that AOM is going on at this site. This question is discussed in the next section because this result is of particular interest as, to date, this process has been described essentially in marine methane-rich environments.

Anaerobic oxidation of methane

The high amounts of methane together with the assumed marine origin of the mud led to the hypothesis that this system might be a promising place to find terrestrial AOM. Anaerobic oxidation of methane is a microbially mediated process described to occur widely in anoxic marine sediments (e.g. Hinrichs and Boetius, 2002; Valentine, 2002). As indicated by geochemical profiles, this process is generally linked to sulfate reduction (Reeburgh, 1980; Devol and Ahmed, 1981). Field and laboratory studies, including phylogenetic analyses, carbon-isotopic analyses of biomarker lipids, and fluorescent *in situ* hybridizations, indicate that AOM is linked to associations of archaea and bacteria (Hoehler *et al*., 1994; Hinrichs *et al*., 1999; Boetius *et al*., 2000; Orphan *et al*., 2001; Elvert *et al*., 2003). So far, three major groups of putative anaerobic methane-oxidizing archaea (ANME-1, ANME-2 and ANME-3) and several SRB groups have been identified in methane-rich marine sediments (Boetius *et al*., 2000; Orphan *et al*., 2002; Knittel *et al*., 2005; T. Lösekann *et al*., in preparation). Specific ANME–SRB physical associations, including formation of aggregates and mats (Boetius *et al*., 2000; Lanoil *et al*., 2001; Michaelis *et al*., 2002; Knittel *et al*., 2005), have been observed, but the exact nature of their metabolic interaction and the mechanisms underlying AOM have not been fully elucidated. Two models are currently discussed: the first suggests that ANME cells are able to mediate the whole process alone (Strous and Jetten, 2004); the second hypothesizes that ANME cells carry out the oxidation of methane and that the electrons or by-products of this reaction are transferred to sulfate reducers (Valentine, 2002; Strous and Jetten, 2004). Both models assume that the methane oxidizers harbour elements of the methanogenic pathway, reversing key steps to enable methane oxidation anaerobically (Hallam *et al*., 2003; 2004; Krüger *et al*., 2003).

Several lines of evidence are consistent with the occurrence of AOM in the PMMV. The archaeal 16S rRNA gene library is dominated by sequences affiliated to anaerobic methanotrophs of the ANME-2 group. Additionally, few sequences related to ANME-1 were also recovered. The detected ANME-2 sequences were found to form a monophyletic group related to ANME-2a, sharing only 95–96% 16S rDNA similarity with the ANME-2a sequences detected to date from marine methane-rich habitats. The phylogenetic divergence might display the evolutionary history of this population after its geographic isolation consecutive to the Carpathian Mountains orogeny during

the Miocene Epoch (23.8 to 5.32 million years ago). The phylogenetic affiliation of indigenous microorganisms to ANME-2 is further supported by the detection of McrA sequences belonging to the McrA group e (Hallam *et al*., 2003; Inagaki *et al*., 2004). As indicated by the conservation of their active site positions, such McrA may be part of the enzyme that catalyses the first step in AOM.

Lipid biomarker analyses provided further evidence that AOM takes place at PMMV. Among the detected lipid biomarkers, the *Methanosarcinales* marker hydroxyarchaeol displayed a carbon isotopic signature around −52‰, i.e. more than 20‰ lighter in its isotopic signal than the methane released by the mud volcano. The hydroxyarchaeol would be depleted in ^{13}C relative to the methane for two reasons: isotope effects and resulting fractionations associated with (i) the assimilation of methane (Whiticar, 1999) and (ii) isotopic fractionations associated with lipid biosynthesis. Such an isotopic value is consistent with the fractionation reported for the biomass of anaerobic methanotrophs. In order to evaluate AOM activity, we conducted incubations with radiotracers as well as sulfide-production time-series under elevated methane partial pressure. Definite AOM activity was detected in samples, compared with negative controls, using radiolabelled methane. Nevertheless, the AOM rate was very low compared with other advective systems (Treude *et al*., 2003; Joye *et al*., 2004) (Fig. 2), and rather in a magnitude comparable to diffusive systems (Treude *et al*., 2005). This indicates that although the process is present, it is probably not very important *in situ*. This low magnitude of AOM is consistent with the low archaeal cell number detected at the depth zone the samples were collected. The observation that the AOM rate doubled when sulfate was increased from 2 mM to 12 mM suggests that sulfate might be a limiting factor for this process in the mud volcano. Despite high methane concentration *in situ*, the AOM community is not as well developed as those in marine cold seeps because its activity is probably limited by the low concentration of sulfate. Sediment samples incubated with methane as the sole electron and carbon donor were found to produce detectable sulfide from sulfate only after 160 days of incubation, confirming that AOM might not be a major process in the upper part of this mud volcano. However, AOM might be more important in the deeper anoxic zones of the mud volcano. The detected ANME might be cells originating from deeper areas, which have been carried away by the mud flow. Further investigations will be necessary to address the question of the relevance of AOM at greater depth.

Conclusion

This multidisciplinary study provided clues about the composition and functions of the microbial community of a terrestrial mud volcano. The PMMV field is a remarkable example of an ecosystem in which geological and chemical processes mediate the formation of methane and oil compounds, which in turn provide energy for a diverse microbial population. The results of the integrated approach presented herein demonstrate that sulfate reducers, methanogens, anaerobic and aerobic methanotrophs all occur in close proximity. The microbial community associated with sulfate-reduction processes is very abundant and active in this mud volcano. It dominates obviously the microflora of the anoxic areas. In addition, microbial communities associated with the metabolisms of methane and oil components, which represent relevant substrates at this site, are significant components of the indigenous microflora. Different lines of evidence demonstrate the significant contribution of aerobic methanotrophy/methylotrophy and methanogenesis to the carbon cycle of the field. Aerobic methanotrophs should be the major microbial actors in the microniches where there is a supply of oxygen.

Additionally, results of phylogenetic analyses, radioisotope techniques, lipid biomarker and isotopic surveys provide convergent lines of evidence that methane is consumed by AOM. The archaeal groups likely to mediate this process were identified to belong to ANME-2 and ANME-1. To our knowledge, this study is the first to report on the presence of ANME cells in a terrestrial environment, as so far ANME have been detected only in anoxic, methane-rich marine sediments. Considering that the new ANME sequences share less than 97% 16S rRNA sequence similarity (Rossello-Mora and Amann, 2001) with sequences detected from marine methane-rich areas, they represent at least new species, and maybe even new genera. Detection of ANME in this non-marine habitat suggests that ANME and AOM will be found in other terrestrial environments where sulfate and methane are present in substantial amounts.

Experimental procedures

Study site and sampling

In May 2004, samples were collected from several mud volcanoes of the Carpathian Mountains. The sampling site was a volcano field of 0.63 km^2 called Paclele Mici (PMMV), consisting of a high central active dome surrounded by other active and inactive smaller gryphons and dozens of active salses. Due to the instability of its walls and its height, it was impossible to collect samples from the central dome. Samples were collected from five active salses located close to the central dome, showing the frequent development of gas-mud bubbles. Our studies were focused on the salse (diameter < 2 m) which was closest to the central dome (< 10 m away).

Mud samples were collected from the upper 20 cm of the salse and transferred to the laboratory under cooled (4°C)

and dark conditions. In the laboratory, samples were aseptically subsampled and prepared for microbiological and geochemical studies as follows: samples for molecular and geochemical analyses (except the ones for inductively coupled plasma spectroscopy (ICP) analyses that were stored at 4°C) were stored at –80°C; samples for microbiological studies were stored at 4°C in the dark under aerobic and anaerobic conditions; samples for lipids analyses were extracted from 20 ml of wet sediment using dichloromethane–methanol mixtures.

Gas bubbles were sampled from the central part of the salse using inverted gas bottles and analysed immediately in the laboratory by gas chromatography.

Analytical procedures

Temperature, salinity. Temperature of the mud was measured in the central part and in the periphery of salse 1 using a digital thermometer (Amarell, precision ± 0.1°C). Porewater salinity was measured with a refractometer S/Mill-E (Atago, Tokyo, Japan).

Gas bubble analysis. Samples were analysed for methane, ethane, propane, *iso*-butane and butane on a Shimadzu GC-14B gas chromatograph equipped with a Supel-Q PLOT column (30 m × 0.53 mm; Supelco) and a flame ionization detector. The detection and injection temperatures were 280°C and 150°C respectively. The initial temperature of the column was 35°C and the final temperature 140°C. The experiment was run on a period of 8.25 min with a programme rate of 20°C min^{-1}. The carrier phase was N_2 at a flow rate of 3 ml min^{-1}.

Sulfate concentration. Samples were thawed and centrifuged (2200 *g*, 20 min). Pore water sulfate concentration was measured in the supernatant using non-suppressed ion chromatography with a Waters 510 HPLC pump, Waters WISP 712 autosampler (100 µl injection volume), Waters IC-Pak anion exchange column (50 × 4.6 mm), and a Waters 430 conductivity detector. The eluent was 1 mM isophthalatic acid with 10% methanol, adjusted to pH 4.5 (flow: 1.0 ml min^{-1}).

Total organic and inorganic carbon, C/N/S analysis. Prior to elemental analysis, samples were freeze-dried and homogenized. Total carbon (TC), total nitrogen (TN) and total sulfur (TS) concentrations were measured by combustion/gas chromatography on a Carlo Erba NA-1500 CNS analyser. Total inorganic carbon was determined on a CM 5012 CO_2 coulometer after acidification with H_3PO_4. Total organic carbon was deduced from the difference between TC and TIC. The C/N ratio is given as the molar ratio of TOC and TN.

Pore waters analysis. The cationic composition of the pore waters was analysed by inductively coupled plasma optical emission spectrometry (ICP-OES) on a JY 166 ULTRACE instrument (HORIBA Jobin Yvon, USA).

The chlorinity was measured on a Dionex DX-500 Ion Chromatograph (IC) equipped with a AS9-HC (4 mm column) using a 9 mM sodium carbonate solution as eluent (flow rate: 1.0 ml min^{-1}; injection volume: 100 µl).

Sulfide concentration. Sulfide production in cultures was determined using the colorimetric assay based on the formation of copper sulfide as described in Cord-Ruwisch (1985). Sulfide production rates were calculated as described in Nauhaus and colleagues (2002).

$\delta^{13}C$ of methane. Stable isotopic analysis of methane was performed by gas chromatograph-combustion isotope-ratio-mass-spectrometry (GC-IRMS) as described in Krüger and colleagues (2001). Carbon dioxide (99.998% purity, Messer-Griessheim, Düsseldorf, Germany) calibrated against Vienna Pee Dee Belemnite carbonate was used as working standard. The $\delta^{13}C$ of methane was measured on three samples from the mud pool neighbouring the central crater, and on three additional samples from other vents.

Anaerobic oxidation of methane (AOM) and sulfate reduction determined with radiotracer techniques. The activity of AOM was investigated in three different incubation applications: (i) sediment amended with methane (0.6 mM) exhibiting natural sulfate concentration (2 mM), (ii) sediment diminished in methane concentration (0.02 mM) exhibiting natural sulfate concentration (2 mM) and (iii) sediment slurry (1:1 mixture of sediment and basal mineral medium; Widdel *et al.*, 2004) amended with methane (0.6 mM) and sulfate (12 mM). Except for (iii), applications were the same for sulfate reduction. Sediment or slurry was filled anoxically into 6 ml Hungate tubes (five replicates per application and radiotracer method) and closed bubble-free with rubber stoppers. Radioactive tracers, i.e. $^{14}CH_4$ (dissolved in water, injection volume 30 µl, activity 2.8 kBq) and $^{35}SO_4$ (dissolved in water, injection volume 6 µl, activity 163 kBq), were injected into AOM and sulfate reduction samples respectively. During incubation (10 days, room temperature) the samples were shaken permanently. Hungate tubes filled with basal mineral medium (0.6 mM, five replicates per radiotracer method) amended with methane were injected and incubated concurrently (negative controls). After incubation, AOM samples were transferred into 50 ml glass vials filled with 25 ml of sodium hydroxide (2.5% w/w) to stop bacterial activity and closed quickly with rubber stoppers. Sulfate reduction samples were transferred into plastic tubes filled with 25 ml of zinc acetate (20% w/w). AOM rates were determined according to Treude and colleagues (2003) (gas chromatography and $^{14}CH_4$ combustion) and Joye and colleagues (2004) ($^{14}CO_2$ trapping). Sulfate-reduction rates were determined using the cold chromium distillation procedure (Kallmeyer *et al.*, 2004).

Microbial activities, enrichment and isolation of microorganisms

In order to measure potential rates of sulfate reduction, methanogenesis, methanotrophy and AOM, incubations were performed with different substrates. All anoxic incubations, with the exceptions of those aiming at culturing hydrogenotrophic methanogens and microorganisms involved in AOM, were carried out in 22 ml Hungate tubes sealed with butyl-rubber stoppers and screw caps, containing 2 ml of original sediment and 10 ml of basal mineral medium (Widdel *et al.*, 2004). For the enrichments of sulfate reducers and of microorganisms involved in sulfate-dependent AOM, medium was prepared with 8 mM sulfate. The medium contained (per litre): 20 g of NaCl, 3 g of $MgCl_26H_2O$, 0.15 g of $CaCl_22H_2O$,

1.14 g of Na_2SO_4, 0.5 g of KCl, 0.1 g of KH_2PO_4, 0.3 g of NH_4Cl. The remaining incubations were conducted with sulfate-free medium. All these media were amended with mineral trace elements, vitamins and bicarbonate (30 mM) (Widdel and Bak, 1992). The pH was adjusted to 7.5 and the media were reduced with 0.5 mM sodium sulfide. All manipulations were carried out under anoxic conditions using either an anoxic chamber (Mecaplex) or the Hungate technique and its modifications (Widdel and Bak, 1992; Breznak and Costilow, 1994). If not stated otherwise, the headspace in the incubation tubes consisted in N_2/CO_2 (90/10 v/v). Each application was tested in triplicate and with three negative controls. Enrichments of methanotrophic bacteria and of hydrogenotrophic microorganisms were carried out in 150 ml of serum vials, containing 10 ml of medium and 2 ml of original sediment under a gas phase of CH_4/O_2 (97/3 v/v). The determination of sulfate-dependent AOM was performed in triplicate under high methane partial pressure (4 atm) in a high-pressure incubation device, as described elsewhere (Nauhaus *et al*., 2002).

To test the ability of indigenous microorganisms to degrade different substrates, a first experiment was conducted in which the substrate concentrations were adjusted in order to be comparable in terms of electrons. As potential electron donor and carbon source of methanogenesis and sulfate reduction, the following substrates were added in different applications: acetate (5 mM), formate (20 mM) and H_2/CO_2 (80/20 v/v; four bars).

Less common substrates of sulfate reduction, methanogenesis and syntrophic reactions were added directly as follows: ethane (headspace: 100%), *n*-butane (headspace: 100%), propane (headspace: 100%), palmitate (5 mM), hexadecane (2% v/v) and crude oil (1% v/v). Different hydrocarbons comprising benzene and naphthalene were also tested as potential substrates of methanogenesis. These hydrocarbons were diluted (0.7% v/v) in sterile, anoxic 2,2,4,4,6,8,8-heptamethylnonane (HMN) as an inert carrier phase to avoid toxic effect of the pure substances.

Triplicate tubes and vials were incubated horizontally at 20°C for the common substrates and palmitate, and at 28°C for the less common substrates. In order to analyse the metabolic end-products, samples were withdrawn (every 2 days) with hypodermic needles and sterile plastic syringes pre-flushed with N_2 through the butyl-rubber stoppers and chemically analysed as described in the analytical procedure section. Rates were calculated per g_{dwt} of sediment from the slope of the curves.

After the first incubation, positive cultures were subcultured, and then purified using the dilution-to-extinction technique under the same conditions.

DNA extraction, 16S rRNA and mcrA gene libraries

Total community DNA was extracted from 300 mg of thawed mud (dry weight) with a protocol combining enzymatic and chemical lysis procedures as described elsewhere (Alain *et al*., 2002). Then, community 16S rDNAs were selectively amplified using universal oligonucleotide primers (MWG-Biotech, Ebersberg, Germany). Two universal bacterial 16S rRNA gene primers, referenced as 8f (5′-AGA GTT TGA TCA TGG CTC AG-3′) and 1492r (5′-GTT ACC TTG TTA CGA CTT-3′), and two universal archaeal 16S rRNA gene primers, respectively, A21f (5′-TTC CGG TTG ATC CTG CCG GA-3′) and A958r (5′-YCC GGC GTT GAM TCC AAT T-3′), were used to amplify 16S rRNA genes from the extracted genomic DNA. Community DNA fragments encoding the *mcrA* (methyl coenzyme M reductase A) were selectively amplified by using the primers MCRf (5′-TAY GAY CAR ATH TGG YT-3′) and MCRr (5′-ACR TTC ATN GCR TAR TT-3′) (Springer *et al*., 1995). Polymerase chain reactions were performed with a Mastercycler Gradient (Eppendorf, Hamburg, Germany) by amplifying approximately 100 ng of bulk DNA in 50 μl of reaction mixtures containing (final concentrations): 1× ReDTaq PCR buffer, 200 μM of each deoxyribonucleoside triphosphate, 100 μM of each reverse and forward primers, and 2.5 U of *Taq* polymerase. The cycling programme was as follows: 94°C for 3 min, 28 cycles of 94°C for 1 min, 48°C (bacterial 16S rDNA and MCR) or 58°C (archaeal 16S rDNA) for 1.5 min, 72°C for 2 min and a final extension period of 6 min at 72°C.

McrA, bacterial and archaeal 16S rRNA gene libraries were constructed by pooling products of two parallel PCR amplifications. Then the combined PCR products were cloned directly using the TOPO TA Cloning® kit (pCR®4-TOPO® suicide vector) according to the manufacturer's specifications (Invitrogen, Carlsbad, CA, USA). Clone libraries were constructed by transforming *E. coli* TOP10F cells. In order to reduce cloning biases, clones of two parallel cloning experiments were combined to construct each library.

Plasmid DNA from each clone was extracted from 2 ml of overnight cultures using the QIAprep® Miniprep Kit (Qiagen, Hilden, Germany), according to the manufacturer's recommendations. Plasmids were checked for the presence of inserts on agarose gels, and then plasmids containing correct-size inserts were used as template for sequencing. Inserts were sequenced by *Taq* cycle on an ABI 3100 sequencer (Applied Biosystems, Foster City, CA, USA), using the following primers: 8f, 520f (5′-GCG CCA GCA GCC GCG GTA A-3′) and 1492r for the bacterial 16S rRNA genes, A21f and A958r for the archaeal 16S rRNA genes, and the vector primer M13f (5′-GTA AAA CGA CGG CCA G-3′) for the genes encoding the *mcrA*.

Phylogenetic analyses

First, insert-containing clones were partially sequenced and fragments were analysed using the DNASTAR Lasergene 6 package (Madison, WI, USA). These partial sequences were aligned in Megalign using the CLUSTALW program, and adjusted to the same size. Sequences displaying more than 99% similarity were considered to be related and grouped in the same phylotype. At least one representative of each unique phylotype was completely sequenced. Sequences were assembled with the SEQMAN program (DNASTAR Lasergene 6 software, Madison, WI, USA).

Sequences were checked for chimera formation by comparing phylogenetic tree topologies constructed from partial sequences. To identify putative close phylogenetic relatives, sequences were compared with those in available databases by use of the BLAST program (Altschul *et al*., 1990). Then, sequences were aligned to their nearest neighbours using either the automated alignment tool of the ARB program pack-

age of the technical university of Munich (http://www.arb-home.de), or the CLUSTALX program (Thompson *et al.*, 1997). Alignments were refined manually using the SEAVIEW program (Galtier *et al.*, 1996). All trees were constructed by the PHYLIP (PHYlogeny Inference Package) version 3.63 software (http://evolution.genetics.washington.edu/phylip/getme.html) on the basis of evolutionary distance (Saitou and Nei, 1987) and maximum likelihood (Felsenstein, 1981). The robustness of inferred topologies was tested by using 100 bootstrap resampling (Felsenstein, 1985). Phylogenetic trees were generated using the SEQBOOT, DNAPARS, DNAML and DNADIST then Neighbour-joining for 16S rDNA sequences, and SEQBOOT, PROTPARS, PROML, PROTDIST then Neighbour-joining for McrA sequences.

Rarefaction curves were calculated with the freeware program ARAREFACTWIN (http://www.uga.edu/strata/software/), based on the analytical approximation algorithm of Hurlbert (1971) with confidence intervals of 95% (Heck *et al.*, 1975).

Quantification of 16S rRNA genes

For quantitative PCR analysis, high-molecular-weight DNA was extracted from 450 mg of frozen sediment samples. Cell lysis was performed with 10% SDS and horizontal shaking for 45 s after addition of zirconium-silica beads. DNA was purified using NH_4 acetate and isopropanol precipitations as described in detail by Henckel and colleagues (1999). Quantitative PCR analysis (ABI Prism 7000, Applied Biosystems) was used to determine the 16S rDNA copy numbers of Archaea (Takai and Horikoshi, 2000) and Bacteria (Nadkarni *et al.*, 2002). 16S rDNA gene copy numbers of Bacteria and Archaea were converted to cell numbers using a conversion factor of 3.6 and 1 respectively (Klappenbach *et al.*, 2001).

Lipid analysis

Free lipids were extracted from the wet mud volcano samples (20 ml) by subsequent ultrasonication using dichloromethane-methanol solvent mixtures of decreasing polarity (1:2 once, 2:1 once, 1:0 twice). Free lipid extracts were separated into four fractions using SPE amino-propyl glass cartridges (1.0 g packing) in a sequence of solvent mixtures of increasing polarity: 10 ml of *n*-hexane (hydrocarbons), 10 ml of *n*-hexane/dichloromethane (2:1, ketones/esters), 12 ml of dichloromethane/acetone (9:1, alcohols) and 10 ml of 2% acetic acid in dichloromethane (fatty acids). Prior to identification and compound-specific carbon isotope analysis, alcohols and fatty acids were reacted with *N,O*-bis(trimethylsilyl)triflouracetamid in pyridine-forming trimethylsilyl (TMS) ethers and esters respectively.

Individual compounds were identified by coupled gas chromatography-mass spectrometry (GC-MS) using a Thermo Trace MS plus system. The Trace GC was equipped with a Varian VF-5ms fused silica capillary column (30 m length, 0.25 mm inner diameter, film thickness 0.25 μm). Stable carbon isotopic compositions of individual compounds were determined using a Thermo Delta plus XP mass spectrometer coupled via a combustion interface III to a Trace GC equipped with a J&W DB-5 fused silica capillary column (30 m length, 0.25 mm inner diameter, film thickness 0.25 μm). Helium was used as carrier gas for both GC systems and column temperatures were programmed from 60°C (1 min isothermal) to 150°C at a rate of 10°C min^{-1}, and then to 310°C at a rate of 4°C min^{-1} (50 min isothermal). Stable isotope ratios are given in the δ-notation against Vienna Pee Dee Belemnite. $\delta^{13}C$-values of alcohols were corrected for the introduction of additional carbon atoms during derivatization. Due to the presence of an unresolved complex mixture in all fractions measurements were complicated and not possible for all biomarker components. Accordingly, reported $\delta^{13}C$-values (means of two measurements where possible) show differences between individual measurements of up to 2‰.

Nucleotide sequence accession numbers

The clone sequence data reported in this article appear in the EMBL, GenBank and DDBJ sequence database under the Accession No. AJ937678–AJ937701 for the 16S rRNA genes, and under the Accession No. AJ937704–AJ937707 for the *mcrA* genes.

The nucleotide accession numbers of the isolates are AJ937702–AJ937703.

Acknowledgements

We are grateful to Oana Iftime (University of Bucharest) and Alexandru Iftime (National Museum of Natural History 'Grigore Antipa', Bucharest) for giving us information about the study site, and to Ion Musat for guiding us in the Carpathian Mountains. We acknowledge Paul Faber (BGR) for gas isotope analyses, and Imke Müller (MPI), Ramona Appel (MPI) and Xavier Prieto (RCOM) for technical assistance. We thank Michael Böttcher, Jens Harder and Katrin Knittel for fruitful discussions during the preparation of the manuscript, and one anonymous reviewer for comments and suggestions improving the manuscript. Special thanks to Friedrich Widdel and Antje Boetius for helpful discussions and review of the manuscript. We acknowledge Tina Lösekann for kindly supplying us with unpublished sequences. This work was funded by the Max Planck Society (Germany), the Deutsche Forschungsgemeinschaft as part of the DFG-Research Center 'Ocean Margins' at the University of Bremen, by the Alexander von Humboldt Stiftung (Germany) through a postdoctoral fellowship for K.A. and by the GEOTECHNOLOGIEN project MUMM (Fkz 03G0554A, Fkz G0608A). This is publication n°GEOTECH-183 of the GEOTECHNOLOGIEN programme of the BMBF project MUMM.

References

Aeckersberg, F., Rainey, F.A., and Widdel, F. (1998) Growth, natural relationships, cellular fatty acids and metabolic adaptation of sulphate-reducing bacteria that utilize long-chain alkanes under anoxic conditions. *Arch Microbiol* **170:** 361–369.

Alain, K., Olagnon, M., Desbruyères, D., Pagé, A., Barbier, G., Juniper, S.K., *et al.* (2002) Phylogenetic characterization of the bacterial assemblage associated with mucous

secretions of the hydrothermal vent polychaete *Paralvinella palmiformis*. *FEMS Microbiol Ecol* **42:** 463–476.
Altschul, S., Gish, W., Miller, W., Myers, E., and Lipman, D. (1990) Basic local alignment search tool. *J Mol Biol* **215:** 403–410.
Bak, F., and Widdel, F. (1986) Anaerobic degradation of phenol and phenol derivatives by *Desulfobacterium phenolicum*. *Arch Microbiol* **146:** 177–180.
Boetius, A., Ravenschlag, K., Schubert, C., Rickert, D., Widdel, F., Gieseke, A., *et al.* (2000) A marine microbial consortium apparently mediating anaerobic oxidation of methane. *Nature* **407:** 623–626.
Boschker, H.T.S., and Middelburg, J.J. (2002) Stable isotopes and biomarkers in microbial ecology. *FEMS Microbiol Ecol* **40:** 85–95.
Breznak, J.A., and Costilow, R.N. (1994) Physicochemical factors in growth. In *Methods for General and Molecular Bacteriology.* Gerhard, P., Murray, R.G.E., Wood, W.A., and Krieg, N.R. (eds). Washington, USA: American Society for Microbiology Press, pp. 137–154.
Cord-Ruwisch, R. (1985) A quick method for the determination of dissolved and precipitated sulfides in cultures of sulphate-reducing bacteria. *J Microbiol Methods* **4:** 33–36.
Devol, A.H., and Ahmed, S.L. (1981) Are high rates of sulphate reduction associated with anaerobic methane oxidation? *Nature* **291:** 407–408.
Dimitrov, L.I. (2002) Mud volcanoes – the most important pathway for degassing deeply buried sediments. *Earth Sci Rev* **59:** 49–76.
Dinh, H.T., Kuever, J., Mußmann, M., Hassel, A.W., Stratmannn, M., and Widdel, F. (2004) Iron corrosion by novel anaerobic microorganisms. *Nature* **427:** 829–832.
Dojka, M.A., Harris, J.K., and Pace, N.R. (2000) Expanding the known diversity and environmental distribution of an uncultured phylogenetic division of bacteria. *Appl Environ Microbiol* **66:** 1617–1621.
Elvert, M., Boetius, A., Knittel, K., and Jørgensen, B.B. (2003) Characterization of specific membrane fatty acids as chemotaxonomic markers for sulphate-reducing bacteria involved in the anaerobic oxidation of methane. *Geomicrobiol J* **20:** 403–419.
Etiope, G., Baciu, C., Caracausi, A., Italiano, F., and Cosma, C. (2004) Gas flux to the atmosphere from mud volcanoes in eastern Romania. *Terra Nova* **16:** 179–184.
Felsenstein, J. (1981) Evolutionary trees from DNA sequences: a maximum likelihood approach. *J Mol Evol* **17:** 368–376.
Felsenstein, J. (1985) Confidence limits on phylogenies: an approach using the bootstrap. *Evolution* **30:** 783–791.
Findlay, R.H., and Dobbs, F.C. (1993) Quantitative description of microbial communities using lipid analysis. In *Handbook of Methods of Aquatic Microbial Ecology*. Kemp, P.F., Sherr, B.F., Sherr, E.B., and Cole, J.J. (eds). Boca Raton, FL, USA: Lewis Publishers, pp. 271–284.
Galtier, N., Gouy, M., and Gautier, C. (1996) SEAVIEW and PHYLO_WIN: two graphic tools for sequence alignment and molecular phylogeny. *CABIOS* **12:** 543–548.
Hallam, S.J., Girguis, P.R., Preston, C.M., Richardson, P.M., and DeLong, E.F. (2003) Identification of methyl coenzyme M reductase A (*mcrA*) genes associated with methane-oxidizing Archaea. *Appl Environ Microbiol* **69:** 5483–5491.
Hallam, S.J., Putnam, N., Preston, C.M., Detter, J.C., Rokhsar, D., Richardson, P.M., and DeLong, E.F. (2004) Reverse methanogenesis: testing the hypothesis with environmental genomics. *Science* **305:** 1457–1462.
Heck, K.L., van Belle, G., and Simberloff, D. (1975) Explicit calculation of the rarefaction diversity measurement and the determination of sufficient sample size. *Ecology* **56:** 1459–1461.
Heijs, S.K., Sinninghe Damsté, J.S., and Forney, L.J. (2005) Characterization of a deep-sea microbial mat from an active cold seep at the Milano mud volcano in the Eastern Mediterranean Sea. *FEMS Microbiol Ecol* **54:** 47–56.
Henckel, T., Friedrich, M., and Conrad, R. (1999) Molecular analyses of the methane-oxidizing microbial community in rice field soil by targeting the genes of the 16S rRNA, particulate methane monooxygenase, and methanol dehydrogenase. *Appl Environ Microbiol* **65:** 1980–1990.
Hinrichs, K.-U., and Boetius, A. (2002) The anaerobic oxidation of methane: new insights in microbial ecology and biogeochemistry. In *Ocean Margin Systems*. Wefer, G., Billett, D., Hebbeln, D., *et al.* (eds). Berlin, Germany: Springer-Verlag, pp. 457–477.
Hinrichs, K.U., Hayes, J.M., Sylva, S.P., Brewer, P.G., and DeLong, E.F. (1999) Methane-consuming archaebacteria in marine sediments. *Nature* **398:** 802–805.
Hinrichs, K.-U., Hmelo, L.R., and Sylva, S.P. (2003) Molecular fossil record of elevated methane levels in late Pleistocene coastal waters. *Science* **299:** 1214–1217.
Hoehler, T.M., Alperin, M.J., Albert, D.B., and Martens, C.S. (1994) Field and laboratory studies of methane oxidation in an anoxic marine sediment – evidence for a methanogen-sulphate reducer consortium. *Global Biogeochem Cycles* **8:** 451–463.
Hovland, M., Hill, A., and Stokes, D. (1997) The structure and geomorphology of the Dashgil mud volcano, Azerbaidjan. *Geomorphology* **21:** 1–15.
Hurlbert, S.H. (1971) The nonconcept of species diversity: a critique and alternative parameters. *Ecology* **52:** 577–586.
Inagaki, F., Tsunogai, U., Suzuki, M., Kosaka, A., Machiyama, H., Takai, K., *et al.* (2004) Characterization of C_1-metabolizing prokaryotic communities in methane seep habitats at the Kuroshima Knoll, southern Ryukyu arc, by analyzing *pmoA*, *mmoX*, *mxaF*, *mcrA*, and 16S rRNA genes. *Appl Environ Microbiol* **70:** 7445–7455.
Joye, S.B., Boetius, A., Orcutt, B.N., Montoya, J.P., Schulz, H.N., Erickson, M.J., and Logo, S.K. (2004) The anaerobic oxidation of methane and sulfate reduction in sediments from Gulf of Mexico cold seeps. *Chem Geol* **205:** 219–238.
Kallmeyer, J., Ferdelman, T.G., Weber, A., Fossing, H., and Jørgensen, B.B. (2004) A cold chromium distillation procedure for radiolabeled sulfide applied to sulfate reduction measurements. *Limnol Oceanogr Methods* **2:** 171–180.
Klappenbach, J.L., Saxman, P.R., Cole, J.R., and Schmidt, T.M. (2001) rrndb: the ribosomal RNA operon copy number database. *Nucleic Acids Res* **29:** 181–184.
Knittel, K., Boetius, A., Lemke, A., Eilers, H., Lochte, K., Pfannkuche, O., and Linke, P. (2003) Activity, distribution, and diversity of sulphate reducers and other bacteria in

sediments above gas hydrates (Cascadia Margin, Oregon). *Geomicrobiol J* **20:** 269–294.

Knittel, K., Lösekann, T., Boetius, A., Kort, R., and Amann, R. (2005) Diversity and distribution of methanotrophic archaea at cold seeps. *Appl Environ Microbiol* **71:** 467–479.

Knoblauch, C., Sahm, K., and Jørgensen, B.B. (1999) Psychrophilic sulphate-reducing bacteria isolated from permanently cold arctic marine sediments: description of *Desulfofrigus oceanense* gen. nov., sp. nov., *Desulfofrigus fragile* sp. nov., *Desulfofaba gelida* gen. nov., sp. nov., *Desulfotalea psychrophila* gen. nov., sp. nov. and *Desulfotalea arctica* sp. nov. *Int J Syst Bacteriol* **49:** 1631–1643.

Koga, Y., Nishihara, M., Morii, H., and Akagawa-Matsushita, M. (1993) Ether polar lipids of methanogenic bacteria: structures, comparative aspects and biosyntheses. *Microbiol Rev* **57:** 164–182.

Koga, Y., Morii, H., Akagawa-Matsushita, M., and Ohga, M. (1998) Correlation of polar lipid composition with 16S rRNA phylogeny in methanogens. Further analyses of lipid component parts. *Biosci Biotech Biochem* **62:** 230–236.

Kopf, A.J. (2002) Significance of mud volcanism. *Rev Geophys* **40:** 2.1–2.52.

Krüger, M., Frenzel, P., and Conrad, R. (2001) Microbial processes influencing methane emission from rice fields. *Global Change Biol* **7:** 49–63.

Krüger, M., Meyerdierks, A., Glöckner, F.O., Amann, R., Widdel, F., Kube, M., *et al.* (2003) A conspicuous nickel protein in microbial mats that oxidize methane anaerobically. *Nature* **426:** 878–881.

Kuever, J., Könneke, M., Galushko, A., and Drzyzga, O. (2001) Reclassification of *Desulfobacterium phenolicum* as *Desulfobacula phenolica* comb. nov. and description of strain Sax (T) as *Desulfotignum balticum* gen. nov., sp. nov. *Int J Syst Evol Microbiol* **51:** 171–177.

Lanoil, B.D., Sassen, R., La Duc, M.T., Sweet, S.T., and Nealson, K.H. (2001) *Bacteria* and *Archaea* physically associated with Gulf of Mexico gas hydrates. *Appl Environ Microbiol* **67:** 5143–5153.

Luton, P.E., Wayne, J.M., Sharp, R.J., and Riley, P.W. (2002) The *mcrA* gene as an alternative to 16S rRNA in the phylogenetic analysis of methanogen populations in landfill. *Microbiology* **148:** 3521–3530.

Michaelis, W., Seifert, R., Nauhaus, K., Treude, T., Thiel, V., Blumenberg, M., *et al.* (2002) Microbial reefs in the Black Sea fueled by anaerobic oxidation of methane. *Science* **297:** 1013–1015.

Milkov, A.V., Sassen, R., Apanasovich, T.V., and Dadashev, F.G. (2003) Global gas flux from mud volcanoes: a significant source of fossil methane in the atmosphere and the ocean. *Geophys Res Lett* **30:** 1037.

Milkov, A.V., Vogt, P.R., Crane, K., Lein, A.Y., Sassen, R., and Cherkashev, G.A. (2004) Geological, geochemical, and microbial processes at the hydrate-bearing Haakon Mosby mud volcano: a review. *Chem Geol* **205:** 347–366.

Morse, J.W., and Mackenzie, F.T. (1990) Geochemistry of sedimentary carbonate. *Dev Sedimentol* **48:** 707.

Nadkarni, M., Martin, F.E., Jacques, N.A., and Hunter, N. (2002) Determination of bacterial load by real-time PCR using a broad range (universal) probe and primer set. *Microbiology* **148:** 257–266.

Nauhaus, K., Boetius, A., Krüger, M., and Widdel, F. (2002) *In vitro* demonstration of anaerobic oxidation of methane coupled to sulphate reduction in sediment from a marine gas hydrate area. *Environ Microbiol* **4:** 296–305.

Orphan, V.J., House, C.H., Hinrichs, K.-U., McKeegan, K.D., and DeLong, E.F. (2001) Methane-consuming archaea revealed by directly coupled isotopic and phylogenetic analysis. *Science* **293:** 484–487.

Orphan, V.J., House, C.H., Hinrichs, K.-U., McKeegan, K.D., and DeLong, E.F. (2002) Multiple archaeal groups mediate methane oxidation in anoxic cold seep sediments. *Proc Natl Acad Sci USA* **99:** 7663–7668.

Reeburgh, W.S. (1980) Anaerobic methane oxidation; rate depth distributions in Skan Bay sediments. *Earth Planet Sci Lett* **47:** 345–352.

Rohmer, M., Bouvier-Nave, P., and Ourisson, G. (1984) Distribution of hopanoid triterpenes in prokaryotes. *J Gen Microbiol* **130:** 1137–1150.

Rossello-Mora, R., and Amann, R. (2001) The species concept for prokaryotes. *FEMS Microbiol Rev* **25:** 39–67.

Rütters, H., Sass, H., Cypionka, H., and Rullkötter, J. (2001) Monoalkylether phospholipids in the sulphate-reducing bacteria *Desulfosarcina variabilis* and *Desulforhadus amnigenus*. *Arch Microbiol* **176:** 435–442.

Saitou, N., and Nei, M. (1987) The neighbour-joining method: a new method for reconstructing phylogenetic trees. *Mol Biol Evol* **4:** 406–425.

So, C.M., and Young, L.Y. (1999) Isolation and characterization of a sulphate-reducing bacterium that anaerobically degrades alkanes. *Appl Environ Microbiol* **65:** 2969–2976.

Springer, E., Sachs, M.S., Woese, C.R., and Boone, D.R. (1995) Partial gene-sequences for the α-subunit of methylcoenzyme M reductase (MCRI) as a phylogenetic tool for the family *Methanosarcinaceae*. *Int J Syst Bacteriol* **45:** 554.559.

Strous, M., and Jetten, M.S.M. (2004) Anaerobic oxidation of methane and ammonium. *Annu Rev Microbiol* **58:** 99–117.

Szewzyk, R., and Pfennig, N. (1987) Complete oxidation of catechol by the strictly anaerobic sulphate-reducing *Desulfobacterium catecholicum* sp. nov. *Arch Microbiol* **147:** 163–168.

Takai, K., and Horikoshi, K. (2000) Rapid detection and quantification of members of the archaeal community by quantitative PCR using fluorogenic probes. *Appl Environ Microbiol* **66:** 5066–5072.

Taylor, J., and Parkes, R.J. (1983) The cellular fatty acids of the sulphate-reducing bacteria, *Desulfobacter* sp., *Desulfobulbus* sp. and *Desulfovibrio desulfuricans*. *J Gen Microbiol* **129:** 3303–3309.

Thompson, J.D., Gibson, T.J., Plewniak, F., Jeanmougin, F., and Higgins, D.G. (1997) The CLUSTALX windows interface: flexible strategies for multiple sequence alignment aided by quality analysis tools. *Nucleic Acids Res* **24:** 4876–4882.

Treude, T., Boetius, A., Knittel, K., Wallmann, K., and Jørgensen, B.B. (2003) Anaerobic oxidation of methane above gas hydrates at Hydrate Ridge, NE Pacific Ocean. *Mar Ecol Prog Ser* **264:** 1–14.

Treude, T., Niggemann, J., Kallmeyer, J., Wintersteller, P., Schubert, C.J., Boetius, A., and Jørgensen, B.B. (2005)

Anaerobic oxidation of methane and sulfate reduction along the Chilean continental margin. *Geochim Cosmochim Acta* **69:** 2767–2779.

Valentine, D.L. (2002) Biogeochemistry and microbial ecology of methane oxidation in anoxic environments: a review. *Antonie Van Leeuwenhoek* **81:** 271–282.

Whiticar, M.J. (1999) Carbon and hydrogen isotope systematics of bacterial formation and oxidation of methane. *Chem Geol* **161:** 291–314.

Widdel, F., and Bak, F. (1992) Gram-negative mesophilic sulphate-reducing bacteria. In *The Prokaryotes*. Balows, A., Trüper, H.G., Dworkin, M., Harder, W., and Schleifer, K.-H. (eds). New York, USA: Springer, pp. 3352–3378.

Widdel, F., Boetius, A., and Rabus, R. (2004) Anaerobic biodegradation of hydrocarbons including methane. In *The Prokaryotes*, release, 3.18 (21/12/2004) [WWW document]. URL http://link.springer-ny.com/link/service/books/10125/

Willems, A., and Collins, M.D. (1996) Phylogenetic relationships of the genera *Acetobacterium* and *Eubacterium sensu stricto* and reclassification of *Eubacterium alactolyticum* as *Pseudoramibacter alactolyticus* gen. nov., comb. nov. *Int J Syst Bacteriol* **46:** 1083–1087.

Yakimov, M.M., Giuliano, L., Crisafi, E., Chernikova, T.N., Timmis, K.N., and Golyshin, P.N. (2002) Microbial community of a saline mud volcano at San Biagio-Belpasso, Mt. Etna (Italy). *Environ Microbiol* **4:** 249–256.

III.4

Thermophilic anaerobic oxidation of methane by marine microbial consortia

Thomas Holler,[1] Friedrich Widdel,[1] Katrin Knittel,[1] Rudolf Amann,[1]
Matthias Y. Kellermann,[2] Kai-Uwe Hinrichs,[2] Andreas Teske,[3]
Antje Boetius,[1,2,4] and Gunter Wegener[1,2]*

Manuskript eingereicht

---

[1]Max Planck Institute for Marine Microbiology, Celsiusstr.1, 28359 Bremen, Germany

[2]Organic Geochemistry Group, Department of Geosciences and MARUM Center for Marine Environmental Sciences, University of Bremen, 28359 Bremen, Germany

[3]Department of Marine Sciences, The University of North Carolina at Chapel Hill, Chapel Hill, North Carolina, 27599, USA

[4]Alfred Wegener Institute for Polar and Marine Research, 27515 Bremerhaven, Germany

*** Corresponding author**

Abstract

The anaerobic oxidation of methane with sulfate (AOM) controls the emission of the greenhouse gas methane from the ocean floor. AOM is performed by microbial consortia of archaea (ANME) associated with partners related to sulfate-reducing bacteria. *In vitro* enrichments of AOM were so far only successful at temperatures ≤ 25 °C, however energy gain for growth by AOM with sulfate is in principle also possible at higher temperatures. Sequences of 16S rRNA genes and core lipids characteristic for ANME as well as hints of *in situ* AOM activity were indeed reported for geothermally heated marine environments, yet no direct evidence for thermophilic growth of marine ANME consortia was obtained to date. To study possible thermophilic AOM we investigated hydrothermally influenced sediment from the Guaymas Basin. *In vitro* incubations showed activity of sulfate-dependent methane oxidation between 5 and 70 °C with an apparent optimum between 45 and 60 °C. AOM was absent at temperatures ≥75 °C. Long-term enrichment of AOM was fastest at 50 °C, yielding a 13-fold increase of methane-dependent sulfate reduction within 250 days, equivalent to an apparent doubling time of 68 days. The enrichments were dominated by novel ANME-1 consortia, mostly associated with bacterial partners of the deltaproteobacterial HotSeep-1 cluster, a deeply branching phylogenetic group previously found in a Butane-amended 60 °C-enrichment culture of Guaymas sediments. Its closest relatives (*Desulfurella* spp.; *Hippea maritima*) are moderately thermophilic sulfur reducers. Results indicate that AOM, and ANME archaea, could be more widespread than previously known and of biogeochemical relevance in hot marine habitats.

Introduction

Methane, the simplest hydrocarbon, is an atmospheric trace gas of climatic relevance. Vast amounts of methane are formed by anaerobic microbial degradation of organic matter as well as by geothermal processes (Schoell 1980) and may eventually reach the atmosphere. In the ocean, however, most methane migrating upwards from deep sediment strata is already consumed within the anoxic seafloor at distinct horizons characterized by simultaneous methane and sulfate depletion (Reeburgh 2007). These horizons are usually populated by archaea (ANME groups) and bacteria of distinct phylogenetic lineages clustering with methanogens and Deltaproteobacteria, respectively (Boetius *et al* 2000, Knittel and Boetius 2009). The ANME archaea are thought to oxidize the methane, in principle via a reversal of the reactions of methanogenesis (Zehnder and Brock 1979, Krüger *et al* 2003, Hallam *et al* 2004, Scheller *et al* 2010). Biochemical studies so far focused on the ANME-associated protein that is closely related to methyl-coenzyme M reductase (Mcr), the nickel enzyme catalyzing the terminal step in methanogenesis (Thauer 1998, Hallam *et al* 2003, Krüger *et al* 2003, Scheller *et al* 2010). The associated Deltaproteobacteria most likely perform the sulfate reduction, using methane-derived reducing equivalents (Hoehler *et al*. 1994). Yet, the mechanism of the intercellular transfer of reducing equivalents between the partners has not been elucidated, and axenic binary cultures have not been reported to date.

ANME-2 is a prominent phylogenetic archaeal group at most marine cold gas seeps (e.g. Orphan *et al* 2001, Mills *et al* 2003, Wegener *et al* 2008b, Knittel and Boetius 2009) and some sulfate-methane transition zones where the temperature is 4–14 °C (Knittel and Boetius 2009). Another group, ANME-3, occurs for instance at Haakon Mosby Mud Volcano (Niemann *et al* 2006; *in situ* temperature –1.5 °C) and the Eastern Mediterranean seepages (Omoregie et al. 2008; 14 °C). Cells of both groups form dense consortia with specific bacterial phylotypes clustering with sulfate-reducing Deltaproteobacteria (most often a cluster within *Desulfosarcina,* SEEP-SRB1a, Schreiber *et al* 2010) or relatives of *Desulfobulbus* (Knittel *et al* 2003, Lösekann *et al* 2007, Pernthaler *et al* 2008, Schreiber *et al* 2010), respectively. A third phylogenetic group, ANME-1, is dominant in the microbial biomass layers covering chimney structures at methane seeps in the Black Sea (Michaelis *et al* 2002; *in situ* temperature of ~10 °C), and in several diffusive methane interfaces (Thomsen *et al* 2001, Lanoil *et al* 2005, Harrison *et al* 2009, Aquilina *et al* 2010). The AOM habitats with these ANME-types exhibit temperatures between –1.5 and 25 °C (Boetius *et al* 2009, Supporting Table 1). First hints of anaerobic methanotrophs thriving at higher temperatures were obtained by identification of 16S rRNA genes of ANME-1 (Teske *et al* 2002, Schrenk *et*

al 2004, Roussel *et al* 2008) and ANME-specific core lipids (Schouten *et al* 2003) in hydrothermally influenced marine sediments. Also radiotracer incubation of such sediment indicated thermophilic AOM (Kallmeyer and Boetius 2004).

Indeed, AOM according to $CH_4 + SO_4^{2-} \rightarrow HCO_3^- + HS^- + H_2O$ should in principle be possible also under thermophilic conditions (ΔG with 100 kPa CH_4, 0.028 M SO_4^{2-}, 0.03 M HCO_3^- and 0.001 M HS^- between 25 and 80 °C ranges from –30 to –34 kJ mol^{-1}; for calculations see Material and Methods). Also from an enzymatic point of view a restriction of AOM to low temperatures is not expected. Methanogenesis as a metabolically related process (see above) and sulfate reduction with electron donors other than methane have been reported to occur at temperatures up to 100 °C (Jørgensen *et al* 1992, Stetter 1996).

Here, we investigated possible thermophilic AOM and the responsible microorganisms in hydrothermally influenced sediments from the Guaymas Basin, Gulf of California. We combined rate measurements, enrichment cultivation with methane as sole organic substrate, and analyses of molecular markers. Hydrothermal Guaymas Basin sediments are characterized by rapid thermochemical transformation of labile fractions of settled detritus to volatile fatty acids, methane and higher hydrocarbons (Simoneit *et al* 1988, Martens 1990). These compounds act as substrates for diverse microorganisms such as sulfate reducers. The high microbial sulfide production in these sediments fosters patchy mats of sulfide-oxidizing bacteria such as *Beggiatoa* (Jannasch *et al* 1989). From such areas a variety of sulfate-reducing bacteria (Rueter *et al*. 1994; Jeanthon *et al* 2002), sulfate-reducing archaea (Burggraf *et al* 1990, Khelifi *et al* 2010) and methanogenic archaea (Kurr *et al* 1991) have been isolated.

Material and Methods

Sediment characterization and sampling

Samples from a hydrothermal vent site in the Guaymas Basin were obtained during the RV *Atlantis* cruise AT15-56 in November/December 2009 with the submersible *Alvin* (Dive 4570; 27°00.437 N, 111°24.548 W) from bacterial mats (Supporting Figure 1). Temperature profiles were measured *in situ* and the retrieved sediment was sectioned into the following horizons: (A) 2–13 cm, 4–30 °C; (B) 14–25 cm, 30–60 °C; and (C) 26–45 cm, 60–85 °C (Supporting Figure 1c). The cored material consisted of unconsolidated, methane-rich clays. The sections were transferred to glass bottles, diluted 1:1 with artificial anoxic seawater medium (Widdel and Bak 1992) and stored anaerobically with a methane headspace until further processing.

Determination of sulfate reduction rates

Sulfate reduction rates were determined by injection of 25 µl $^{35}SO_4^{2-}$ tracer (Amersham) so as to achieve ~75 kBq per horizon (~ 30 cm^3) into push cores at intervals of 1 cm and incubation at *in situ* temperature for 12 to 48 h. Cores were sliced into 1 cm sections and transferred to zinc acetate solution (0.9 M) to stop the reaction and fix sulfide. The radiolabeled reactant ($^{35}SO_4^{2-}$) and products (total reduced inorganic sulfur) were separated by reduction with Cr^{2+} and cold distillation (Kallmeyer *et al* 2004). The radioactivity of both pools was quantified by scintillation counting (scintillation cocktail, LumaSafe™ Plus; scintillation counter, 2900TR LSA, Packard), and rates were calculated as described (Jørgensen and Fenchel 1974).

Determination of methane oxidation rates

Methane oxidation to inorganic carbon was determined via radiolabelling of homogeneous sediment slurries prepared from defined proportions of medium and sediment. Samples (2 ml slurry; dry weight 195 mg) were distributed to culture tubes (5 ml) and sealed with butyl rubber stoppers inside an anoxic chamber. The headspace was completely filled with methane-saturated (250 kPa) synthetic seawater while gas was allowed to escape via an inserted hypodermic needle. Samples were pre-incubated for 5 days at the designated temperatures. Control samples were inactivated with concentrated formaldehyde solution (final concentration, 20 g l^{-1}). Upon pre-incubation, carrier-free $^{14}CH_4$ (15 kBq) dissolved in 50 µl of anoxic water 50 µl was added per tube. Tubes were further incubated for 48 h. Activity was stopped by alkalization with NaOH. The total methane concentration was determined by gas chromatography using a 5890A instrument (Hewlett Packard) equipped with a Porapak-Q column (6 ft, 0.125 in, 80/100 mesh; Agilent) and a flame ionization detector, and operated at 40 °C with helium as carrier gas. Radioactivity in methane and inorganic carbon was determined after their separation and conversion to CO_2 as described (Treude *et al* 2003). Label in the trapped CO_2 fractions was determined by scintillation counting (cocktail Ultima Gold™ XR, Perkin Elmer; instrument 2900TR LSA, Packard). Rates were calculated as described previously (Treude *et al* 2003).

Enrichment of anaerobic methanotrophic microorganisms

Microorganisms were enriched in culture vials (156 ml) at 37 °C (samples from horizon A), 50 °C (horizon B) and 60 °C (horizon B) with synthetic seawater medium (Widdel and Bak 1992) under a headspace (56 ml) of 250 kPa CH_4 and 40 kPa CO_2. Controls for each temperature were incubated with N_2 and CO_2. Vials were incubated at the indicated

temperatures on rotary shakers at low speed (50 rpm). Activity was followed by quantification of sulfide using a rapid colorimetric test (Cord-Ruwisch 1985). The sulfidic supernatant was replaced by fresh medium every 4 to 8 weeks.

Determination of the methane oxidation to sulfide production ratio

To measure methane consumption coupled to sulfate reduction (and resulting sulfide production), sediment slurries (50 ml) were added to culture vials (250 ml) inside an anoxic chamber. Bottles were completely filled with CH_4-saturated (250 kPa) anoxic seawater medium (see above), incubated at 50°C, and intensely shaken by hand once per day. Per time point, 1 ml supernatant was withdrawn and replaced with the same volume of sterile medium. The sample was injected into rubber-sealed vials (6 ml) containing 0.5 ml $ZnCl_2$ (50 g l^{-1}) to bind sulfide. Methane was quantified in the headspace by gas chromatography (see above). Sulfide was liberated from ZnS (by acidification) and quantified colorimetrically using the methylene blue-forming reaction in a miniaturized assay (Aeckersberg *et al* 1991).

DNA extraction, PCR, and clone library construction

DNA was extracted as described by Zhou *et al* (1996) from a 9 ml subsample of an enrichment cultures incubated for 3 and 9 months. After 9 months, only the supernatant after 1 hour settling time was used for the extraction. The protocol encompassed three cycles of freezing and thawing, chemical lysis in a high-salt extraction buffer (1.5 M NaCl) by heating of the suspension in the presence of sodium dodecyl sulfate (SDS) and hexadecyltrimethylammonium bromide, and treatment with proteinase K. The following domain-specific primers were used to amplify almost-full-length 16S rRNA genes from the extracted chromosomal DNAs: Bacteria, primers GM3F (Muyzer *et al* 1995) and EUB1492R (Kane *et al* 1993); Archaea, primers 20F (Massana *et al* 1997) and Arc1492R (Teske *et al* 2002). In addition, fragments of the gene coding for the alpha subunit of methyl-coenzyme M reductase (*mcrA*) were amplified using the primers ME1 and ME2 (Hales *et al* 1996).

PCR reactions were performed in a Mastercycler Gradient (Eppendorf, Germany) in a 20 µl reaction volume. Each PCR reaction contained: 0.5 µM of each primer, 200 µM of each deoxyribonucleoside triphosphate, 6 µg bovine serum albumin, 1 × PCR buffer (5Prime, Germany), 1 × PCR Enhancer (5Prime), 0.25 U *Taq* DNA Polymerase (5Prime) and 5–10 ng of template DNA. The following cycling conditions were applied: one initial step at 95 °C for 5 min; 26 cycles, each at 95 °C for 1 min, 42 °C (58 °C for Arch20F/Arc1492R; 48 °C for ME1/ME2) for 1.5 min, and 72 °C for 3 min; and final step at 60 °C for 60 min. After PCR,

the DNA of 10 reactions was pooled, gel extracted and purified by using the QIAquick PCR Purification Kit (Qiagen) according to the manufacturer's recommendations. The DNA was ligated to the pGEM-T-Easy vector (Promega) and transformed into *Escherichia coli* One Shot Top10 cells (Invitrogen) according to the manufacturer's recommendations. Taq cycle sequencing was performed using ABI BigDye Terminator chemistry and an ABI377 sequencer (Applied Biosystems, USA).

Phylogenetic analysis

The phylogenetic affiliation was inferred with the ARB software package (Ludwig *et al* 2004) based on Release 102 of the ARB SILVA database (Pruesse *et al* 2007). Comparative sequence analyses were performed with representative sequences from the Guaymas Basin enrichments together with sequences of related archaea (Figure 4a), Deltaproteobacteria (Figure 4b), and methyl coenzyme M reductases (Figure 4c), found in public databases. In total, 877 (deltaproteobacterial) and 1090 (archaeal) nearly full-length 16S rRNA gene sequences (> 1350 bp) were used for tree construction. For *mcrA* tree construction, 483 sequences (>230 amino acids) were considered. Phylogenetic trees were calculated by maximum likelihood analysis (PhyML, RAxML) and the neighbor-joining algorithm. A 50% base frequency filter was used for 16S rRNA gene tree calculation to exclude highly variable positions. The phylogenetic McrA tree was generated from *mcrA*-deduced amino acid sequences using PhyML and RAxML with a 30% amino acid frequency filter. The resulting trees were compared manually and, if necessary, a consensus tree was constructed. Relevant partial sequences were subsequently added to the tree according to maximum parsimony criteria, without allowing changes in the overall tree topology.

Nucleotide sequences have been deposited at EMBL, GenBank and DDBJ under accession numbers FR682488 to FR682496 (archaeal 16S rRNA genes), FR682813 to FR682818 (*mcrA*) and FR682644 to FR682663 (bacterial 16S rRNA genes).

Design and application of oligonucleotide probes

Oligonucleotide probes HotSeep-1-590, ANME-1-GI812, and ANME-1-GII186 (Supporting Table 2) were designed using the ARB probe tool. Specificity of the probes was evaluated by Clone-FISH (Schramm *et al* 2002) for probe HotSeep-1-590, or directly on enrichment samples for probes ANME-1-GI812 and ANME-1-GII186. To generate melting curves, the probes were hybridized to clones at formamide concentrations of 0%, 10%, 20%, 30%, 40%, 50%, 60% and 70%. To increase the accessibility of the HotSeep-1-590 probe, target site on

the 16S rRNA, helper oligonucleotides were designed. In addition, the probes were tested for sensitivity (target group hits) and specificity (outgroup hits) *in silico* with the ARB probe match tool. Probe HotSeep-1-590 has at least 3 mismatches to non-target sequences. Probes ANME-1-GI812 and ANME-1-GII186 were designed to discriminate between the two ANME-1 Guaymas subclusters: Probe ANME-1-GI812 has 2 mismatches to cluster II and ANME-1-GII186 has 5 mismatches to cluster I. Oligonucleotide probes were synthesized by Biomers (Germany).

Samples for cell hybridization were fixed with formaldehyde (30 g l^{-1}, final concentration) for 2 h at room temperature, washed with 1 × phosphate-buffered saline (PBS), pH 7.2, and stored in PBS:ethanol (1:1) at –20 °C until further processing. Fixed samples were treated by mild sonication for 20 s with a MS73 probe (Sonopuls HD70, Bandelin) at ≤10 W.

Catalyzed reporter deposition fluorescence hybridization (CARD-FISH) of cells was performed as described previously (Pernthaler *et al* 2004) with the following modifications: Aliquots of the enrichment samples were filtered onto 0.2 μm pore-size GTTP polycarbonate filters (Millipore, Germany). For cell wall permeabilization, filters were sequentially incubated in SDS solution (0.5%) for 10 min and proteinase K solution (15 μg ml^{-1} , 0.1 M Tris-HCl, 0.05 M EDTA, pH 8, 0.5 M NaCl) for 2 min at room temperature. Endogenous peroxidases were inactivated by incubating the filters in 0.01 M HCl for 5 min at room temperature. Permeabilization with higher HCl concentrations or lysozyme caused damage of cells and disturbance of their arrangement within the ANME-1/HotSeep-1 sheaths. The oligonucleotide probes were applied with formamide concentrations according to literature data or Clone-FISH results, respectively (Supporting Table 2). For dual-CARD-FISH, peroxidases of initial hybridizations were inactivated by 30 min incubation in 0.3% H_2O_2 in methanol at room temperature. Catalyzed reporter deposition was performed using the fluorochromes Alexa Fluor 488 and Alexa Fluor 594. Finally, samples were stained with 4′,6′-diamidino-2-phenylindole (DAPI). Micrographs were obtained by confocal laser scanning microscopy (LSM510; Zeiss, Germany).

Lipid extraction and analyses

Total lipid extracts were retrieved by modified Bligh and Dyer extraction (Sturt *et al* 2004). Fractions of core glycerol dibiphytanyl glycerol tetraethers (CDGTs) were purified by preparative liquid chromatography (ThermoFinnigan Surveyor equipped with preparative LiChrosphere Si60 column, 250 mm × 10 mm × 5 μm, Alltech) connected to a Gilson FC204

fraction collector. Analysis of core GDGTs followed the described procedure (Huguet *et al* 2006) with C_{46}-GDGT as injection standard. Analysis was done by combined liquid chromatography-quadrupol mass spectrometry (1200 series, Agilent,) using a Prevail Cyano column (3 × 150 mm; Grace, USA). GDGTs were eluted isocratically. Compounds were detected by atmospheric pressure positive ion chemical ionization mass spectrometry

For isotopic analysis, GDGTs were subjected to ether cleavage using BBr_3 (Aldrich) in dichloromethane (Bradley *et al* 2009). Carbon isotopic composition of produced biphytanes was determined using gas chromatography combustion isotope ratio mass spectrometry (gas chromatography: Hewlett Packard 5890 series II equipped with a 30 m TRX-5MS fused silica column; combustion: ThermoFinnigan Combustion Interface-II: mass spectrometry: Finnigan MAT252). Carbon isotopic values are expressed in per mil (‰) deviations from the Pee Dee Belemnite standard. The analytical error was < 1‰.

Thermodynamic calculations

The standard free energy change of AOM was calculated from free energies of formation (Stumm and Moran 1996). The free energy change for non-standard conditions was calculated using the van t'Hoff equation, concentrations in the medium at the beginning of incubation, and activity coefficients from the IUPAC project on ionic strength corrections for stability constants (www.iupac.org/web/ins/2000-003-1-500).

Results and Discussions

Sediment cores were taken from underneath a bacterial mat (identified as *Beggiatoa* by microscopy, and in prior analyses by Jannasch *et al* 1989; Supporting Figure 1a,b). The development of *Beggiatoa* was indicative of high rates of sulfate reduction. Sulfate reduction rates determined in replicate cores peaked between 3 and 6 cm with 1500 nmol d^{-1} ml^{-1} (average throughout the upper 15 cm: 530 $nmol^{-1}$ d^{-1} ml^{-1}, corresponding to roughly 0.25 µmol d^{-1} g_{dw}^{-1}; Supporting Figure 1d).

Homogenized material from the three horizons was further diluted, equilibrated with methane (250 kPa), and incubated without headspace in a temperature gradient block (0 to 90 °C; Kallmeyer *et al*. 2003). After 5 days of pre-incubation methane oxidation rates were determined using ^{14}C-methane. We measured substantial AOM rates between 4 and 70 °C (Figure 1). Highest rates occurred between 42 and 65 °C, with approx. 1.2 µmol d^{-1} g_{dw}^{-1}. AOM was not observed at ≥75 °C.

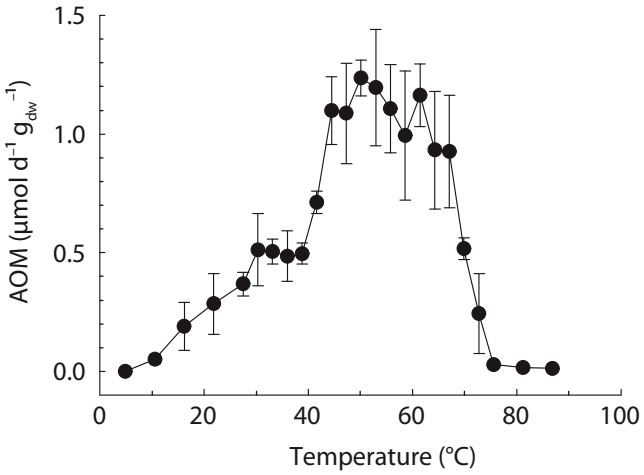

Figure 1: Rates of anaerobic oxidation of methane in Guaymas Basin sediment at different temperatures measured as $^{14}CH_4$ conversion to $^{14}CO_2$. Homogenous samples (2–45 cm sediment depth, *in situ* temperature, 4–85 °C) were pre-incubated for five days at designated temperatures followed by incubation with labeled methane for 48 h.

To test the stoichiometry of observed methane oxidation and sulfate reduction in our enrichments, methane consumption and sulfide production were chemically quantified in headspace-free subsamples (two month after start addition of methane) at 50 °C. Within two weeks methane consumption occurred simultaneously with sulfide production (Figure 2). As in previous low-temperature enrichments (Nauhaus *et al* 2002, Holler *et al* 2009), the ratio between methane consumed and sulfide formed (corrected against the background) was in accordance with the expected stoichiometry of one mol CH_4 oxidized per mol SO_4^{2-}. The proportion of methane channeled into biosynthesis and not used for sulfate reduction was previously shown to be extremely low (around 1%; Nauhaus *et al* 2007, Wegener *et al* 2008a), hence it can be neglected in the AOM stoichiometry. In controls without methane no production of methane (methanogenesis) was detected and sulfide production was only ~10% of rates in the presence of methane. These measurements gave evidence for thermophilic AOM in the natural enrichment.

To further increase the biomass and activity of the organisms responsible for thermophilic AOM, horizon A (37 °C) and B (50 °C and 60 °C) were incubated for 10 months in anoxic synthetic seawater medium with methane as sole energy source. To avoid the inhibition of growth by sulfide accumulation (Boetius et al. 2009), the supernatant was replaced by fresh medium at sulfide concentrations of 10 mM every 40–70 days (Figure 3a). Within these periods, the increase in sulfide appeared linear, indicating an inhibitory effect of

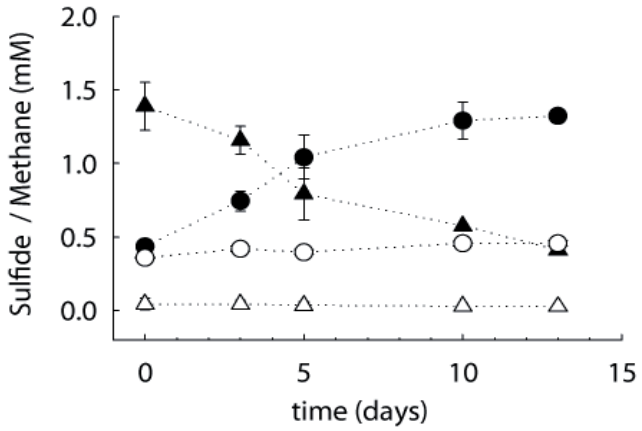

Figure 2: Time course experiment of AOM enrichment incubated without headspace at 50 °C. Sulfide formation (black circles) and methane consumption (black triangles) in the enrichment. A control without methane addition (open triangles, background methane) showed only minor sulfide formation (open circles).

accumulating sulfide on the microbial activity already at concentrations <10 mM, which may have counteracted the increase in activity due to growth of AOM consortia. Accordingly, after each addition of new medium, (dry-weight dependent) sulfide production with methane became faster than in the previous period (Figure 3a, b). Over the total incubation time of 250 days methane-dependent sulfate reduction rates of the 50 °C culture increased exponentially from 3 to 34 µmol d^{-1} g_{dw}^{-1} (Figure 3b) which indicates significant increase of active methanotrophic biomass during the enrichment, equaling a doubling time of 68 days. The doubling time at 50 °C was higher than in incubations at 37 °C (77 days), and at 60 °C (112 days) (see Supporting Figure 2). Thus, we assume an apparent optimum for the growth of thermophilic methanotrophs around 50 °C. In all control experiments without methane, sulfate reduction declined and was below detection limit after 5 months of incubation (data not shown).

To identify phylotypes responsible for AOM with sulfate at 50 °C, the enrichment was examined by cloning of genes encoding 16S rRNA genes and methyl coenzyme M reductase (Mcr) subunit A (*mcrA*). The most frequently obtained archaeal 16S rRNA genes and transcribed *mcrA* genes were affiliated with *mcrA* of ANME-1 (Figure 4 a, c; Table 1), matching sequences previously isolated from Guaymas Basin sediment (Teske *et al* 2002). The retrieved ANME-1 16S rRNA gene sequences cluster together with other sequences previously retrieved from Guaymas Basin (Teske *et al.,* 2002 and clone G72_C2 and

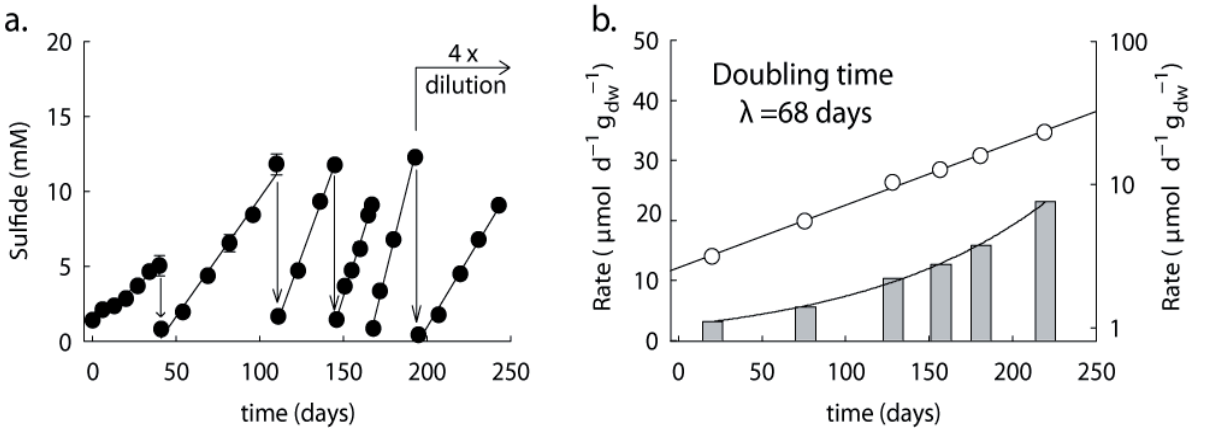

Figure 3: Long-term enrichment of anaerobic methanotrophs at 50 °C. a. Sulfide formation (black circles) in the initial sediment suspension and upon five exchanges of the sulfide-rich supernatant. Medium exchanges are indicated by arrows. b. Linear (vertical bars) and semi-logarithmic (open circles) illustration of methane-dependent sulfide production of the different incubation periods over time; normalized by dry-weights.

G72_C59, Longnecker and Reysenbach, database release) and form two Guaymas-specific subclusters named ANME-1-Guaymas I and II (Figure 4a, Table 1). Sequence similarity within subcluster ANME-1-Guaymas I ranged between 97.9 and 99.9% and within subcluster Guaymas II between 97.9 and 99.8%. The retrieved *mcrA*-derived sequences form a separate cluster with at least 6% amino acid divergence to other sequences within the *mcrA* group a–b (Figure 4c). In comparison to *mcrA* from methanogenic archaea, the present sequence contains a modification (motif $VX_2CCX_4CX_5C$) which has been previously observed in the abundant nickel protein of ANME-1 consortia in a cold habitat (Krüger *et al* 2003). The most frequently retrieved bacterial 16S rRNA clone sequences represent a lineage distantly related to *Desulfurella* spp., sulfur-reducing thermophilic Deltaproteobacteria (Figure 4b, Table 1).

16S rRNA gene sequences representing this lineage were previously obtained from a heterogeneous sulfate-reducing enrichment culture from Guaymas Basin sediment amended with butane and grown at 60 °C (Kniemeyer *et al* 2007). However, the presently obtained AOM enrichment characterized by a high proportion of related 16S rRNA genes did not show detectable sulfate reduction activity with butane instead of methane within an incubation time of 7 weeks. Corresponding to the naming of bacterial seep clusters identified at cold seeps ('SeepSRB-1 to -4'and subgroups; Knittel *et al* 2003, Schreiber *et al* 2010) we named this new group of thermophilic, ANME-associated bacteria 'HotSeep-1'.

Table 1. Numbers of retrieved clones for genes encoding 16S rRNA and McrA (subunit a of methyl-coenzyme M reductase) from a methane-oxidizing anaerobic enrichment culture analyzed after 3 months (enrichment subsample) and 9 months (supernatant subsample) of incubation at 50 °C.

Phylogenetic affiliation	**16S rRNA (3 months)**	**16S rRNA (9 months)**	***mcrA***
Archaea			
Euryarchaeota			
ANME-1			64
ANME-1-Guaymas I	19		
ANME-1-Guaymas II	27		
Methanosarcinales			
ANME-2c			3
others		1	
Thermoplasmatales	6		
Halobacteriales	4		
Total archaeal clones analyzed	**56**	**n.a.**	**68**
Bacteria			
Proteobacteria			
Betaproteobacteria		3	
Gammaproteobacteria	1	10	
Deltaproteobacteria			
HotSeep-1-cluster	53	71	
DSS group (Desulfosarcinales)		1	
Desulfuromonadales	1		
Syntrophobacterales	1		
others	2	12	
Acidobacteria		1	
Actinobacteria		3	
Bacteriodetes		1	
Candidate division OD1	5	1	
Candidate division OP3	3	2	
Candidate division OP8	8	13	
Chloroflexi 3	5		
Deferribacteres	1		
Planctomycetes		2	
unaffiliated 2	2		
total bacterial clones analyzed	**80**	**127**	

n.a. not analzyed

Fluorescence *in situ* hybridization with specific 16S rRNA targeting fluorescent oligonucleotide probes (Supporting Table 2) revealed spherical ANME-1 cell aggregates associated with Deltaproteobacteria of the HotSeep-1 group after two months of incubation (Figure 4d). The consortia varied in size and harbored between a few and several hundred cells. ANME-1 cells in these aggregates were identified by the new probe ANME-1-GII186 as members of subgroup ANME-1-Guaymas II. In addition, hybridization showed ANME-1 aggregates without partner bacteria (Figure 4e). ANME-1 cells in these aggregates typically have a length of 1.2 μm and a width of 0.3–0.4 μm. After five months, chain-forming aggregates with more than 100 ANME-1 cells appeared (Figure 4f-g) associated in a 1:1 ratio with rod-shaped bacteria appearing thinner (0.4 μm in width) than the archaeal cells (Fig. 4g)

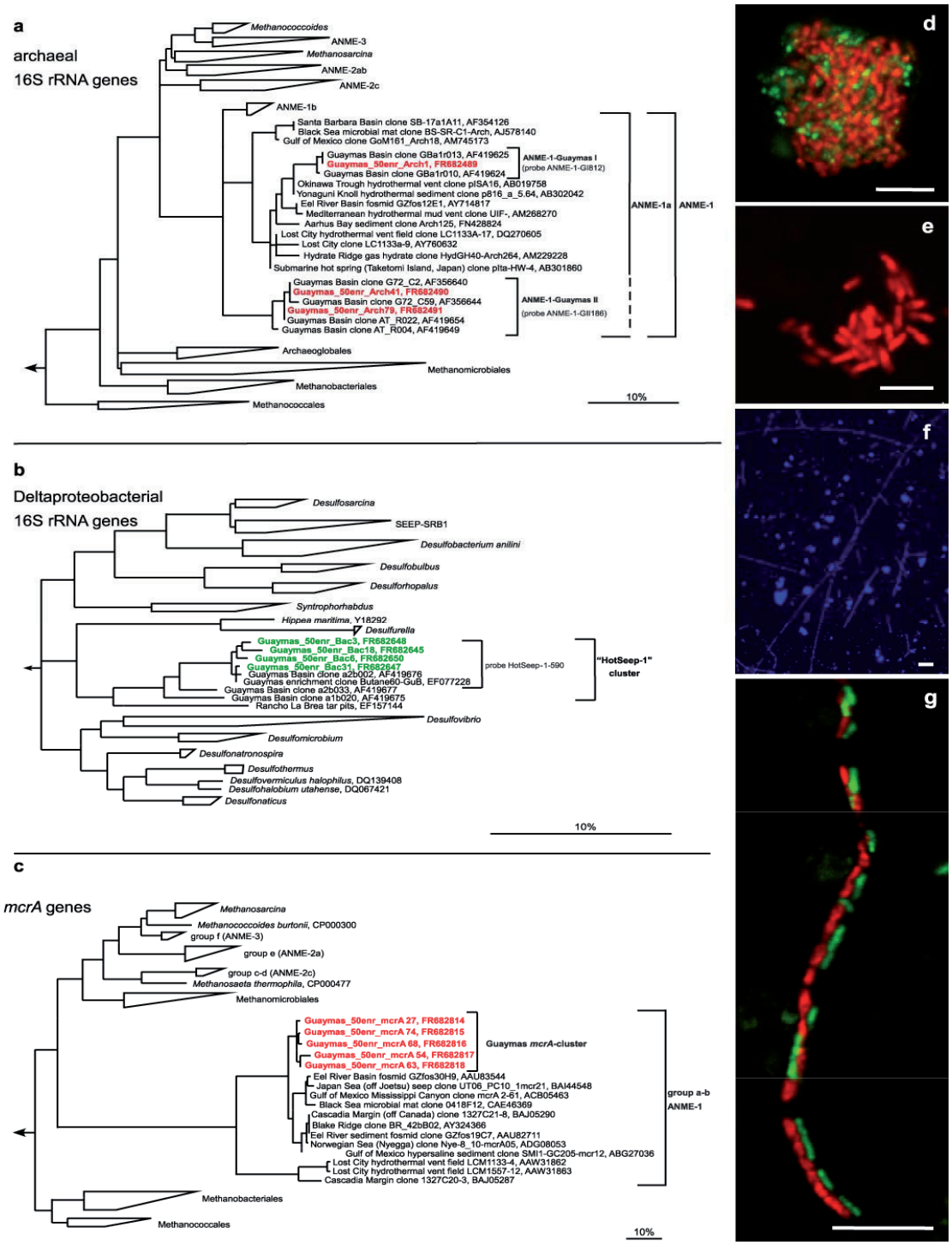

Figure 4: Phylotypes and cell aggregates in the methane-oxidizing anaerobic enrichment culture grown at 50 °C. Phylogenetic trees showing the affiliations of 16S rRNA gene sequences retrieved from Guaymas methane-oxidizing enrichments with selected reference sequences of (a) Euryarchaeota and (b) Deltaproteobacteria. Sequences from this study are printed in bold red (archaea) and bold green (bacteria). Probe specificity is indicated by brackets. Bar = 10% estimated sequence divergence. (c) phylogenetic tree of gene sequences coding for the alpha subunit of methyl-coenzyme M-reductase (*mcrA*), (d–g) cell aggregates of ANME-1 visualized by CARD-FISH. Scale bars = 10 µm. Panels d, e, and g are confocal laser scanning micrographs. Panel f is a regular epifluorescence micrograph. (d) spherical ANME-1/HotSeep-1 aggregates stained with probe ANME-1-350 (red) and probe HotSeep-1-590 (green). (e) Monophyletic ANME-1 aggregate stained with probe ANME-1-350. (f) DAPI staining showing long chain-forming ANME-1 aggregates. (g) chain-forming ANME-1/HotSeep-1 aggregates. ANME-1 cells were identified as members of subcluster ANME-1-Guaymas I (probe ANME-1-GI812, red) and bacterial partners as members of the HotSeep-1 cluster (probe HotSeep-1-590, green).

The ANME-1 cells in these chain-forming aggregates are larger than those in spherical aggregates with a length of 2-2.5 µm and a width of 0.7 µm. Hybridization with the new probe, ANME-1-GI812, identified chain-forming ANME-1 as members of subgroup ANME-1-Guaymas I (Figure 4g). The partner bacteria were attached to the ANME-1 cells, and both cell types were enclosed in a common sheath. We observed growth of these ANME-1 chains with time. The longest chains observed after 11 month of incubation had a length of >250 µm. Aggregations of coiled ANME-1 chains have also been detected. Hybridization with probe HotSeep-1-590 showed that these partner bacteria belong as well to the HotSeep-1 cluster. Based on the observation of significant increase of activity, and ANME-1 HotSeep-1 chains in the 50 °C enrichments we propose that members of the ANME-I Guaymas clades and their partner bacteria of the HotSeep-1 cluster are thermophiles and oxidize methane with sulfate at an apparent temperature optimum of 45–60 °C.

As an independent complementary method for the chemotaxonomic identification of ANME we analyzed the archaeal glycerol dialkylglycerol tetraether (GDGT) lipids in the enrichment. The intact lipids contained mostly diglycosides, which are abundant in lipids in ANME-1 dominated habitats (Rossel *et al* in press). The GDGT cores were dominated by chains without or with four or five cyclopentane rings. GDGTs with one to three rings, which were previously assigned to thermophilic ANME-1 (Schouten *et al* 2003), were significantly depleted in ^{13}C as compared to typical planktonic signals (Table 2). The isoprenoids prepared from the GDGTs, especially mono- and bicyclic biphytane, were depleted in ^{13}C ($\delta^{13}C$, –49‰). This indicates utilization of methane or its metabolites (CO_2) as shown for lipids of anaerobic methanotrophs (Wegener *et al* 2008a). These results are consistent with earlier analyses of hydrothermally influenced Guaymas Basin sediment (Schouten *et al* 2003).

Apart from the hot Guaymas Basin sediments and some calcified gas vents in cold to moderately thermophilic habitats such as the Black Sea (Michaelis *et al* 2002) and the Lost City Hydrothermal Field (Schrenk *et al* 2004), most shallow gas-rich habitats investigated so far were dominated by the methanotrophic clades ANME-2 and ANME-3 (Knittel and Boetius 2009). Also, all prior cultivation attempts using environmental samples from marine cold seeps selected for these groups (Boetius *et al* 2009). Here, propagation of methane oxidation (Figure 1–3) as well as comparative sequence analysis, hybridization and membrane lipid information demonstrate that thermophilic AOM up to at least 60 °C is mediated by members of the ANME-1 group. Hence, considering previous findings of ANME sequences and lipids in hot environments (Schouten *et al* 2003, Schrenk *et al* 2004, Roussel *et al* 2008) together with our results, we suggest that AOM could be widespread in hot marine habitats

Table 2. Concentrations of archaeal glycerol dibiphytanyl glycerol tetraethers (GDGTs) in the enrichment culture (top) and stable carbon isotopic compositions of GDGT-derived biphytane derivatives obtained by ether cleavage (bottom). Structures of the GDGTs are shown in Schouten *et al* 2003.

Tetraethers	**Concentration µg g_{dw}^{-1}**	**Rel. abundance (%)**
GDGT-0	1.90	25
GDGT-1	0.49	6
GDGT-2	0.70	9
GDGT-3	0.47	6
GDGT-4	1.78	23
GDGT-cr.	2.24	29
GDGT-cr. (iso)	0.07	1
Isoprenoids	**Isotopic composition ($\delta^{13}C$ vs. PDB)**	**Rel. abundance (%)**
Acyclic biphytane	–25.2‰	40
Monocyclic biphytane	–49.1‰	13
Bicyclic biphytane	–41.6‰	29
Tricyclic biphytane	–20.0‰	18

including e.g. hydrothermal crusts, brine lakes and subsurface gas reservoirs. Furthermore, it would be interesting to investigate whether thermophilic ANME groups may be involved in the widely observed transformation of anhydrite to calcite according to

$$CaSO_4 + CH_4 \rightarrow CaCO_3 + H_2S + H_2O \quad (\Delta G^\circ = -21.4 \text{ kJ mol}^{-1}) \qquad (1)$$

in evaporitic cap rocks of moderately heated gas reservoirs (Werner *et al* 1988), which would extend the importance of ANME driven methanotrophy in the global carbon cycle and in deep subsurface diagenesis.

Acknowledgements

We are indebted to the crew and pilots of Research Vessel *Atlantis* and Research Submersible *Alvin*. We thank Nicole Rödiger, Viola Krukenberg, Philipp Hach, Viola Beier, Gabriele Schüssler, Dennis Enning, and Florin Musat for technical support. This study was supported by grant NSF OCE-0647633 to A.T., by the Leibniz program of the Deutsche Forschungsgemeinschaft to A.B., the DFG Research Center and Cluster of Excellence MARUM, and the Max Planck Society.

References

Aeckersberg F, Bak F, Widdel F (1991). Anaerobic oxidation of saturated hydrocarbons to CO_2 by a new type of sulfate-reducing bacterium. *Arch Microbiol* **156:** 5–14.

Aquilina A, Knab NJ, Knittel K, Kaur G, Geissler A, Kelly SP *et al* (2010). Biomarker indicators for anaerobic oxidizers of methane in brackish-marine sediments with diffusive methane fluxes. *Org Geochem* **41:** 414–426.

Boetius A, Ravenschlag K, Schubert CJ, Rickert D, Widdel F, Gieseke A *et al* (2000). A marine microbial consortium apparently mediating anaerobic oxidation of methane. *Nature* **407:** 623–626.

Boetius A, Holler T, Knittel K, Felden J, Wenzhöfer F (2009). The seabed as natural laboratory: lessons from uncultivated methanotrophs. In: Epstein SS (ed). *Microbiology Monographs: Uncultivated Microorganisms*. Springer: Berlin. pp 59–82.

Bradley AS, Fredricks HF, Hinrichs K-U, Summons RE (2009). Structural diversity of diether lipids in carbonate chimneys at the lost City Hydrothermal Field. *Org Geochem* **40:** 1169–1178.

Burggraf S, Jannasch HW, Nicolaus B, Stetter KO (1990). *Archaeoglobus profundus* sp. nov., represents a new species within the sulfate-reducing archaebacteria. *Syst Appl Microbiol* **13:** 24–28.

Cord-Ruwisch R (1985). A quick method for the determination of dissolved and precipitated sulfides in cultures of sulfate-reducing bacteria. *J Microbiol Methods* **4:** 33–36.

Hales BA, Edwards C, Ritchie DA, Hall G, Pickup RW, Saunders JR (1996). Isolation and identification of methanogen-specific DNA from blanket bog peat by PCR amplification and sequence analysis. *Appl Environ Microbiol* **62:** 668–675.

Hallam SJ, Girguis PR, Preston CM, Richardson PM, DeLong EF (2003). Identification of methyl coenzyme M reductase A (*mcrA*) genes associated with methane-oxidizing archaea. *Appl Environ Microbiol* **69:** 5483–5491.

Hallam SJ, Putnam N, Preston CM, Detter JC, Rokhsar D, Richardson PM *et al* (2004). Reverse methanogenesis: testing the hypothesis with environmental genomics. *Science* **305:** 1457–1462.

Harrison BK, Zhang H, Berelson W, Orphan VJ (2009). Variations in archaeal and bacterial diversity associated with the sulfate-methane transition zone in continental margin sediments (Santa Barbara Basin, California). *Appl Environ Microbiol* **75:** 1487–1499.

Hoehler TM, Alperin MJ, Albert DB, Martens CS (1994) Field and laboratory studies of methane oxidation in an anoxic marine sediment: Evidence for a methanogen-sulfate reducer consortium. *Global Biogeochem Cy* **8**, 451-464.

Holler T, Wegener G, Knittel K, Boetius A, Brunner B, Kuypers MMM *et al* (2009). Substantial $^{13}C/^{12}C$ and D/H fractionation during anaerobic oxidation of methane by marine consortia enriched *in vitro*. *Environ Microbiol Rep* **1:** 370–376.

Huguet C, Hopmans E, Febo-Ayala W, Thompson D, Damstè JSS, Schouten S (2006). An improved method to determine the absolute abundance of glycerol dibiphytanyl glycerol tetraether lipids. *Org Geochem* **37:** 1036–1041.

Jannasch HW, Nelson DC, Wirsen CO (1989). Massive natural occurrence of unusually large bacteria (*Beggiatoa* sp.) at a hydrothermal deep-sea vent site. *Nature* **342:** 834–836.

Jeanthon C, L'Haridon S, Cueff V, Banta A, Reysenbach AL, Prieur D (2002). *Thermodesulfobacterium hydrogeniphilum* sp. nov., a thermophilic, chemolithoautotrophic, sulfate-reducing bacterium isolated from a deep-sea hydrothermal vent at Guaymas Basin, and emendation of the genus *Thermodesulfobacterium*. *Int J Syst Evol Microbiol* **52:** 765–772.

Jørgensen BB, Fenchel T (1974). The sulfur cycle of a marine sediment model system. *Mar Biol* **24:** 189–201.

Jørgensen BB, Isaksen MF, Jannasch HW (1992). Bacterial sulfate reduction above 100°C in deep-sea hydrothermal vent sediments. *Science* **258:** 1756–1757.

Kallmeyer J, Ferdelman TG, Jansen K-H, Jørgensen BB (2003). A high pressure thermal grandient block for investigating microbial activity in multiple deep-sea samples. *J Microbiol Methods* **55:** 165–172.

Kallmeyer J, Boetius A (2004). Effects of temperature and pressure on sulfate reduction and anaerobic oxidation of methane in hydrothermal sediments of Guaymas Basin. *Appl Environ Microbiol* **70:** 1231–1233.

Kallmeyer J, Ferdelman TG, Weber A, Fossing H, Jørgensen BB (2004). A cold chromium distillation procedure for radiolabeled sulfide applied to sulfate reduction measurements. *Limnol Oceanogr: Methods* **2:** 171–180.

Kane MD, Poulsen LK, Stahl DA (1993). Monitoring the enrichment and isolation of sulfate-reducing bacteria by using oligonucleotide hybridization probes designed from environmentally derived 16S rRNA sequences. *Appl Environ Microbiol* **59:** 682–686.

Khelifi N, Grossi V, Hamdi M, Dolla A, Tholozan J-L, Ollivier B *et al* (2010). Anaerobic oxidation of fatty acids and alkenes by the hyperthermophilic sulfate-reducing archaeon *Archaeoglobus fulgidus*. *Appl Environ Microbiol* **76:** 3057–3060.

Kniemeyer O, Musat F, Sievert SM, Knittel K, Wilkes H, Blumenberg M *et al* (2007). Anaerobic oxidation of short-chain hydrocarbons by marine sulphate-reducing bacteria. *Nature* **449:** 898–901.

Knittel K, Boetius A, Lemke A, Eilers H, Lochte K, Pfannkuche O *et al* (2003). Activity, distribution, and diversity of sulfate reducers and other bacteria in sediments above gas hydrate (Cascadia Margin, Oregon). *Geomicrobiol J* **20:** 269–294.

Knittel K, Boetius A (2009). Anaerobic oxidation of methane: progress with an unknown process. *Annu Rev Microbiol* **63:** 311–334.

Krüger M, Meyerdierks A, Glöckner FO, Amann R, Widdel F, Kube M *et al* (2003). A conspicuous nickel protein in microbial mats that oxidize methane anaerobically. *Nature* **426:** 878–881.

Kurr M, Huber R, König H, Jannasch HW, Fricke H, Trincone A *et al* (1991). *Methanopyrus kandleri*, gen. and sp. nov. represents a novel group of hyperthermophilic methanogens, growing at 110°C. *Arch Microbiol* **156:** 239–247.

Lanoil BD, Duc MT, Wright M, Kastner M, Nealson KH, Bartlett D (2005). Archaeal diversity in ODP legacy borehole 892b and associated seawater and sediments of the Cascadia Margin. *FEMS Microbiol Ecol* **54:** 167–177.

Lösekann T, Knittel K, Nadalig T, Fuchs B, Niemann H, Boetius A *et al* (2007). Diversity and abundance of aerobic and anaerobic methane oxidizers at the Haakon Mosby Mud Volcano, Barents Sea. *Appl Environ Microbiol* **73:** 3348–3362.

Ludwig W, Strunk O, Westram R, Richter L, Meier H, Yadhukumar *et al* (2004). ARB: a software environment for sequence data. *Nucleic Acids Res* **32:** 1363–1371.

Martens CS (1990). Generation of short chain acid anions in hydrothermally altered sediments of the Guaymas Basin, Gulf of California. *Appl Geochem* **5:** 71–76.

Massana R, Murray AE, Preston CM, Delong EF (1997). Vertical distribution and phylogenetic characterization of marine planktonic *Archaea* in the Santa Barbara channel. *Appl Environ Microbiol* **63:** 50–56.

Michaelis W, Seifert R, Nauhaus K, Treude T, Thiel V, Blumenberg M *et al* (2002). Microbial reefs in the Black Sea fueled by anaerobic oxidation of methane. *Science* **297:** 1013–1015.

Mills HJ, Hodges C, Wilson K, MacDonald IR, Sobecky PA (2003). Microbial diversity in sediments associated with surface-breaching gas hydrate mounds in the Gulf of Mexico. *FEMS Microbiol Ecol* **46:** 39–52.

Muyzer G, Teske A, Wirsen CO, Jannasch HW (1995). Phylogenetic relationships of *Thiomicrospira* species and their identification in deep-sea hydrothermal vent samples by denaturing gradien gel electrophoresis of 16S rDNA fragments. *Arch Microbiol* **164:** 165–172.

Nauhaus K, Boetius A, Krüger M, Widdel F (2002). *In vitro* demonstration of anaerobic oxidation of methane coupled to sulphate reduction in sediment from a marine gas hydrate area. *Environ Microbiol* **4:** 296–305.

Nauhaus K, Albrecht M, Elvert M, Boetius A, Widdel F (2007). *In vitro* cell growth of marine archaeal-bacterial consortia during anaerobic oxidation of methane with sulfate. *Environ Microbiol* **9:** 187–196.

Niemann H, Lösekann T, de Beer D, Elvert M, Nadalig T, Knittel K *et al* (2006). Novel microbial communities of the Haakon Mosby Mud Volcano and their role as a methane sink. *Nature* **443:** 854–858.

Omoregie EO, Mastalerz V, de Lange G, Straub KL, Kappler A, Røy H, *et al* (2008). Biogeochemistry and community composition of iron- and sulfur-precipitating microbial mats at the Chefren Mud Volcano (Nile Deep Sea Fan, Eastern Mediterranean). *Appl Environ Microbiol* **74.** 3198–3215.

Orphan VJ, House CH, Hinrichs K-U, McKeegan KD, DeLong EF (2001). Methane-consuming archaea revealed by directly coupled isotopic and phylogenetic analysis. *Science* **293:** 484–487.

Pernthaler A, Pernthaler J, Amann R (2004). Sensitive multi-color fluorescence *in situ* hybridization for the identification of environmental microorganisms. In: Kowalchuk GA, Bruijn FJd, Head IM, Akkermans AD, van Elsas JD (eds). *Molecular microbial ecology manual*, 2nd ed. edn. Kluwer Academic Publishers: Dordrecht. pp 711–726.

Pernthaler A, Dekas AE, Brown CT, Goffredi SK, Embaye T, Orphan VJ (2008). Diverse syntrophic partnerships from deep-sea methane vents revealed by direct cell capture and metagenomics. *Proc Natl Acad Sci U S A* **105:** 7052–7057.

Pruesse E, Quast C, Knittel K, Fuchs B, Ludwig W, Peplies J *et al* (2007). SILVA: a comprehensive online resource for quality checked and aligned ribosomal RNA sequence data compatible with ARB. *Nucleic Acids Res* **35:** 7188–7196.

Reeburgh WS (2007). Oceanic methane biogeochemistry. *Chem Rev* **107:** 486–513.

Rossel PE, Elvert M, Ramette A, Boetius A, Hinrichs K-U (2011). Factors controlling the distribution of anaerobic methanotrophic communities in marine environments: Evidence from intact polar membrane lipids. In press.

Roussel EG, Bonavita M-AC, Querellou J, Cragg BA, Webster G, Prieur D *et al* (2008). Extending the sub-sea-floor biosphere. *Science* **320:** 1046–1056.

Rueter P, Rabus R, Wilkes H, Aeckersberg F, Rainey FA, Jannasch HW, Widdel F (1994) Anaerobic oxidation of hydrocarbons in crude oil by new types of sulphate-reducing bacteria. *Nature* **372**: 455–458.

Scheller S, Goenrich M, Boecher R, Thauer RK, Jaun B (2010). The key nickel enzyme of methanogenesis catalyses the anaerobic oxidation of methane. *Nature* **465:** 606–608.

Schoell M (1980). The hydrogen and carbon isotopic composition of methane from natural gases of various origins. *Geochim Cosmochim Acta* **44:** 649–661.

Schouten S, Wakeham SG, Hopmans EC, Damsté JSS (2003). Biogeochemical evidence that thermophilic archaea mediate the anaerobic oxidation of methane. *Appl Environ Microbiol* **69:** 1680–1686.

Schramm A, Fuchs BM, Nielsen JL, Tonolla M, Stahl DA (2002). Fluorescence *in situ* hybridization of 16S rRNA gene clones (Clone-FISH) for probe validation and screening of clone libraries. *Environ Microbiol* **4:** 713–720.

Schreiber L, Holler T, Knittel K, Meyerdierks A, Amann R (2010). Identification of the dominant sulfate-reducing bacterial partner of anaerobic methanotrophs of the ANME-2 clade. *Environ Microbiol* **12:** 2327–2340.

Schrenk MO, Kelley DS, Bolton SA, Baross JA (2004). Low archaeal diversity linked to subseafloor geochemical processes at the Lost City Hydrothermal Field, Mid-Atlantic Ridge. *Environ Microbiol* **6:** 1086–1095.

Simoneit BRT, Kawka OE, Brault M (1988). Origin of gases and condensates in the Guaymas Basin hydrothermal system (Gulf of California). *Chem Geol* **71:** 169–182.

Stetter KO (1996). Hyperthermophilic procaryotes. *FEMS Microbiol Rev* **18:** 149–158.

Stumm W, Morgan JJ (1996). *Aquatic Chemistry*, 3rd edn. John Wiley & Sons: New York.

Sturt HF, Summons RE, Smith K, Elvert M, Hinrichs K-U (2004). Intact polar membrane lipids in prokaryotes and sediments deciphered by high-performance liquid chromatography/electrospray ionization multistage mass spectrometry - new biomarkers for biogeochemistry and microbial ecology. *Rapid Commun Mass Spectrom* **18:** 617–628.

Teske A, Hinrichs K-U, Edgcomb V, de Vera Gomez A, Kysela D, Sylva SP *et al* (2002). Microbial diversity of hydrothermal sediments in the Guaymas Basin: evidence for anaerobic methanotrophic communities. *Appl Environ Microbiol* **68:** 1994–2007.

Thauer RK (1998). Biochemistry of methanogenesis: a tribute to Marjory Stephenson. 1998 Marjory Stephenson Prize Lecture. *Microbiol* **144:** 2377–2406.

Thomsen TR, Finster K, Ramsing NB (2001). Biogeochemical and molecular signatures of anaerobic methane oxidation in a marine sediment. *Appl Environ Microbiol* **67:** 1646–1656.

Treude T, Boetius A, Knittel K, Wallmann K, Jørgensen BB (2003). Anaerobic oxidation of methane above gas hydrates at Hydrate Ridge, NE Pacific Ocean. *Mar Ecol Prog Ser* **264:** 1–14.

Wegener G, Niemann H, Elvert M, Hinrichs K-U, Boetius A (2008a). Assimilation of methane and inorganic carbon by microbial communities mediating the anaerobic oxidation of methane. *Environ Microbiol* **10:** 2287–2298.

Wegener G, Shovitri M, Knittel K, Niemann H, Hovland M, Boetius A (2008b). Biogeochemical processes and microbial diversity of the Gullfaks and Tommeliten methane seeps (Northern North Sea). *Biogeosciences* **5:** 1127–1144.

Werner ML, Feldman MD, Knauth LP (1988). Petrography and geochemistry of water-rock interactions in Richton Dome cap rock (southeastern Mississippi, USA). *Chem Geol* **74:** 113–135.

Widdel F, Bak F (1992). Gram-negative mesophilic sulfate-reducing bacteria. In: Balows A, Trüper HG, Dworkin M, Harder W, Schleifer K-H (eds). *The Prokaryotes*, 2 edn. Springer: New York. pp 3352–3378.

Zehnder AJB, Brock TD (1979). Methane formation and methane oxidation by methanogenic bacteria. *J Bacteriol* **137:** 420–432.

Zhou J, Bruns MA, Tiedje JM (1996). DNA recovery from soils of diverse composition. *Appl Environ Microbiol* **62:** 316–322.

Supporting Information Holler *et al*. Thermophilic anaerobic oxidation of methane by marine microbial consortia

Supporting Table 1. *In vitro* studies of AOM and apparent temperature ranges (modified from ref. Boetius *et al* 2009).

Sampling site	**Dominating ANME[a] population**	***In situ* temperature**	***In vitro* temperature optimum of AOM**	**Reference**
Haakon Mosby Mud Volcano (North Atlantic)	ANME-3/DBB[b]	–1.5	4–8	(Krüger *et al* 2005)
Hydrate Ridge (East Pacific)	ANME-2/DSS[c]	4	10–15	(Nauhaus *et al* 2005)
Monterey Basin (East Pacific)	ANME-2/DSS	4	5	(Girguis *et al* 2003)
Gulf of Mexico	ANME-2/DSS	6	16–20	(Krüger *et al* 2005)
Black Sea	ANME-1/DSS ANME-2/DSS	8	16–25	(Nauhaus *et al* 2005, Deusner *et al 2010*)
Amon/Isis Mud Volcano (Eastern Mediterranean)	ANME-2/DSS	14	20	(Holler *et al* 2009, Schreiber *et al* 2010)
Eckernförde Bay (Baltic Sea)	ANME-2/DSS	5–20	20	(Krüger *et al* 2005, Treude *et al* 2005, Jagersma *et al* 2009, Meulepas *et al 2009*)
Kattegat (Baltic Sea)	ANME-2/DSS, DBB	5–20	20–25	(Krüger *et al* 2005)

[a] ANME, clusters of anaerobic methanotrophs (Euryarchaeota)
[b] DBB, *Desulfobulbus*
[c] DSS, *Desulfosarcina/Desulfococcus*

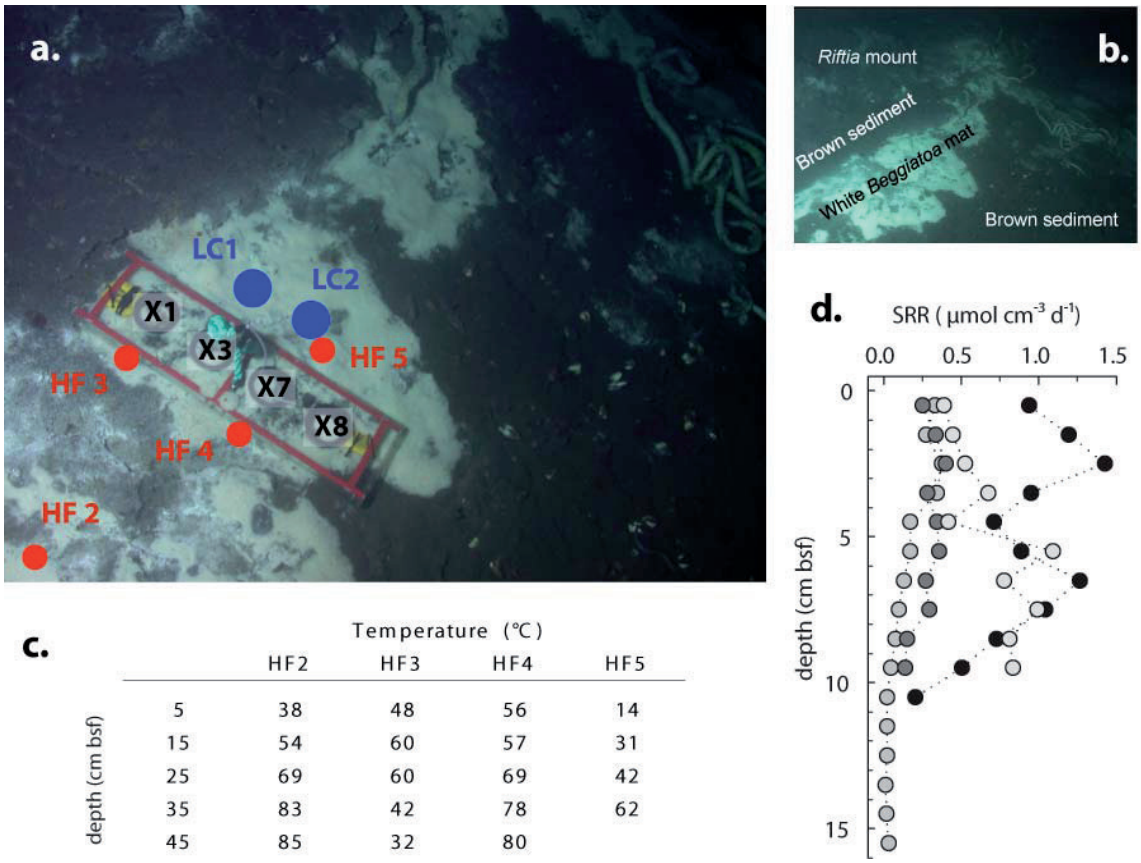

c.

depth (cm bsf)	Temperature (°C) HF2	HF3	HF4	HF5
5	38	48	56	14
15	54	60	57	31
25	69	60	69	42
35	83	42	78	62
45	85	32	80	

Supporting Figure 1: Images and data from sampling site. a. Placement of long cores (LC1,2), incubation cores (X1, X3, X7 and X8), and temperatures loggers (HF2, HF3, HF4, HF5) on *Beggiatoa*-covered sediment in Guaymas Basin (*ALVIN* Dive 4570). b. Contextual information of the sampling site. c. Temperature profiles from the sampling site. d. Sulfate reduction rates derived from *in vivo* radiotracer incubations.

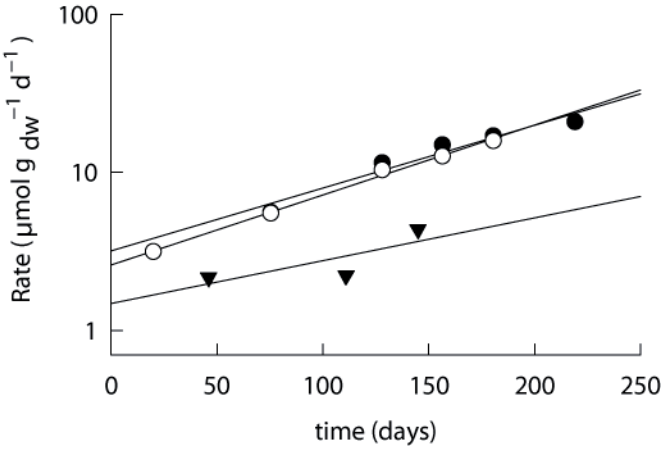

Supporting Figure 2: Semi- logarithmic plot of sulfide production in methane-amended sediment slurries incubated at 37 °C (open circle), 50 °C (filled circles) and triangles (60 °C) yielding doubling times of 77, 68 and 112 days for the 37 °C, 50 °C and 60 °C enrichments, respectively.

Supporting Table 2. Oligonucleotide probes used for fluorescence *in situ* hybridization.

Probe	Specificity	Probe sequence (5´-3´)	Target site[a]	FA conc.[b] [%]	Reference
NON338	Background control	ACTCCTACGGGAGGCAGC	338–355	10	(Wallner *et al* 1993)
EUB338 I-III	most *Bacteria*	GCTGCCTCCCGTAGGAGT GCAGCCACCCGTAGGTGT GCTGCCACCCGTAGGTGT	338–355	35	(Daims *et al* 1999)
Arch915	most *Archaea*	GTGCTCCCCCGCCAATTCC T	915–935	35	(Stahl and Amann 1991)
DSS658	*Desulfosarcina* spp./ *Desulfococcus* spp. and relatives	TCCACTTCCCTCTCCCAT	658–685	50	(Manz *et al* 1998)
ANME1-350	ANME-1 archaea	AGTTTTCGCGCCTGATGC	350–367	40	(Boetius *et al* 2000)
ANME-1-GI812	ANME-1 subgroup Guaymas I	CTGGCCCACATCGTTTAC	812–829	30	This study
cANME-1-GI812[c]	competitor oligonucleotide targeting Guaymas I	CTAGCCCGCATCGTTTAC	812–829	30	This study
ANME-1-GII186	ANME-1 subgroup Guaymas II	GGACATCCTGCATTCCAG	186–203	10	This study
ANME-2-538	ANME-2 archaea	GGCTACCACTCGGGCCGC	538–555	50	(Treude *et al* 2005)
HotSeep-1-590	HotSeep-1 cluster of Deltaproteobacteria	ACACGCTCAACTTGCCTT	590–608	20–25	This study
HotSeep-1-H5	helper probes for HotSeep-1-590	CCCGCCTRCGCGCCCTTT	572–589	20–25	This study
HotSeep-1-H3		ARGTTGAGCCTCAGGCTT	608–625		This study
HotSeep-1-H3-3		GTTTTGAGCGCCATTCTG	626–643		This study
HotSeep-1-H3-3-3		CGGGACTCAAGAAAGGCA	644–661		This study

[a] Position in the 16S rRNA of *E.coli*
[b] FA: formamide concentration in the hybridization buffer
[c] used as an unlabelled competitor oligonucleotide in hybridization with probe ANME-1-GI812 to limit cross-hybridizations with Guaymas II cluster

References

Boetius A, Ravenschlag K, Schubert CJ, Rickert D, Widdel F, Gieseke A *et al* (2000). A marine microbial consortium apparently mediating anaerobic oxidation of methane. *Nature* **407:** 623–626.

Boetius A, Holler T, Knittel K, Felden J, Wenzhöfer F (2009). The seabed as natural laboratory: lessons from uncultivated methanotrophs. In: Epstein SS (ed). *Microbiology Monographs: Uncultivated Microorganisms*. Springer: Berlin. pp 59–82.

Daims H, Bruhl A, Amann R, Schleifer KH, Wagner M (1999). The domain-specific probe EUB338 is insufficient for the detection of all Bacteria: Development and evaluation of a more comprehensive probe set. *Syst Appl Microbiol* **22:** 434–444.

Deusner C, Meyer V, Ferdelman TG (2010). High-pressure systems for gas-phase free continuous incubation of enriched marine microbial communities performing anaerobic oxidation of methane. *Biotechnol Bioeng* **105:** 524–533.

Girguis PR, Orphan VJ, Hallam SJ, DeLong EF (2003). Growth and methane oxidation rates of anaerobic methanotrophic archaea in a continuous-flow bioreactor. *Appl Environ Microbiol* **69:** 5472–5482.

Holler T, Wegener G, Knittel K, Boetius A, Brunner B, Kuypers MMM *et al* (2009). Substantial $^{13}C/^{12}C$ and D/H fractionation during anaerobic oxidation of methane by marine consortia enriched *in vitro*. *Environ Microbiol Rep* **1:** 370–376.

Jagersma GC, Meulepas RJW, Jong IH, Gieteling J, Klimiuk A, Schouten S *et al* (2009). Microbial diversity and community structure of a highly active anaerobic methane-oxidizing sulfate-reducing enrichment. *Environ Microbiol* **11:** 3223–3232.

Krüger M, Treude T, Wolters H, Nauhaus K, Boetius A (2005). Microbial methane turnover in different marine habitats. *Palaegeogr Paleoclimatol Paleoecol* **227:** 6–17.

Manz W, Eisenbrecher M, Neu TR, Szewzyk U (1998). Abundance and spatial organization of Gram-negative sulfate-reducing bacteria in activated sludge investigated by *in situ* probing with specific 16S rRNA targeted oligonucleotides. *FEMS Microbiol Ecol* **25:** 43–61.

Meulepas RJW, Jagersma CG, Khadem AF, Buisman CJN, Stams AJM, Lens PNL (2009). Effect of environmental conditions on sulfate reduction with methane as electron donor by an Eckernförde Bay enrichment. *Environ Sci Technol* **43:** 6553–6559.

Nauhaus K, Treude T, Boetius A, Krüger M (2005). Environmental regulation of the anaerobic oxidation of methane: a comparison of ANME-I and ANME-II communities. *Environ Microbiol* **7:** 98–106.

Schreiber L, Holler T, Knittel K, Meyerdierks A, Amann R (2010). Identification of the dominant sulfate-reducing bacterial partner of anaerobic methanotrophs of the ANME-2 clade. *Environ Microbiol* **12:** 2327–2340.

Stahl DA, Amann R (1991). Development and application of nucleic acid probes. In: Stackebrandt E, Goodfellow M (eds). *Nucleic Acid Techniques in Bacterial Systematics*. John Wiley&Sons Ltd.: Chichester. pp 205–248.

Treude T, Krüger M, Boetius A, Jørgensen BB (2005). Environmental control on anaerobic oxidation of methane in the gassy sediments of Eckernförde Bay (German Baltic). *Limnol Oceanogr* **50:** 1771–1786.

Wallner G, Amann R, Beisker W (1993). Optimizing fluorescent *in situ* hybridization with rRNA-targeted oligonucleotide probes for flow cytometric identification of microorganism. *Cytometry* **14:** 136–143.

IV. Weitere Beteiligungen an Arbeiten zur Mikrobiologie von Methan

IV.1 The seabed as natural laboratory: Lessons from uncultivated methanotrophs

Antje Boetius, Thomas Holler, Katrin Knittel, Janine Felden & Frank Wenzhöfer

Microbiology Monographs 10 (2009): 59–82

IV.2 Identification of the dominant sulfate-reducing bacterial partner of anaerobic methanotrophs of the ANME-2 clade

Lars Schreiber, Thomas Holler, Katrin Knittel, Anke Meyerdierks & Rudolf Amann

Environmental Microbiology 12 (2010): 2327–2340

IV.3 Metagenomic analysis of the dominating sulfate-reducing bacteria in ANME-2 dominated enrichments catalyzing the anaerobic oxidation of methane

Lars Schreiber, Thomas Holler, Michael Kube, Richard Reinhard, Anke Meyerdierks & Rudolf Amann

Manuskript in Vorbereitung

IV.4 Diversity of adenosine-5'-phosphosulfate reductase and dissimilatory sulfite reductase in microbial communities mediating the anaerobic oxidation of methane

Lars Schreiber, Friedrich Reinhard, Thomas Holler, Martin Krüger, Jan Küver, Marc Mussmann, Anke Meyerdierks & Rudolf Amann

Manuskript in Vorbereitung

IV.5 Polyphasic comparative analysis of microbial reef communities along the northwestern Black Sea shelf

Julia Arnds, Pamela Rossel, Katrin Knittel, Tina Treude, Thomas Holler, Markus Elvert, Kai-Uwe Hinrichs, Antje Boetius & Rudolf Amann

Manuskript in Vorbereitung

IV.6 Effect of storage conditions on archaeal and bacterial communities in subsurface marine sediments

Yu-Shih Lin, Jennifer F. Biddle, Julius S. Lipp, Beth! N. Orcutt, Thomas Holler, Andreas Teske & Kai-Uwe Hinrichs

Geomicrobiology Journal 27 (2010): 261–272

IV.7 Stable carbon isotope probing of intact polar lipids from benthic archaea in marine subsurface sediment

Yu-Shih Lin, Jennifer F. Biddle, Julius S. Lipp, Thomas Holler, Andreas Teske & Kai-Uwe Hinrichs

Manuskript in Vorbereitung

IV.1

The seabed as natural laboratory: Lessons from uncultivated methanotrophs

Antje Boetius, [1,2]* Thomas Holler,[1] Katrin Knittel, [1] Janine Felden[1] and Frank Wenzhöfer[1]

Microbiology Monographs 10 (2009): 59–82

[1]Max Planck Institute for Marine Microbiology, Celsiusstr.1, 28359 Bremen, Germany

[2]Jacobs University Bremen, Campusring 1, 28759 Bremen, Germany

*** Corresponding author**

Abstract

The anaerobic oxidation of methane (AOM) by archaeal methanotrophs (ANME) functions as a major sink in oceanic methane geochemistry, and is a key biogeochemial process in the anoxic seabed. Unfortunately, demonstration of the biochemical pathway of AOM has not been possible because of the lack of pure cultures of ANME and their partner sulfate-reducing bacteria. The main reason for failing to isolate these microorganisms by cultivation is their slow growth, which is most likely a consequence of the low energy yield of the AOM reaction. This chapter discusses how *in situ* biogeochemical and microbiological observations of natural seabed communities and *in vitro* enrichments contribute to understanding of the ecology and physiology of these "uncultivables". Successful *in vitro* enrichment strategies include selecting seabed inoculates with abundant ANME populations, increasing the availability of dissolved methane and sulfate by flow through reactors and hydrostatic pressure, and maintaining the apparent temperature, pH, and salinity optima of AOM, the energy delivering process.

IV.2

Identification of the dominant sulfate-reducing bacterial partner of anaerobic methanotrophs of the ANME-2 clade

Lars Schreiber,[1] Thomas Holler,[1] Katrin Knittel,[1] Anke Meyerdierks[1]* and Rudolf Amann[1]

Environmental Microbiology 12 (2010): 2327–2340

[1]Max Planck Institute for Marine Microbiology, Celsiusstr.1, 28359 Bremen, Germany

*** Corresponding author**

Abstract

The anaerobic oxidation of methane (AOM) with sulfate as terminal electron acceptor is mediated by consortia of methanotrophic archaea (ANME) and sulfate-reducing bacteria (SRB). Whereas three clades of ANME have been repeatedly studied with respect to phylogeny, key genes, and genomic capabilities, little is known about their sulfate-reducing partner. In order to identify the partner of anaerobic methanotrophs of the ANME-2 clade, bacterial 16S rRNA gene libraries were constructed from cultures highly enriched for ANME-2a and ANME-2c in consortia with *Deltaprotobacteria* of the *Desulfosarcina/Desulfococcus* group (DSS). Phylogenetic analysis of those and publicly available sequences from AOM sites supported the hypothesis that the DSS partner belongs to cluster SEEP-SRB1. Six subclusters of SEEP-SRB1, SEEP1a to SEEP1f, were proposed and specific oligonucleotide probes were designed. Using fluorescence *in situ* hybridization on samples from four distinctly different AOM sites, SEEP1a was identified as sulfate-reducing partner in up to 95% of total ANME-2 consortia. SEEP1a cells exhibited a rod-shaped, vibrioid, or coccoid morphology and were found to be associated with subgroups ANME-2a and ANME-2c. Moreover, SEEP1a was also detected in 8% to 23% of ANME-3 consortia in Haakon Mosby Mud Volcano sediments, previously described to be predominantly associated with SRB of the *Desulfobulbus* group. SEEP1a contributed to only 0.3% to 0.7% of all single cells indicating that the association with ANME may be highly beneficial or even obligate.

IV.3

Metagenomic analysis of the dominating sulfate-reducing bacteria in ANME-2 dominated enrichments catalyzing the anaerobic oxidation of methane

Lars Schreiber,[1] Thomas Holler,[1] Michael Kube,[2] Richard Reinhard,[2] Anke Meyerdierks[1]* & Rudolf Amann[1]

Manuskript in Vorbereitung

[1]Max Planck Institute for Marine Microbiology, Celsiusstr.1, 28359 Bremen, Germany

[2]Max Planck Institute for Molecular Genetics, Ihnestr. 63–73, 14195 Berlin, Germany

*** Corresponding author**

Abstract

The anaerobic oxidation of methane with sulfate (AOM) is a widespread process and the main methane sink in marine systems. AOM is catalyzed by consortia of anaerobic methanotrophic archaea (ANME) and sulfate-reducing bacteria (SRB). In spite of the importance of AOM, our understanding of the interaction between ANME and SRB as well as the underlying biochemistry of AOM is still limited. Attempts to answer these questions are hampered by the current inability to cultivate the involved microorganisms in pure culture. Here we used a culture-independent metagenomic approach to attempt a genome reconstruction of SEEP-SRB1a, the main sulfate-reducing partner of anaerobic methanotrophs of the ANME-2 clade. We used DNA from an enrichment culture dominated by ANME-2 and SEEP-SRB1a for constructing a large-insert fosmid library and for performing next-generation pyrosequencing. Almost 92% of the assembled contigs featured a length of only 1.5 kbp or shorter indicating an insufficient coverage of the enrichment community. Within the metagenome, we detected 11 contigs carrying 16S rRNA genes of SEEP-SRB1a. This observation indicated a considerable microdiversity of SEEP-SRB1a within the enrichment. The metagenome contained too few long contigs to reconstruct the genome of SEEP-SRB1a. However, we identified the 23S rRNA gene as well as putative *apr* and *dsr* genes of SEEP-SRB1a which might be used as alternative genetic markers in future studies. *Apr* and *dsr* genes of SEEP-SRB1a identified two contigs with a length of >18kbp and thereby provided a first glimpse of the genetic potential of SEEP-SRB1a. Finally, we identified 211 fosmid inserts whose end-sequences map onto the genome of *Desulfococcus oleovorans* Hxd3, the closest fully-sequenced relative of SEEP-SRB1a. Sequencing of these inserts might provide a robust scaffold for the reconstruction the SEEP-SRB1a genome.

IV.4

Diversity of adenosine-5'-phosphosulfate reductase and dissimilatory sulfite reductase in microbial communities mediating the anaerobic oxidation of methane

Lars Schreiber,[1] Friedrich Reinhard,[1] Thomas Holler,[1] Martin Krüger,[2] Jan Küver,[3] Marc Mussmann,[1] Anke Meyerdierks[1]* & Rudolf Amann[1]

Manuskript in Vorbereitung

---

[1]Max Planck Institute for Marine Microbiology, Celsiusstr.1, 28359 Bremen, Germany

[2] Federal Institute for Geosciences and Natural Resources, Stillweg 2, 30655 Hannover, Germany

[3]Bremen Institute for Material Testing, Paul-Feller-Str. 1, 28199 Bremen, Germany

*** Corresponding author**

Abstract

Sulfate reducing bacteria (SRB) are associated with anaerobic methanotrophic archaea in consortia mediating the anaerobic oxidation of methane (AOM). Furthermore, a significant fraction of SRB is present as free-living cells at AOM sites. In this study, the diversity of SRB in AOM habitats, more precisely different microbial mats from the Black Sea, and enrichment cultures from the sediment above gas hydrates at Hydrate Ridge, was characterized by using the AprA and DsrAB genes as functional markers. The diversity of SRB was well covered by comparative analysis of 37–71 clones (≥ 92% coverage for Black Sea samples and Hydrate Ridge subjected to intermediate high, 15 mM, methane pressure; 79–86% coverage for Hydrate Ridge sediment kept at low, 1.5 mM, methane partial pressure). Within the Black Sea mat sections the diversity of SRB (2–8 retrieved OTUs) was comparable to the diversity in Hydrate Ridge enrichment cultures after high methane pressure incubation and considerably lower compared to Hydrate Ridge sediment kept at low methane concentration (14–19 OTUs). Clone libraries from Black Sea mats were dominated by sequences assigned to *Desulfobacteraceae*. Nonetheless, several different *Desulfobacteraceae* groups were detected in these mats and the SRB communities of the mat sections were heterogeneous with similarities scores of only 17–30%. Clone libraries from Hydrate Ridge enrichment cultures after high methane pressure incubation were also dominated by sequences related to *Desulfobacteraceae* (98–100% of the analyzed clones); also here a considerable diversity within this family was detected. Finally, many *Desulfobacteraceae* sequences were also retrieved from Hydrate Ridge sediment kept at low methane concentration. However, a *dsrAB* clone library from that sample was dominated by a group of deep-branching sequences (63% of analyzed clones) previously retrieved from other marine habitats and a salt marsh. With a fluorescence-activated cell sorting approach, the AprA of the yet uncultivated dominant partner of ANME-2, SEEP-SRB1a, was tentatively assigned to a sequence cluster within the *Desulfobacteraceae*.

IV.5

Polyphasic comparative analysis of microbial reef communities along the northwestern Black Sea shelf

Julia Arnds,[1] Pamela Rossel,[2] Katrin Knittel,[1]* Tina Treude,[1] Thomas Holler,[1] Markus Elvert,[2] Kai-Uwe Hinrichs,[2] Antje Boetius[1,3] & Rudolf Amann[1]

Manuskript in Vorbereitung

---

[1]Max Planck Institute for Marine Microbiology, Celsiusstr.1, 28359 Bremen, Germany

[2]Organic Geochemistry Group, Department of Geosciences and MARUM Center for Marine Environmental Sciences, University of Bremen, 28359 Bremen, Germany

[3]Alfred Wegener Institute for Polar and Marine Research, 27515 Bremerhaven, Germany

*** Corresponding author**

Abstract

Massive microbial reefs, fueled by the anaerobic oxidation of methane (AOM) with sulfate, grow along the deep anoxic shelf of the northwestern Black Sea. The key microbes have been identified as ANME-1, ANME-2, and sulfate reducers of the *Desulfosarcina/Desulfococcus* cluster (DSS), but little is known about their *in situ* abundance and spatial distribution. In this study, we used two (semi) quantitative methods (i.e. intact polar lipid (IPL) and CARD-FISH analysis) to investigate the composition of the microbial community in various reef samples and methane seeping sediments. IPL composition of the reef communities was most often consistent with their phylogenetic diversity and structure. Comparisons of the microbial community structure of reefs from three distinct areas showed only little variations suggesting stable environmental conditions along the Black Sea shelf. Distribution of key methanotrophs varied in distinct reef zones: the youngest, top zones characterized by high AOM rates [940 μmol (gram dry weight) $^{-1}$ d^{-1}] were dominated by ANME-2 archaea (15–24% of total cells) and sulfate reducers of the DSS (15–21%). In contrast, exterior and interior zones of the reef showed threefold lower AOM rates and were characterized by a dominance of ANME-1 archaea (27–32%) but absence of ANME-2 archaea (<1%) and DSS bacteria (<1%). Bacterial IPL composition reflected the difference in the AOM community. The ANME-2 zones were dominated by phosphatidylethanolamine (PE) derivatives of mixed acyl/ether glycerol (AEG) lipids or diacyl glycerol (DAG) lipids whereas ANME-1 zones were dominated by PEs of dietherglycerol (DEG) lipid types with the exception of the interior reef zone where DEG-PEs were absent. In conclusion, our FISH and IPL data suggest that ANME-1 archaea have i) a single or ii) diverse non-DSS sulfate-reducing partners, or iii) might be even independent on any bacterial partner to perform AOM.

IV.6

Effect of storage conditions on archaeal and bacterial communities in subsurface marine sediments

Yu-Shih Lin,[1]* Jennifer F. Biddle,[2]* Julius S. Lipp,[1] Beth! N. Orcutt,[3] Thomas Holler,[4] Andreas Teske[2] and Kai-Uwe Hinrichs[1]

Geomicrobiology Journal 27 (2010): 261–272

---

[1]Organic Geochemistry Group, Department of Geosciences and MARUM Center for Marine Environmental Sciences, University of Bremen, 28359 Bremen, Germany

[2]Department of Marine Sciences, The University of North Carolina at Chapel Hill, Chapel Hill, North Carolina, 27599, USA

[3]Department of Marine Sciences, University of Georgia, Athens, Georgia, USA

[4]Max Planck Institute for Marine Microbiology, Celsiusstr.1, 28359 Bremen, Germany

*** Corresponding author**

Abstract

We have studied the effects of slow infiltration of oxygen on microbial communities in refrigerated legacy samples from ocean drilling expeditions. Storage was in heat-sealed, laminated foil bags with a N_2 headspace for geomicrobiological studies. Analysis of microbial lipids suggests that *Bacteria* were barely detectable *in situ* but increased remarkably during storage. Detailed molecular examination of a methane-rich sediment horizon showed that refrigeration triggered selective growth of ANME-2 archaea and a drastic change in the bacterial community. Subsequent enrichment targeting methanogens yielded exclusively methylotrophs, which were probably selected for by high sulfate levels caused by oxidation of reduced sulfur species. We provide recommendations for sample storage in future ocean drilling expeditions.

IV.7

Stable carbon isotope probing of intact polar lipids from benthic archaea in marine subsurface sediment

Yu-Shih Lin,[1] Jennifer F. Biddle,[2] Julius S. Lipp,[1] Thomas Holler,[3]
Andreas Teske[2] & Kai-Uwe Hinrichs[1]*

Manuskript in Vorbereitung

---

[1]Organic Geochemistry Group, Department of Geosciences and MARUM Center for Marine Environmental Sciences, University of Bremen, 28359 Bremen, Germany

[2]Department of Marine Sciences, The University of North Carolina at Chapel Hill, Chapel Hill, North Carolina, 27599, USA

[3]Max Planck Institute for Marine Microbiology, Celsiusstr.1, 28359 Bremen, Germany

*** Corresponding author**

Abstract

Recent studies based on intact polar lipids (IPLs) have suggested that Archaea make a significant contribution of the extant biomass on Earth, but the linkage between the archaeal IPLs and marine benthic archaea have not been demonstrated by *in vitro* studies. With a combined goal of elucidating the substrate specificity of marine benthic archaea, an intact polar lipid-stable carbon isotope probing (IPL-SIP) experiment was performed on a subseafloor sediment sample with ^{13}C-labeled bicarbonate, methane, acetate, or *Spirulina platensis* cells. After prolonged incubation for up to 468 days, the hydrophobic moieties of the archaeal IPLs showed minimal label incorporation. The strongest shift in carbon isotopic values (up to 4‰) was detected in crenarchaeol-derived tricyclic biphytane in the sediment slurries supplemented with ^{13}C-labeled *S. platensis*. In contrast, under the same labeling condition, close to 5% of the mannose cleaved from the archaeal glycosyl tetraether lipids was ^{13}C-labeled. Our results suggest that archaeal IPLs were being generated in the sediment containing benthic archaeal sequences. The unbalanced ^{13}C uptake between the glycosidic head groups and the hydrocarbon chains implies the presence of an anabolic shortcut that enables benthic archaea to regenerate glycolipids while bypassing the energy-costly tetraether biosynthesis.

V. Danksagung

Ich möchte mich bei allen Personen bedanken, die mich im Laufe der Promotion auf vielfältige Art und Weise unterstützt haben und zum Gelingen dieser Arbeit beigetragen haben.

Außerordentlich dankbar bin ich Prof. Friedrich Widdel für die Möglichkeit an diesem spannenden wie faszinierenden mikrobiologischen Thema arbeiten zu können. Darüber hinaus möchte ich ihm für die interessanten und inspirierenden Diskussionen sowie für das Vertrauen in meine Arbeit danken. Als Betreuer hat er entscheidend zum Gelingen dieser Arbeit beigetragen.

Besonderer Dank gilt Prof. Antje Boetius für die Übernahme des Gutachtens aber vor allem für ihre stete Unterstützung und Motivation. Ohne ihr Engagement wäre diese Arbeit so nicht zustande gekommen.

Mein herzlicher Dank gilt PD Jens Harder. Als sehr langer Begleiter meiner wissenschaftlichen Entwicklung hat er mir bei den Anfängen des Forschens geholfen und nie aufgehört mir mit Rat und Tat zur Seite zu stehen. Seine Bereitschaft zur Übernahme des Zweitgutachtens freut mich besonders und ich danke ihm dafür.

Ohne die konstruktive und freundschaftliche Zusammenarbeit mit den MPI-Kollegen hätte ich so manche Technik nicht kennengelernt, so manche Idee nicht bekommen und einige Versuche nicht machen können. Vielen Dank an all diejenigen, mit denen ich zusammenarbeiten durfte. Besonders bedanke ich mich bei Dr. Gunter Wegener, der mich in der Endphase der Promotion bestens unterstützte. Dr. Katrin Knittel und Dr. Anke Meyerdierks danke ich für die sehr gute Zusammenarbeit in den gemeinsamen AOM-Projekten.

Ich möchte allen jetzigen und früheren Mitarbeitern der Abteilung Mikrobiologie für die angenehme und produktive Arbeitsatmosphäre danken. Die Zusammenarbeit mit Jana Milučkà, Mirko Basen und Christian Deusner war dabei außerordentlich inspirierend. Besonders meinen lieben Büro-Kollegen Lars, Katja und Hoa sei für viele schöne Jahre am MPI gedankt.